Western University
Scholarship@Western

Digitized Theses

Digitized Special Collections

1976

Mechanical Properties Of Chordae Tendineae And Anterior Leaflets From Human Mitral Valves, And Of Aortic Valve Cusps

Koon Ong Lim

Follow this and additional works at: https://ir.lib.uwo.ca/digitizedtheses

Recommended Citation

Lim, Koon Ong, "Mechanical Properties Of Chordae Tendineae And Anterior Leaflets From Human Mitral Valves, And Of Aortic Valve Cusps" (1976). *Digitized Theses*. 890.
https://ir.lib.uwo.ca/digitizedtheses/890

This Dissertation is brought to you for free and open access by the Digitized Special Collections at Scholarship@Western. It has been accepted for inclusion in Digitized Theses by an authorized administrator of Scholarship@Western. For more information, please contact tadam@uwo.ca, wlswadmin@uwo.ca.

INFORMATION TO USERS

THIS DISSERTATION HAS BEEN
MICROFILMED EXACTLY AS RECEIVED

This copy was produced from a microfiche copy of the original document. The quality of the copy is heavily dependent upon the quality of the original thesis submitted for microfilming. Every effort has been made to ensure the highest quality of reproduction possible.

PLEASE NOTE: Some pages may have indistinct print. Filmed as received.

Canadian Theses Division
Cataloguing Branch
National Library of Canada
Ottawa, Canada K1A 0N4

AVIS AUX USAGERS

LA THESE A ETE MICROFILMEE
TELLE QUE NOUS L'AVONS RECUE

Cette copie a été faite à partir d'une microfiche du document original. La qualité de la copie dépend grandement de la qualité de la thèse soumise pour le microfimage. Nous avons tout fait pour assurer une qualité supérieure de reproduction.

NOTA BENE: La qualité d'impression de certaines pages peut laisser à désirer. Microfilmée telle que nous l'avons reçue.

Division des thèses canadiennes
Direction du catalogage
Bibliothèque nationale du Canada
Ottawa, Canada K1A 0N4

MECHANICAL PROPERTIES OF CHORDAE TENDINEAE AND ANTERIOR LEAFLETS FROM HUMAN MITRAL VALVES, AND OF AORTIC VALVE CUSPS

by

Koon Ong Lim, B.Sc., B.Ed.
Department of Biophysics

Submitted in partial fulfillment
of the requirements for the degree of
Doctor of Philosophy

Faculty of Graduate Studies
The University of Western Ontario
London, Ontario
May 1976

© Koon Ong Lim 1976.

ABSTRACT

A knowledge of the mechanical properties of heart valve tissues is a necessary prerequisite for a better understanding of valvular behaviour and the design of leaflet type prosthetic valves. The intention of this thesis is to examine the response to mechanical stress of human mitral valve chordae tendineae, the anterior mitral leaflet and aortic valve tissues.

The elastic response of chordae tendineae was studied by subjecting the tissue to uniaxial tensile stress at strain rates of 6.25% min^{-1} to 1600% min^{-1} and to sinusoidal strain variations (frequency 0.42 to 6.68 Hz). Selective enzymatic digestion and scanning and transmission electron microscopy were employed to relate the observed elastic response of this tissue to its internal structure. The dynamic viscoelasticity of the mitral and aortic leaflets was investigated by subjecting membranous samples of these tissues to sinusoidal fluid pressure variations (frequency 0.5 to 5 Hz).

The stress-strain curves of the chordae were found to be governed primarily by the central collagen core and were non-linear. Scanning electron microscopy revealed that this was due to a network arrangement of collagen fibrils in the central chordal core. The collagen fibres in the core were also found to be wavy in young specimens but were relatively straight in the older specimens. This explains the greater extensibility of young specimens. Chordal extensibility was also found to decrease with increasing strain rates, indicating that this tissue is viscoelastic. Thicker chordae were found to be more extensible than thinner specimens. Transmission electron microscopy showed that this was due to a lower collagen fibril density in the core of the thicker chordae.

Dynamic studies on the chordae showed that the dynamic modulus also decreased with increase in chordal size. At strains of 6.5% to 10.0%, the storage modulus, E', was of the order of 10^8 to 10^9 dynes cm^{-2} and increased with strain but was independent of applied frequency. The loss modulus, E", however, decreased with increasing frequency, and was 18 to 50 times smaller than E'.

The storage moduli for the mitral and aortic leaflets at strains of 1.5% to 5% were also found to be independent of frequency. Values in the order of 10^8 dynes cm^{-2} were obtained, with the mitral values being nearly twice that of the aortic. The loss modulus for the mitral leaflet increased with frequency while that for the aortic was independent of frequency. The loss moduli of both the valve leaflets were 17 to 43 times smaller than their storage moduli.

The study has, therefore, shown that the mitral and aortic tissues are relatively inextensible and have low losses. These characteristics should be considered in the design of leaflet type valve prostheses. The low losses also imply that these tissues are more elastic than viscous. This is advantageous for a structure that is under constant dynamic stress. The collagen fibril network in the central chordal core also ensures that excessive strains are not imposed on these fibrils. The greater extensibility of the thicker chordae serves a useful function. It allows the more centrally inserted larger chordae to maintain an even valve surface on closure. Under the assumption of comparable loading and valve configurations, the higher E' of the mitral leaflet led one to conclude that the vibrations of these two valves cannot contribute in any significant way to the observed frequencies of the first and second heart sounds. In addition, it is believed that the low extensibility of the mitral tissue renders it impossible for this valve to bulge into the left atrium to produce the left atrial pressure 'c' wave.

ACKNOWLEDGEMENTS

I wish to express my gratitude and appreciation to Dr. D.R. Boughner for introducing me to this area of research and for his constant guidance and interest throughout this study. Drs. M.R. Roach, A.C. Groom and J.B. Finlay provided invaluable suggestions throughout the course of this research and I owe them special thanks. I would also like to extend my appreciations to Dr. W.J. Kostuk, my advisor, and to the many faculty members and colleagues in the Biophysics Department with whom I discussed my problems at one time or another.

I am grateful to Dr. L.N. Johnson for the use of the Instron machine and Mr. C. Rupp for his superb technical assistance. Dr. A.C. Wallace of the Department of Pathology permitted the use of the transmission electron microscope and Mrs. E. Hunter provided the technical expertise, and I am indebted to them. My appreciation also goes to the Department of Anatomy for the use of the scanning electron microscope and to Mr. P. Ohara for his indispensible technical assistance.

I would also like to thank Mr. L. Rigutto and Mr. W. Rigg for their expert assistance in the construction of the apparatus and Mrs. E. Swann for the histological sections.

Mrs. R. Norkum patiently deciphered my script during the preparation of the final draft and I would like to thank her.

The Departments of Pathology, University Hospital and St. Joseph's Hospital, London, kindly provided the autopsy specimens without which this work would be impossible.

Finally, special appreciation is expressed to my wife Lee Lee who has to put up with all the frustrations that go with completing a thesis.

KOON ONG LIM

Department of Biophysics,
University of Western Ontario,
May 1st, 1976.

This work was supported by the Ontario Heart Foundation and the author wishes to express his indebtedness to this organisation.

TABLE OF CONTENTS

Page

CERTIFICATE OF EXAMINATION. ii

ABSTRACT. iii

ACKNOWLEDGEMENTS. vi

TABLE OF CONTENTS xi

LIST OF TABLES. xii

LIST OF FIGURES xiii

CHAPTER 1 - INTRODUCTION. 1

1. Anatomy of the Mitral and Aortic Valves 1
2. Aim of the Study 7

CHAPTER 2 - HISTORICAL REVIEWS 13

1. Artificial Heart Valves 13
2. Left Atrial Pressure 'c' Wave 18
3. The First and Second Heart Sounds . . 20
4. Cardiac Valvular Tissue Response Under Mechanical Stress 22

CHAPTER 3 - UNIAXIAL TENSILE TESTS ON CHORDAE TENDINEAE 26

1. Introduction 26
2. Method. 26
3. Results 35
4. Discussion 72
5. Summary 77

Page

CHAPTER 4 - MORPHOLOGY OF CHORDAE TENDINEAE AND ITS RELATION TO THEIR EXTENSIBILITY CURVES 81

1. Introduction. 81
2. Method 82
   a) Selective Enzymatic Digestion 83
   b) Scanning Electron Microscopic Studies 86
   c) Transmission Electron Microscopic Studies 87
3. Results 89
   a) Selective Enzymatic Digestion 89
   b) Scanning Electron Microscopic Studies 94
   c) Transmission Electron Microscopic Studies 101
4. Discussion 110
5. Summary 119

CHAPTER 5 - DYNAMIC ELASTICITY OF CHORDAE TENDINEAE 121

1. Introduction 121
2. Method. 121
   a) Theory 121
   b) Apparatus and Experimental Procedures. 124
3. Results 129

Page

4. Discussion 141
5. Summary 149

CHAPTER 6 - THE LOW FREQUENCY DYNAMIC VISCOELASTICITY OF THE ANTERIOR LEAFLET OF THE HUMAN MITRAL VALVE. . . . 151
1. Introduction 151
2. Method 151
    a) Theory 151
    b) Apparatus and Experimental Procedures 152
    c) Analysis 158
3. Results 161
4. Discussion 169
5. Summary 176

CHAPTER 7 - THE LOW FREQUENCY DYNAMIC VISCOELASTICITY OF THE HUMAN AORTIC VALVE CUSPS 177
1. Introduction 177
2. Method 177
3. Results 180
4. Discussion 188
5. Summary 193

CHAPTER 8 - CONCLUSIONS 195
CHAPTER 9 - SUGGESTIONS FOR FUTURE RESEARCH. 198
APPENDIX 201
REFERENCES 202
VITA 209

LIST OF TABLES

Table	Description	Page
3-I	Strain and stress values at point of transition for different sized chordae tendineae strained at 5 different strain rates	55
3-II	Secant and final elastic moduli of the stress-strain curves of different sized chordae tendineae strained at different strain rates	57
3-III	Stress values of chordae tendineae at 5% strain	60
3-IV	Breaking strain as a function of strain rate and breaking stress as a function of chordal size	66
4-I	Average collagen fibril size and fibril density as a function of chordal size. .	109
5-I	Stress and storage modulus of different sized chordae strained to different levels	134
5-II	Regression coefficients for the loss modulus versus frequency graphs for different sized chordae and for different levels of strain	147

LIST OF FIGURES

Figure	Description	Page
1.1	Diagram of a dissected heart showing the locations of the mitral and aortic valves	3
1.2	Diagram of the aortic and mitral valves	6
1.3	Events of the cardiac cycle	10
3.1	Diagram of the apparatus used for tensile tests on chordae tendineae . .	28
3.2	A parallel plate clamp	31
3.3	Stress-strain curves of chordae tendineae preserved for 2 and 6 days. . . .	34
3.4	Typical stress-strain response of chordae tendineae	37
3.5	Stress-strain curves of chordae tendineae of different sizes.	40
3.6	Stress-strain curves of chordae tendineae under different strain rates. .	48
3.7	Stress-strain curves of chordae tentendineae of different ages.	62
3.8	Toughness of chordae tendineae as a function of chordal size	69
3.9	Echocardiographic trace of the motion of the mitral valve leaflet.	71

Figure	Description	Page
3.10	Histogram of the closure rate for mitral leaflets	74
3.11	Diagrams showing attachment, to the mitral leaflets of different sized chordae tendineae and the response of different sized materials having similar or different mechanical properties. . .	79
4.1	Histological sections of chordae tendineae before and after enzymatic digestion	85
4.2	Stress-strain curves of enzymatically treated chordae tendineae and controls.	91
4.3	Scanning electron micrographs of the chordal core of an old specimen	96
4.4	Scanning electron micrograph of the chordal core of a young specimen. . . .	100
4.5	Scanning electron micrograph of a chorda fixed under tension.	103
4.6	Transmission electron micrographs of transverse sections of chordae tendineae	105
4.7	Size distribution of collagen fibrils in chordae tendineae	112
4.8	Elastic response of young and old chordae tendineae	118

Figure	Description	Page
5.1	Diagram showing phase shift between sinusoidal stress and strain	123
5.2	Diagram of apparatus used for stretching chordae tendineae sinusoidally . .	126
5.3	Response of chordae tendineae under sinusoidal stretch	131
5.4	Storage modulus as a function of frequency of chordae tendineae at 6.5% strain	136
5.5	Storage modulus of chordae tendineae at 10.0% and 9.5% strain	138
5.6	Phase lag between stress and strain for chordae tendineae	140
5.7	Loss modulus of chordae tendineae as a function of frequency at 6.5% strain .	143
5.8	Loss modulus of chordae tendineae at 10.0% and 9.5% strain	145
6.1	Diagram of the apparatus used for the sinusoidal stretching of mitral and aortic valve leaflets	154
6.2	Response of the anterior mitral leaflet when stretched sinusoidally	163
6.3	Phase lag between stressing function and response for the mitral leaflets . .	165

Figure	Description	Page
6.4	Dynamic elastic moduli of mitral leaflets	167
6.5	A pressure versus strain graph for the mitral leaflets	171
7.1	Response of aortic valve cusps when stretched sinusoidally	182
7.2	Phase lag between stressing function and response for the aortic valve leaflets	185
7.3	Dynamic elastic moduli of the aortic valve cusps	187
7.4	A comparison of the storage moduli of the mitral and aortic valve leaflets .	192

The author of this thesis has granted The University of Western Ontario a non-exclusive license to reproduce and distribute copies of this thesis to users of Western Libraries. Copyright remains with the author.

Electronic theses and dissertations available in The University of Western Ontario's institutional repository (Scholarship@Western) are solely for the purpose of private study and research. They may not be copied or reproduced, except as permitted by copyright laws, without written authority of the copyright owner. Any commercial use or publication is strictly prohibited.

The original copyright license attesting to these terms and signed by the author of this thesis may be found in the original print version of the thesis, held by Western Libraries.

The thesis approval page signed by the examining committee may also be found in the original print version of the thesis held in Western Libraries.

Please contact Western Libraries for further information:
E-mail: libadmin@uwo.ca
Telephone: (519) 661-2111 Ext. 84796
Web site: http://www.lib.uwo.ca/

CHAPTER 1

INTRODUCTION

1. ANATOMY OF THE MITRAL AND AORTIC VALVES

The human heart is a four chamber pump consisting of two atria and two ventricles. The atria function primarily as reservoirs to the ventricles but they also pump weakly to move blood from the atria to the ventricles. The ventricles supply the major force propelling blood through the lungs and peripheral circulatory system. The effective and efficient pumping of the heart relies, in part, on the presence of heart valves to prevent retrograde flow. The valve lying between the right atrium and right ventricle is the tricuspid valve and that between the left atrium and left ventricle is the bicuspid or mitral valve. Valves are also present at the entrance to the pulmonary artery and aorta. These are respectively, the pulmonary and aortic valves (figure 1.1). These four cardiac valves as well as the atrial and ventricular muscle masses are attached to the fibrous skeleton of the heart.

The mitral (and also the tricuspid) valve is a funnel shaped, fibroelastic diaphragm that projects into the ventricle,

Figure 1.1. Diagram of a dissected heart showing the locations of the mitral and aortic valves. AA = ascending aorta, RA = right atrium, RV = right ventricle, LA= left atrium, LV = left ventricle, S. = interventricular septum, as = aortic sinus, av = aortic valve, tv = tricuspid valve, ct = chordae tendineae, pm = papillary muscles, al = anterior mitral leaflet, and pl = posterior mitral leaflet.

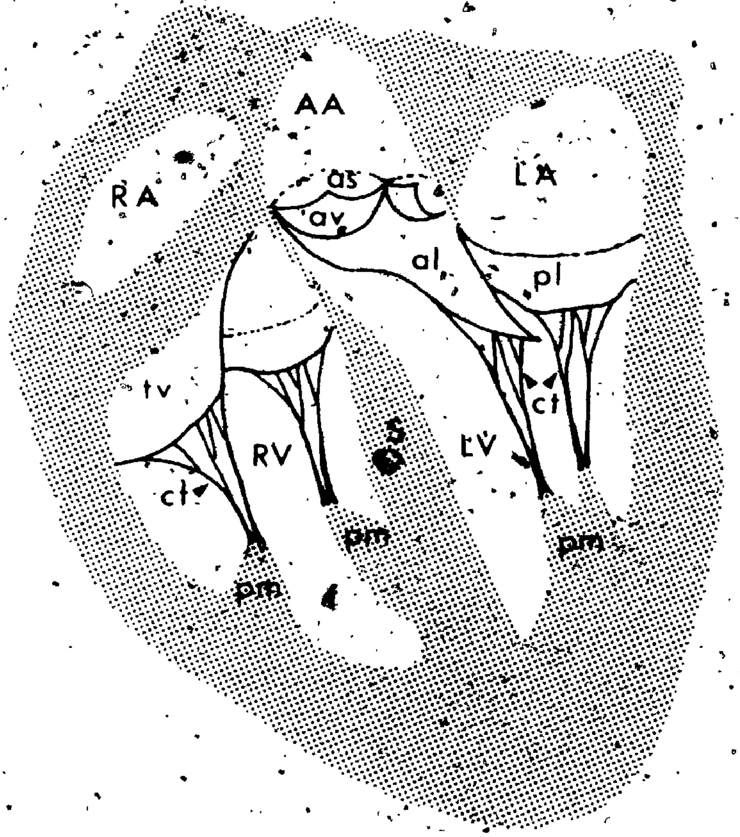
AA
RA
as
av
LA
al
pl
tv
RV
S
LV
ct
ct
pm
pm
pm

The larger base of this funnel shaped structure is firmly attached to the circumference of the fibrous valve ring and the free edge is attached via fibrous tissues, called chordae tendineae, to two papillary muscles which project from the ventricular wall. Anterolateral and posteromedial indentations into this funnel shaped diaphragm divide it into the anteromedial (or anterior) and posterolateral (or posterior) leaflets. These indentations, however, do not proceed as far as the valve ring, thus some bridging commissural tissues are present between the two major leaflets (see figure 1.2). The anterior leaflet, which is somewhat triangular in shape, has a height from apex to base of 1.8 to 3.2 cm and is about twice the height of the quandrangular posterior leaflet. The base length of the anterior leaflet is about 2.4 to 4.5 cm and that of the posterior leaflet is about 2.3 to 4.1 cm (Silverman and Hurst, 1968).

The chordae tendineae radiating from each of the two papillary muscles insert into the ventricular aspect of both the leaflets at different angles and in different locations. Those that insert directly on the free edge of the leaflets are usually smaller in size and are termed the first order chordae (Walmsley, 1929). Larger sized second order chordae insert a short distance away from the free edge and these are termed the critical areas of insertion by Brock (1952).

Figure 1.2. Diagram of the aortic and mitral valves. AA = ascending aorta, LA = left atrium, LV = left ventricle, as = aortic sinus, av = aortic valve, al = anterior mitral leaflet and pl = posterior mitral leaflet.

AORTIC VALVE

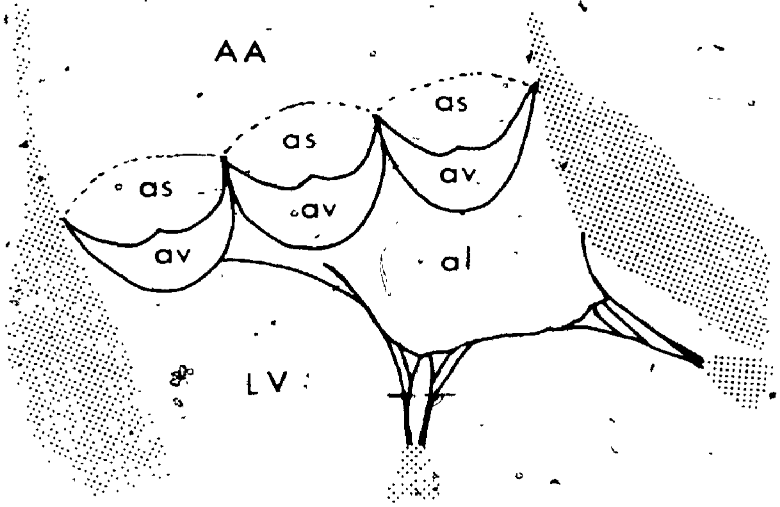
AA
as
as
as
av
av
av
al
LV

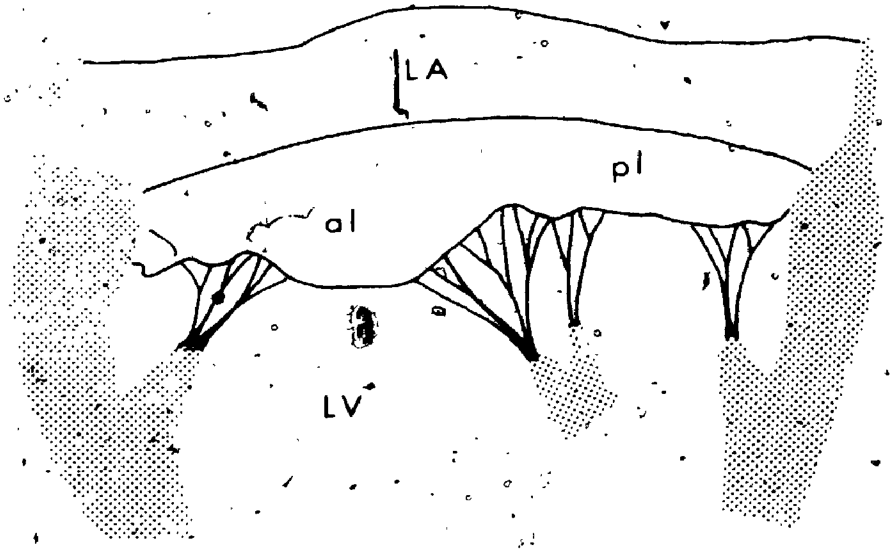

MITRAL VALVE

Some third order chordae insert onto the leaflets directly from the ventricular wall. The presence of the papillary muscles and chordae act to prevent the prolapse of the mitral leaflets into the atrium during ventricular systole. They are all under tension when the valve is completely closed. The area of the mitral orifice is about half the combined area of the valve leaflets. The valve leaflets and chordae are lined by a glistening, slightly opaque endocardium (Silverman and Hurst, 1968).

The aortic valve, in contrast to the mitral valve, is a much simpler structure. It is made up of three fibroelastic cusps or leaflets which are approximately equal in size. Each cusp is about 2 cm long and 1.5 cm wide, and is shaped like a semi-disc (figure 1.2). When the aortic valve is open the size of the orifice is approximately the same as the smaller open end of the funnel shaped diaphragm of the mitral valve. Behind each of the three aortic valve cusps are outpouchings called the sinuses of Valsalva, which help prevent the obstruction of the coronary ostia that are located here.

2. AIM OF THE STUDY.

For over 15 years, cardiac valve replacement has been an accepted form of treatment for patients with diseased and incompetent valves, but the ideal substitute has yet to be found. Valve substitutes can be broadly classified into mechanical prosthetic devices and tissue valves constructed from biological materials such as fascia lata and pericardium.

Whereas mechanical prostheses suffer from the problem of thromboembolism (Kaltman, 1971; Bonchek and Starr, 1975), this complication is seldom observed in tissue valve implants. However, one major disadvantage with tissue valve substitutes is valve incompetence and eventual structural failure (Kaltman, 1971; Wallace, 1975). This could, in part, be due to the unsuitability of the tissue substitutes in both elasticity and mechanical strength. The importance of a knowledge of the mechanical properties of normal valve tissue has been stressed by many as a necessary prerequisite for finding a suitable substitute in the successful design of tissue valve prostheses (Clark, 1973; Mundth, Wright and Austen, 1971).

In addition, the explanations proposed for the occurrence of some events in the cardiac cycle have also implicated the mechanical properties of these cardiac valvular tissues.

In a normal cardiac cycle, pressure in the left atrium is not constant and the atrial pressure curve shows three major pressure elevations, the a, c, and v waves (figure 1.3) The presence of the 'c' wave has been attributed to

Figure 1.3. The events of the cardiac cycle, showing changes in left atrial pressure (ALP), left ventricular pressure (VP), aortic pressure (AP), the electrocardiogram (ECG), and the phonocardiogram (PCG).

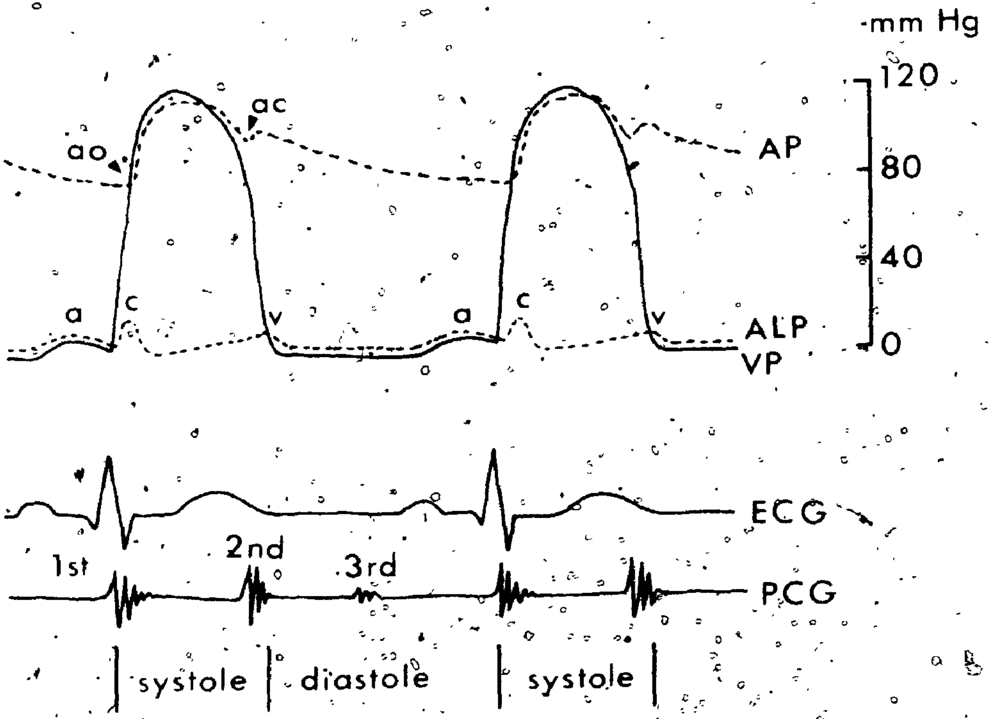
mm Hg
120
80
40
0
ao
ac
AP
a
c
v
a
c
v
ALP
VP
ECG
1st
2nd
3rd
PCG
systole
diastole
systole

the bulging of the mitral valve into the left atrium during ventricular systole, thus suggesting that the mitral tissue is readily extensible (Lakier et al, 1972).

Also, the occurrence of the first and second heart sounds at or near the instant of closure of the mitral and aortic valves (figure 1.3) has led some authors to suggest that these sounds originate from the vibrations of the atrioventricular and semilunar valves on closure. If this contention were true then the frequencies of the first and second heart sounds must be related to the overall geometry and the elastic moduli of the vibrating valve tissues. No comparison of the properties of these tissues has been made.

Yamada (1970) and Clark (1973) reported results on the static elasticity of strips of human aortic and mitral valve leaflets and chordae tendineae. Their results show qualitative similarity but are at variance quantitatively. For example, Yamada found a value of 7.0×10^{9} dynes cm^{-2} for the final elastic moduli of chordae tendineae while Clark reported a value of 3.9×10^{6} dynes cm^{-2}. Mundth et al (1971) reported pressure-volume studies of membranous samples of canine aortic and mitral valve tissues while Wright and Ng (1974) did similar studies on human aortic valve cusps.

All of these preliminary investigations dealt only with the static elastic response of the tissues. Since the cardiac valves are stretched and relaxed for about 2×10^9 times during a normal human life span, and this is done without interruption for repairs or replacements, these preliminary static studies are inadequate for describing the manner in which these tissues respond to the constant dynamic stress. Dynamic investigations would be required. It is to this end that the studies in this thesis are directed.

CHAPTER 2

HISTORICAL REVIEWS

Since the purpose of the studies in this thesis is to provide information believed to be necessary for the successful design of leaflet type valve prostheses and also to contribute to a further and better understanding of the left atrial pressure 'c' wave and the heart sounds, it is deemed proper to present a brief historical review of each of these topics. An account of previous work regarding the response of mitral and aortic valves to mechanical stress will be given.

1. ARTIFICIAL HEART VALVES

Over the last 15 years, cardiac valve replacement has been an accepted form of treatment in humans for diseased valves that are not amenable to commissurotomy or reconstruction.

Attempts at valve replacement dated back as far as 1950, and the first artificial mitral valve that permitted reasonable prolonged survival was used by Denton (1950). Since then, many different types of valve replacements have been tried in animals and later in humans. These included flap valves of various materials, ball valves, sleeve valves, leaflet type valves with "chordae tendineae", homologous aortic, heterologous aortic and autogenous pulmonary transplants (Starr and Edwards, 1961). Many of these showed poor performance and were abandoned.

Nowadays, artificial valve substitutes can be broadly classified into mechanical prostheses of either the caged-ball or low profile disc types and tissue valve substitutes. While mechanical prostheses imitate function but not form, tissue valves were proposed to imitate both.

The first practical mechanical valve was a ball in cage type used by Starr in 1960 for mitral valve replacement in dogs (Starr, 1960). This was followed soon after by its use in humans in both the aortic (Harken et al, 1960) and mitral (Starr and Edwards, 1961) positions. Since these initial attempts, many different types of mechanical prostheses have been developed. However, the major problem encountered in the use of these mechanical prostheses is the frequent occurrence of thromboembolism even with anticoagulant therapy (Kaltman 1971; Kloster, 1975). Mechanical malfunction which resulted from wear and other physical and chemical changes in the valve material and the occurrence of thrombosis of the prostheses are also major set-backs (Kaltman, 1971; Hylen, 1972; Shaw, Gunstensen, and Turner, 1974). These problems were found to be more pronounced in some disc type valves (Lee et al, 1974). In addition, other incidences of postoperative complications have also been documented. Hemolysis, usually caused by paravalvular insufficiency, is still a problem especially in the aortic position (Kaltman, 1971). Hemolysis, though controllable, can sometimes be serious as has been observed in some disc type substitutes (Roberts, Fishbein and Golden, 1975; Nitter-Hauge et al, 1974). All mechanical prostheses are mildly stenotic and show appreciable transvalvular pressure gradients (Bristow and Kremkau, 1975). Problems of sepsis, leak, dislodgement, infection and annular injuries have also been associated with mechanical prosthetic use (Kaltman, 1971; Bowes et al, 1974). More recent improvements in material and structural design have resulted in so called cloth covered prostheses which were first used in 1967. These cloth covered devices have helped reduce the incidence of thromboembolism (Bonchek and Starr, 1975) though hemolysis still occurs (Lefemine, Millar and Pinder, 1974). Hence, though advances have been made in the development of mechanical valve prostheses, the major problems of thromboembolism and mechanical malfunction have yet to be eliminated.

Whereas mechanical prostheses have been used with a certain degree of success, the desire to develop an artificial valve that will simulate much of the in vivo functioning and flow conditions, led to experiments with leaflet type tissue valve substitutes. Valves fashioned from biological tissues such as fascia lata and pericardium were tried. Aortic homografts, aortic heterografts and autologous pulmonary valve grafts were also used.

The use of fascia lata in the construction of a valve substitute was prompted by the initial work of McArthur (1901), and Gallie (1948) who demonstrated histologically that autologous fascia transplants resemble normal fascia even several years after transplantation. Senning (1967) began the use of unsupported autologous fascia lata in aortic valve replacements in 1967 and subsequently others have experimented with either mounted or unsupported grafts fashioned from fascia lata in the mitral, aortic and tricuspid areas (Ionescu and Ross,1969; Joseph et al, 1974; Petch et al, 1974). The immediate results of the fascia valve substitute were good and incidences of thromboembolism were low even in the absence of anticoagulant therapy. However, long term follow up studies have demonstrated a high rate of valve failure resulting from the thickening and stiffening of the valve cusps. This is especially so in the posterior cusp of the mitral position (Petch et al, 1974; Ross and Johnson, 1974). More recent reports on the viability of autologous fascia lata valves after use have indicated that tissue changes do occur and this could result in valve failure (Lincoln et al, 1971; Silver and Trimble, 1972).

The clinical application of aortic valve homografts was initiated by Ross (1962) and Barratt-Boyes (1964) in the early nineteen sixties in the subcoronary position after Murray (1956) demonstrated the long term function of the aortic homograft in the descending thoracic aorta of dogs. Since these early attempts, surgeons in different medical centres have tried using the same grafting technique with preserved and sterilised aortic valve homografts (Ross and Johnson, 1974; Wallace, 1975). Hospital mortality and incidences of thromboembolism were low and good performance was observed in the early postoperative period. However, with a longer follow up, the incidence of valve failure resulting from rupture and tearing of cusps increased. Calcification of the aortic wall was also common (Wallace, 1975). Though Kosek et al (1969) have reported the presence of viable cells five years after implantation of fresh valve grafts, there is still belief that tissue deterioration will occur and this will lead to eventual valve dysfunction, the major problem in tissue valves. Mounted aortic homografts have also been used in the mitral position and the results were equally, if not more disappointing (Ross and Johnson, 1974).

The presence of degenerative changes in aortic homografts prompted Ross in 1967 to use the patient's own pulmonary valve for replacing the diseased aortic valve. The removed pulmonary valve was replaced by an aortic homograft. The use of autologous pulmonary valve has also been tried in the mitral position (Ross, 1967). This procedure, however, has been associated with a higher operative mortality rate and, hence, is not popular. Mounted pulmonary homograft has also been tried without success in the mitral position (Ross and Johnson, 1974). The most recent tissue tried is bovine pericardium. Ionescu et al (1974) have reported reasonable initial results in a recent paper.

Hence, though tissue valve substitutes have low incidences of thromboembolism, even up to seven years postoperatively, are atraumatic to blood cells and have good hemodynamic performance, the greatest problem of eventual tissue failure is still unresolved and hence the long term fate is uncertain.

2. LEFT ATRIAL PRESSURE 'C' WAVE

It is well documented that pressure in the left atrium during a cardiac cycle is not constant but has elevations called the a, c and v waves (figure 1.3). The motion of the mitral valve has been implicated, as early as the beginning of this century, as a possible factor in the production of one of these atrial pressure elevations, the 'c' wave.

Gessel (1911) claimed that high pressure is not necessary to cause the mitral valve to bulge into the left atrium, thus implying, but without adequate substantiation, that the valve tissue is readily extensible.

Wiggers (1934) stated that the atrial pressure 'c' wave, which occurs shortly after the onset of ventricular contraction is doubtless due to the mitral valve pressing back a small volume of blood located between the leaflets during valve closure.

Later, Wynn et al (1952) suggested that the 'c' wave may be due to the inward bulging of the floor of the atrium and of the mitral valve. Since then, many have attributed the 'c' wave to the bulging of the mitral leaflets into the left atrium. Recent advocates of this concept include Nixon and Polis (1962) and Lakier et al (1970).

Lakier et al (1972) reported more recently that the magnitude of the 'c' wave increased with the size of the anterior mitral leaflet. Their conclusions were based on studies where the mitral valves of baboons were replaced by fascia lata of different sizes. This and other similar reports therefore, imply that the mitral valve tissue must be rather distensible, for they postulate the bulging of the valve into the left atrium (Guyton, 1971; Massumi et al, 1973).

In contrast to these, Rushmer, Finlayson and Nash (1956) using cinefluorographic techniques showed that the excursion of the leaflets was small and at no time did the valve edge ascend to the plane of the mitral ring. This suggests that the mitral valve cannot bulge into the left atrium as proposed by other workers.

This difference in opinion could be resolved if the extensibility of the valve leaflets and chordae tendineae under dynamic conditions is known..

3. THE FIRST AND SECOND HEART SOUNDS

The Hippocratic writings of about 400 B.C. indicated that heart sounds had been heard but they were rarely commented upon (McKusick, 1958). It was only after the "visceral lectures" of William Harvey in 1616 that references to the presence of heart sounds and murmurs were documented.

These early reports undoubtedly also brought with them numerous theories for the origin of the normal heart sounds and as many as 40 different theories have been proposed to explain the first sound. In the midst of this uncertainty and controversy, the British Medical Society, on the recommendation of the proposals of an appointed committee, established that the first sound was due to the combined vibrations of the contracting ventricles and atrioventricular valves, and possibly also the semilunars and that the second sound is entirely due to vibrations of the closing semilunar valves (Wiggers, 1915). However, this did not settle the controversy and, since then, two different views have emerged. One view, supported mostly by physiologists, deemphasizes the role of the cardiac valves in the production of the heart sounds; however, a second view, strongly backed by clinicians, contends that either valve closure or valve tension is the only cause of the first and second heart sounds.

The involvement of the valves in the production of the heart sounds was first suggested in 1832 by Rouanet in Paris. This view was supported by studies such as those of Dock (1933), Smith, Essex, and Baldes (1950), Leatham (1954) and Faber (1964). However, Wiggers (1915) provided early evidence to the contrary. MacCannon et al (1969) on the basis of cineangiographic studies and energy considerations, concluded that the energy of a vibrating mitral valve would contribute only about 10% to the total energy of the first sound. This, therefore, denied the possible sole involvement of the mitral valve and chordae tendineae in the production of the first sound. The more recent work of Luisada et al (1974) found that mitral and aortic valve closures, respectively preceded the occurrence of the first and second sounds. This was again supported by the work of Chandraratna and his colleagues (1975) in the case of the aortic valve using echocardiography. These studies therefore, lend support to the idea of Rushmer (1970) that the heart sounds are produced by the accelerations and decelerations of blood which give rise to vibrations of the heart walls and the major blood vessels.

Hence, even after more than a century of investigations there is still no universal agreement regarding the precise nature of the cause or causes of heart sounds. Most of the arguments put forward for supporting any specific cause are based on observations of the temporal relation between sound and some other cardiac events such as valve closure, chordal tensing and muscular contraction. In none of these reports were the physical properties of the structures, supposedly responsible for the sounds, studied.

4. CARDIAC VALVULAR TISSUE RESPONSE UNDER MECHANICAL STRESS

Investigations on the response to mechanical stress of cardiac valvular tissues (human or otherwise) are scarce and the first study on the elastic property of human heart valves was that reported by Yamada (1970) who, with his colleague Yoshimatsu, subjected human chordae tendineae and strips of valvular tissue to uniaxial tensile stress. The work was done in Kyoto Prefectural University of Medicine, Japan in 1958 and the results were presented in the form of stress-strain curves. However, no experimenral details and conditions of testing were reported.

Salisbury, Cross and Rieben (1963) later measured the in situ tension sustained by chordae tendineae during the cardiac cycle, by attaching force transducers to the chordae tendineae of the mitral anterior leaflet in mongrel dogs. This study also investigated changes in the chordal tension with changes in stroke volume, elastic storage capacity of the arterial tree and also changes in coronary artery pressure. The effect on chordal tension with and without a pericardial sac was also studied.

In an effort to characterise the elastic properties of the valve leaflets, Mundth et al (1971) reported pressure-volume studies of canine aortic and mitral valve tissues. Membranous samples instead of strips were used in this investigation.

A theoretical approach to the problem of human mitral tissue response under stress was done by Ghista and Rao (1972). They developed, by quasi-static stress analysis, a relation between stress, Young's modulus, loading pressure and valve dimensions. Using the same technique and in combination with vibration analysis a second relation between Young's modulus loading pressure, valve dimension and the frequency of the first component of the first heart sound was found. In the analysis, the mitral leaflet was assumed to be a semi-disc fixed at the curved edge by the annulus and the straight edge by the chordae.

The next attempt at characterising valvular tissue elastic response was the study of Clark (1973). Tensile tests on fresh and frozen human chordae tendineae and mitral and aortic valve strips were performed. Though stretch rate was constant in his experiments, the initial specimen length during test was quite variable. This will, of course, lead to strain rates that are different in different experiments. This study, though similar to that reported by Yamada, yielded results that were vastly different quantitatively.

Further studies on the response of cardiac valvular tissues to stress were reported by Swanson and Clark (1974). They studied the dimensions and geometric relationships of human aortic valves, as a function of pressure, from silicon rubber valve casts. They found that the axial length of the aortic cusp varied negligibly with pressure (0-120 mm Hg) but that geometry and angular dimensions varied significantly. Studies of this nature are not new; similar preliminary investigations on porcine aortic valves have been done by Wood, Robel and Sauvage (1963), while Mercer, Benedicty and Bahnson (1973) have reported studies on the human aortic root.

The most recent attempt at characterising the mechanical response of valve leaflets was a study by Wright and Ng (1974). Pressure-volume studies similar to the approach of Mundth et al (1971) were performed on human aortic valve cusps. The data were presented in the form of volume of liquid required to increase pressure by a certain amount. Therefore, the smaller the volume the stiffer the valve material. Such a presentation makes data comparison difficult.

Thus, although preliminary attempts at characterising cardiac valve tissue under mechanical stress have been carried out, some of the results are contradictory. In addition, none of these studies has investigated the dynamic response which is surely of greater interest since the valves are under constant dynamic stress in the in vivo state.

CHAPTER 3

UNIAXIAL TENSILE TESTS ON CHORDAE TENDINEAE

1. INTRODUCTION

Since it is possible that chordae tendineae in vivo can be strained at different rates under normal and pathological conditions, this study investigates the elastic response and tensile strength of normal human mitral valve chordae tendineae at varying straining conditions.

2. METHOD

The elastic response and breaking strength of normal human mitral valve chordae tendineae at different strain rates were obtained by applying an uniaxial tensile stress on the chordae. This was achieved by using an Instron Floor Model Tensile Testing Machine (Model TT-C). A load cell C was used. Basically, the Instron consists of a fixed crosshead and a movable crosshead with jaws facing each other for holding the sample. Strain gages at the fixed crosshead measured the load applied to the sample and the motion of the movable crosshead, operated by a servodrive, stretched the specimen uniaxially. The amount of stretch and the force applied were measured simultaneously and continuously on a chart recorder (see figure 3.1).

Figure 3.1. Diagram of the apparatus (the Instron) used for tensile tests on chordae tendineae.

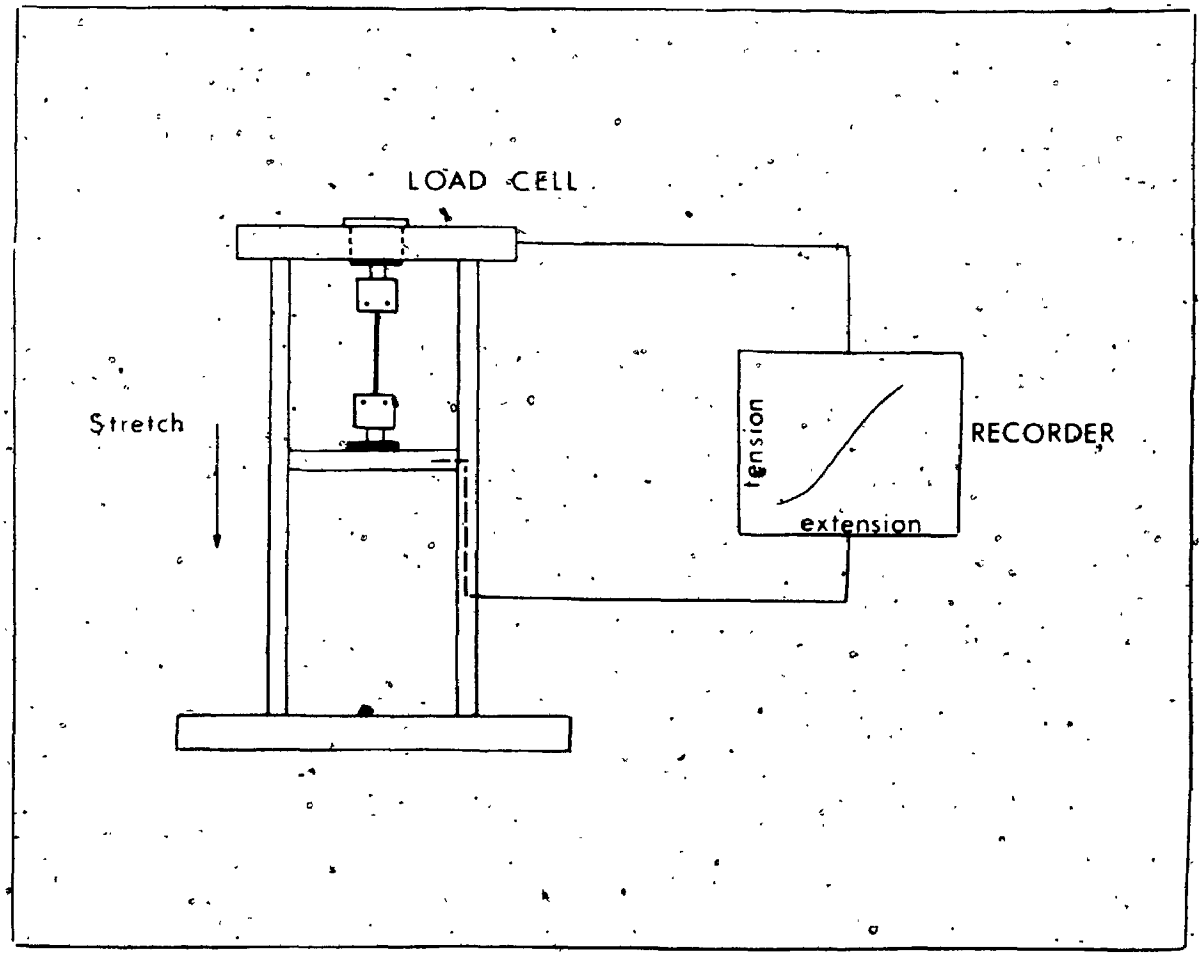
LOAD CELL
Stretch
tension
extension
RECORDER

Preliminary tests showed that tissues cannot be mounted directly between the jaws of the Instron, as the jaws, exerting a pressure of 6.2×10^6 dynes cm^{-2}, damaged the tissue, thus weakening the tissue at the junction of the jaws. Hence, a different clamping device had to be used. Various clamps were designed and tested and I found that clamps with parallel plates having two small pieces of sandpaper (silicon carbide No. 600) facing each other and sandwiched between the plates worked well (figure 3.2). The new clamps held the tissues firmly without crushing them. In tensile testing experiments, specimen slippage from clamps holding them can be a real problem. Hence, the new clamps underwent tests to ensure that slippage did not occur. To do this, several chordae were mounted on the clamps and the exposed tissue stained with black Indian ink. The chordae then underwent uniaxial strain. If slippage did occur unstained tissue would appear at the junctions of the clamps, but no unstained tissue was observed in such tests. To show that staining the exposed tissue did not cause seepage of stains into the clamped tissue, which would invalidate the slippage test, several fresh chordae were again mounted on the clamps and the exposed tissue stained. Without straining the chordae, the clamps were released and a straight clear boundary between the stained and unstained tissue was observed at the junction of the clamps.

Figure 3.2. A parallel plate clamp showing how the specimen was mounted.

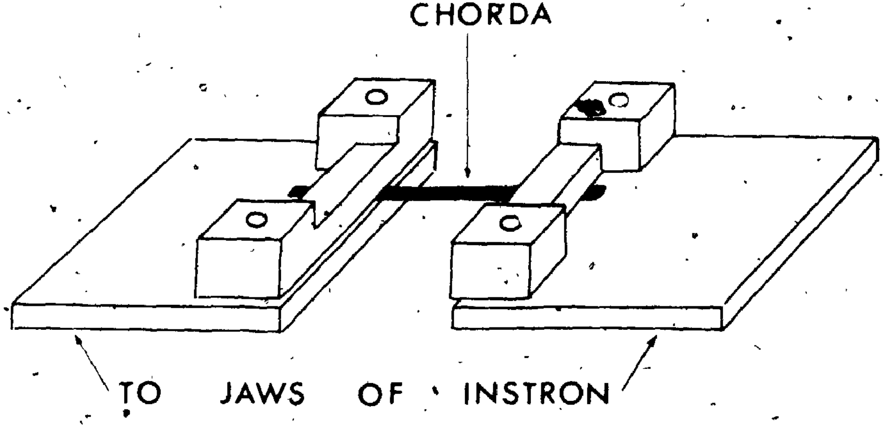
CHORDA
TO JAWS OF INSTRON

The new clamps were then attached to the jaws of the Instron and used in all subsequent experiments. Two hundred chordae, obtained from 20 human mitral valves (13 male, 7 female, ages 5 to 66) at autopsy, were assigned at random to be tested at 5 different strain rates, ranging from 0.05 cm min^{-1} (6.25% min^{-1}) to 12.7 cm min^{-1} (1600% min^{-1}). Due to technical limitations, experiments at high strain rates could not be performed. Valves from patients who had no clinical record of mitral valve disease and which appeared normal at autopsy were selected. The valves were removed not more than 12 hours after death and kept in 0.01% merthiolate solution at a temperature of 6°C until testing. This anti-bacterial solution preserved the mechanical properties of collagen and elastin (Roach and Burton, 1957). The mean cross-sectional area of each chorda was obtained by taking measurements at several places along the chorda with a travelling microscope.

All samples were tested at a room temperature of 21 ± 1°C from 1 to 7 days after removal from the heart and no significant difference in the response curves were observed over this time period (Figure 3.3). The tissue was kept moist throughout the experiment. All chordae samples were mounted with an initial length of 0.8 cm and care was taken to ensure that they were mounted vertically between the jaws of the Instron before an uniaxial tensile stress was applied until tissue rupture occurred. Hence,

Figure 3.3. Stress-strain responses before the proportional limit, of chordae tendineae preserved for 2 and 6 days in 0.01% merthiolate solution. Each curve is an average of the responses of 3 chordae from 3 different mitral valves. SR = strain rate. AREA = cross-sectional area of chordae.

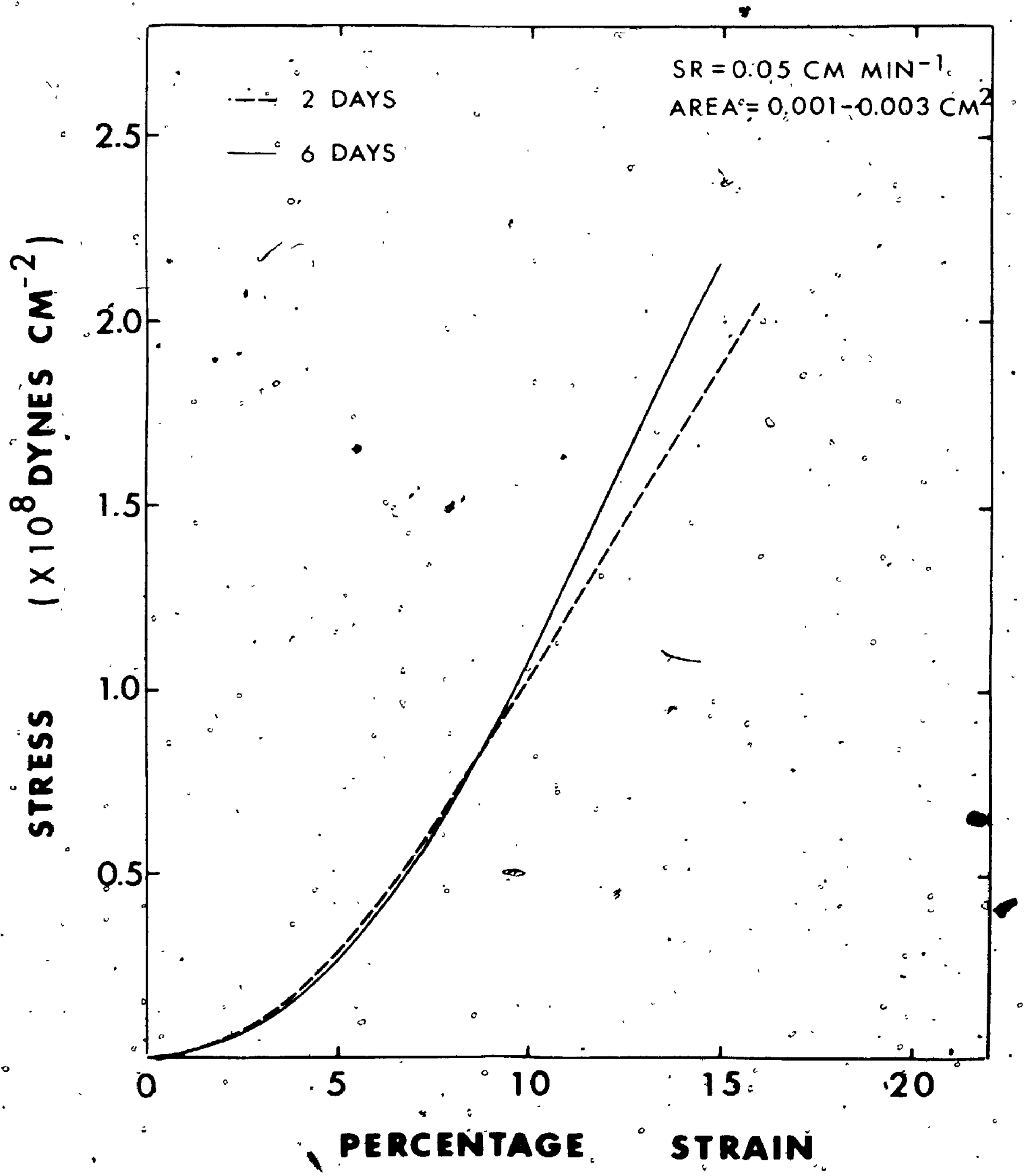
2 DAYS
6 DAYS
SR = 0.05 CM MIN^{-1}
AREA = 0.001-0.003 CM^2
STRESS (X 10^8 DYNES CM^{-2})
2.5
2.0
1.5
1.0
0.5
0
5
10
15
20
PERCENTAGE STRAIN

only one test was performed on each chordae. The tension-time traces were recorded continuously by a chart recorder with speeds that provided a suitable resolution of the different straining conditions. From a knowledge of the initial cross-sectional area and the strain rate, stress-strain diagrams, the secant and final elastic moduli and breaking stress and strain could be obtained from these continuous tension-time records.

3. RESULTS

Figure 3.4 shows an actual typical non-linear stress-strain response of a chordae tendineae under uniaxial tensile stress. The chordae initially responded by developing a low resistance to stretch as indicated by the smaller gradient of the initial segment of the stress-strain curve (A to B). At strains beyond B a greater resistance to stretch developed, as indicated by the steeper gradient of the curve (B to D). Beyond point C the stress-strain curve became linear but on straining the chordae beyond the proportional limit (D), the curve once again became non-linear and the slope of the curve decreased. This behaviour, which persisted until rupture occurred at point E, could either be an indication of plastic deformation and/or the result of a decrease in the cross-sectional area of the chordae at high strain values. Since the stress calculations were based on the initial cross-sectional area, a significant

Figure 3.4. An actual typical continuous stress-strain record of the mechanical response of chordae tendineae.

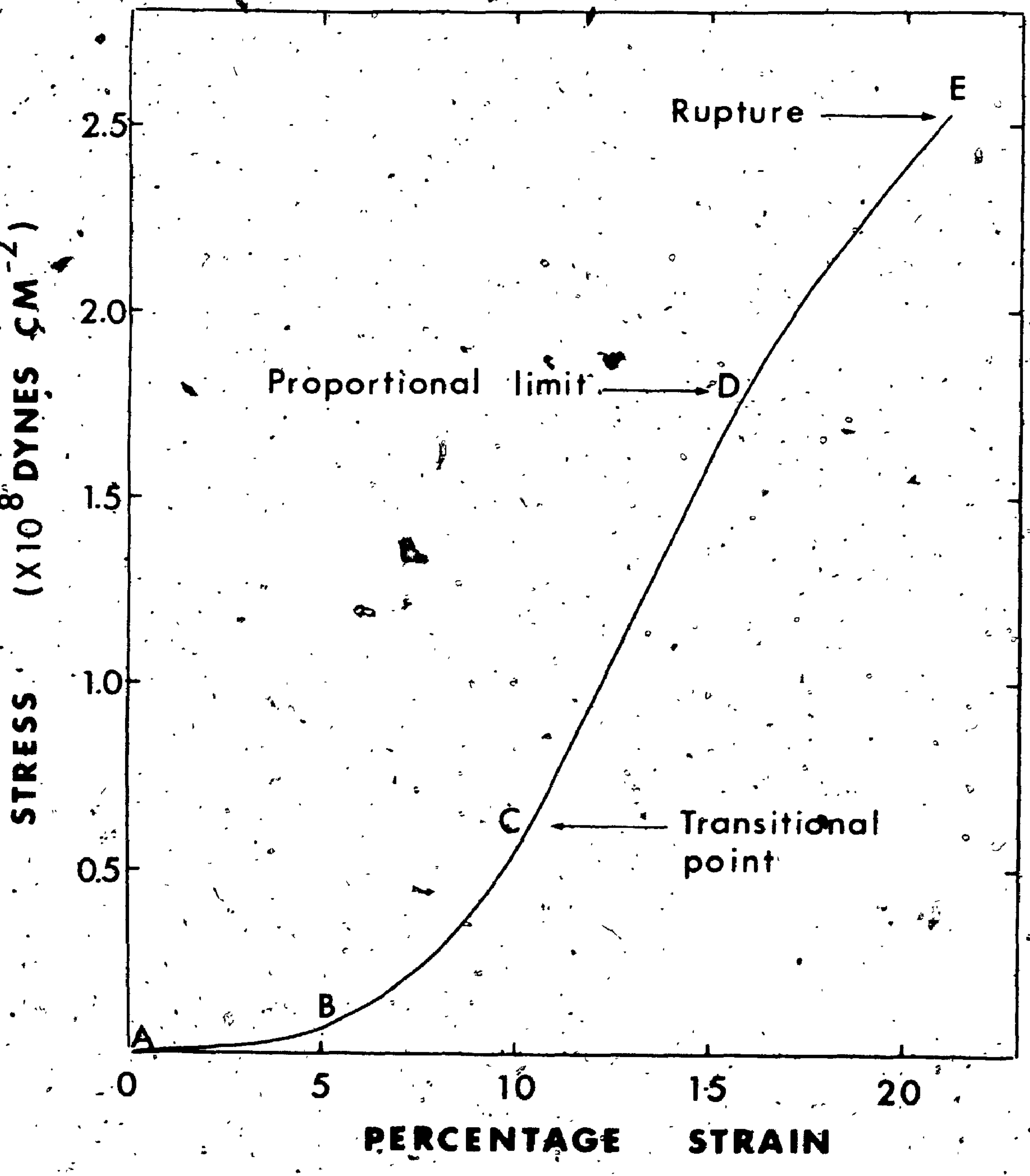
STRESS (X10^8 DYNES CM^{-2})
2.5
2.0
1.5
1.0
0.5
0
5
10
15
20
PERCENTAGE STRAIN
A
B
C
D
E
Rupture
Proportional limit
Transitional point

decrease of this value at high strains would, therefore, give an underestimate of the true stress in this part of the curve. Point C where the linearity of the curve began will, henceforth be called the transitional point.

This non-linear stress-strain response, so typical of biological tissues had also been observed for chordae by Yamada (1970) and Clark (1973). In addition, we found that at higher strain rates and for chordae of smaller cross-sectional area, the proportional limit was reached at lower strain values.

The results shown in Figure 3.5 and 3.6 and Tables 3-I, 3-II, and 3-III were for chordae from the 21-66 age group. Figures 3.5(a) to 3.5 (d) show the elastic response, before reaching the proportional limit, of different sized chordae under 4 different straining conditions. It was observed that the large chordae were initially more extensible than the smaller ones and this behaviour was true for all the different strain rates tested. Figures 3.6(a) to 3.6(c) compare similar elastic response at different strain rates for chordae of approximately the same size. In all cases, they showed that the chordae were more extensible initially at lower rates of strain but became stiffer as strain rates increased.

Since the initial segment of the response curves was non-linear, the response in this segment of the curves cannot be characterized by a single modulus. The nature of

Figure 3.5(a). This and Figures 3.5(b) to 3.5(d) show continuous stress-strain records of different sized chordae under 4 different strain rates (SR). The traces show the response before the proportional limit is reached. The lower case letters after each continuous curve indicate the chordae size. The cross-sectional areas in the groups are: (a) 0.001 to 0.003 cm^2, (b) 0.004 to 0.006 cm^2, (c) 0.006 to 0.008 cm^2, (d) 0.01 to 0.03 cm^2. The broken lines show the standard error. The sample size for each of the curves in this and Figures 3.5(b) to 3.6(c) ranges from 5 to 8 specimens. Similar sample sizes also apply to the entries in Tables 3-I to 3-III.

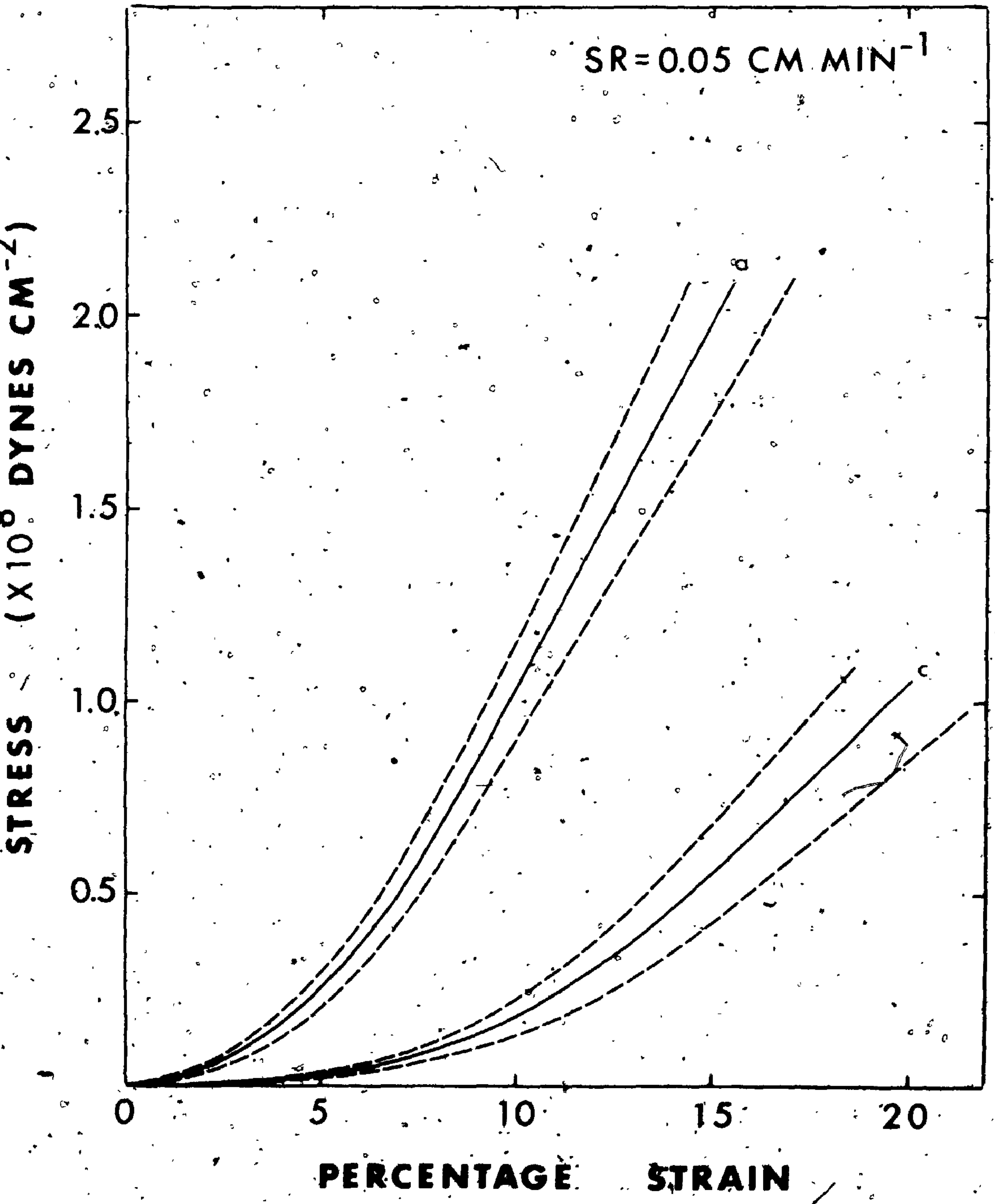
SR=0.05 CM MIN^{-1}
STRESS (X10^{8} DYNES CM^{-2})
2.5
2.0
1.5
1.0
0.5
0
5
10
15
20
a
c
PERCENTAGE STRAIN

Figure 3.5(b) SR = strain rate = 0.13 cm min^{-1}. chordal size: (a) 0.001 to 0.003 cm^2, (b) 0.004 to 0.006 cm^2.

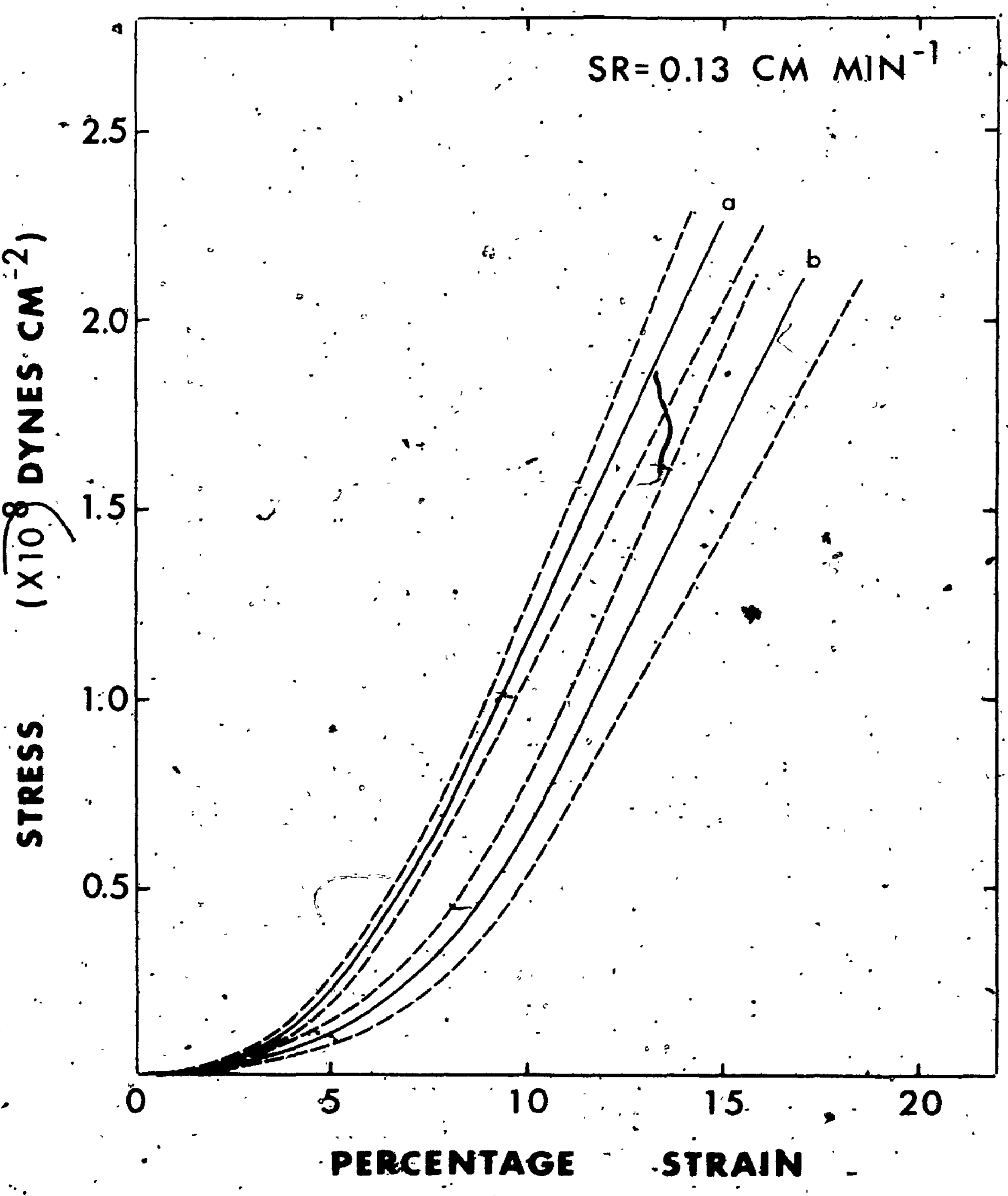
SR= 0.13 CM MIN^{-1}
a
b
STRESS (X10^{8} DYNES CM^{-2})
0.5
1.0
1.5
2.0
2.5
0
5
10
15
20
PERCENTAGE STRAIN

Figure 3.5(c). SR = strain rate = 5.08 cm min^{-1}, chordal size (a) 0.001 to 0.003 cm^2, (c) 0.006 to 0.008 cm^2

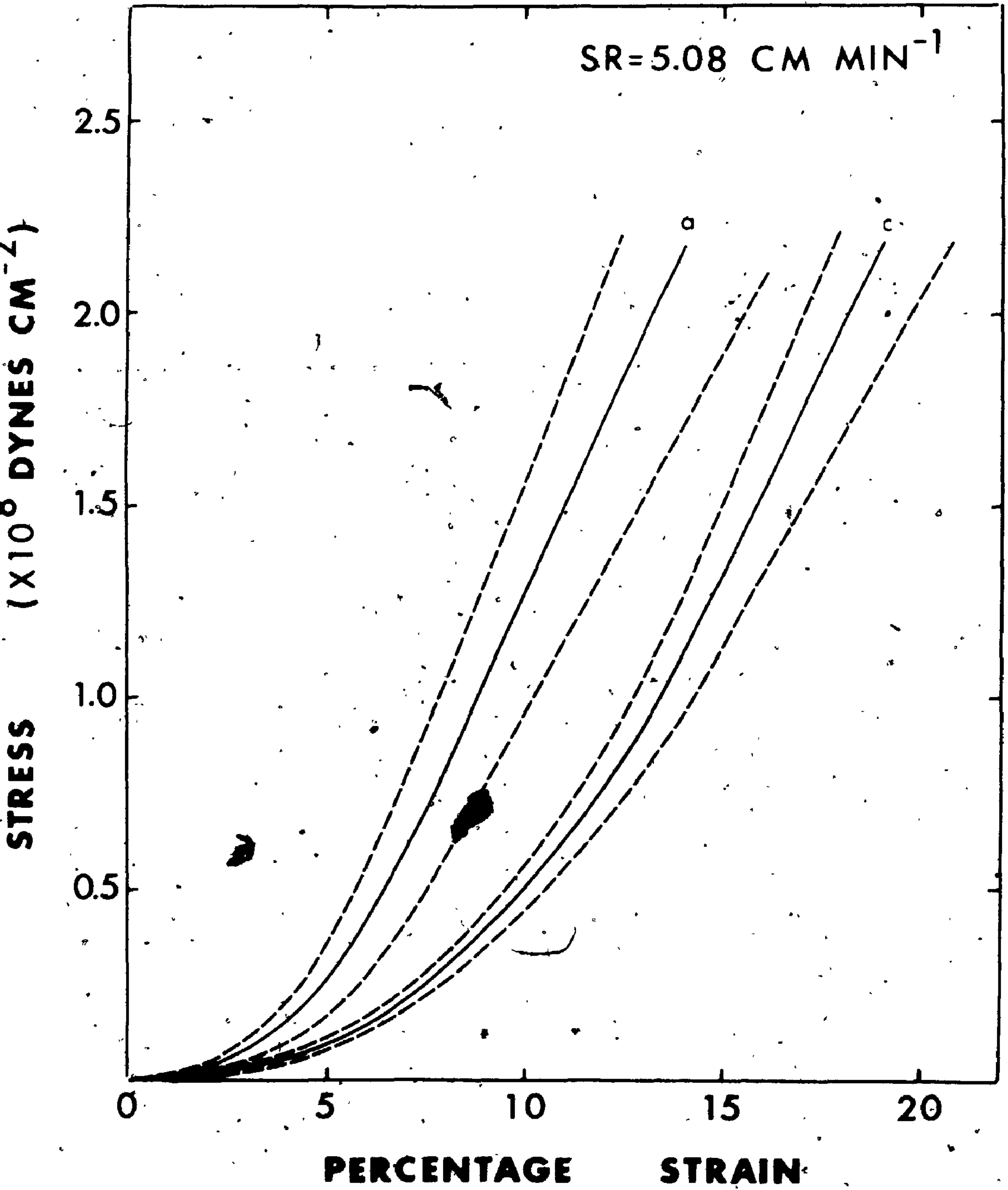
SR=5.08 CM MIN^{-1}
a
c
2.5
2.0
1.5
1.0
0.5
0
5
10
15
20
STRESS (X10^8 DYNES CM^{-2})
PERCENTAGE STRAIN

Figure 3.5(d). SR = strain rate = 12.7 cm min^{-1} chordal size: (a) 0.001 to 0.003 cm^2, (b) 0.004 to 0.006 cm^2, (d) 0.01 to 0.03 cm^2

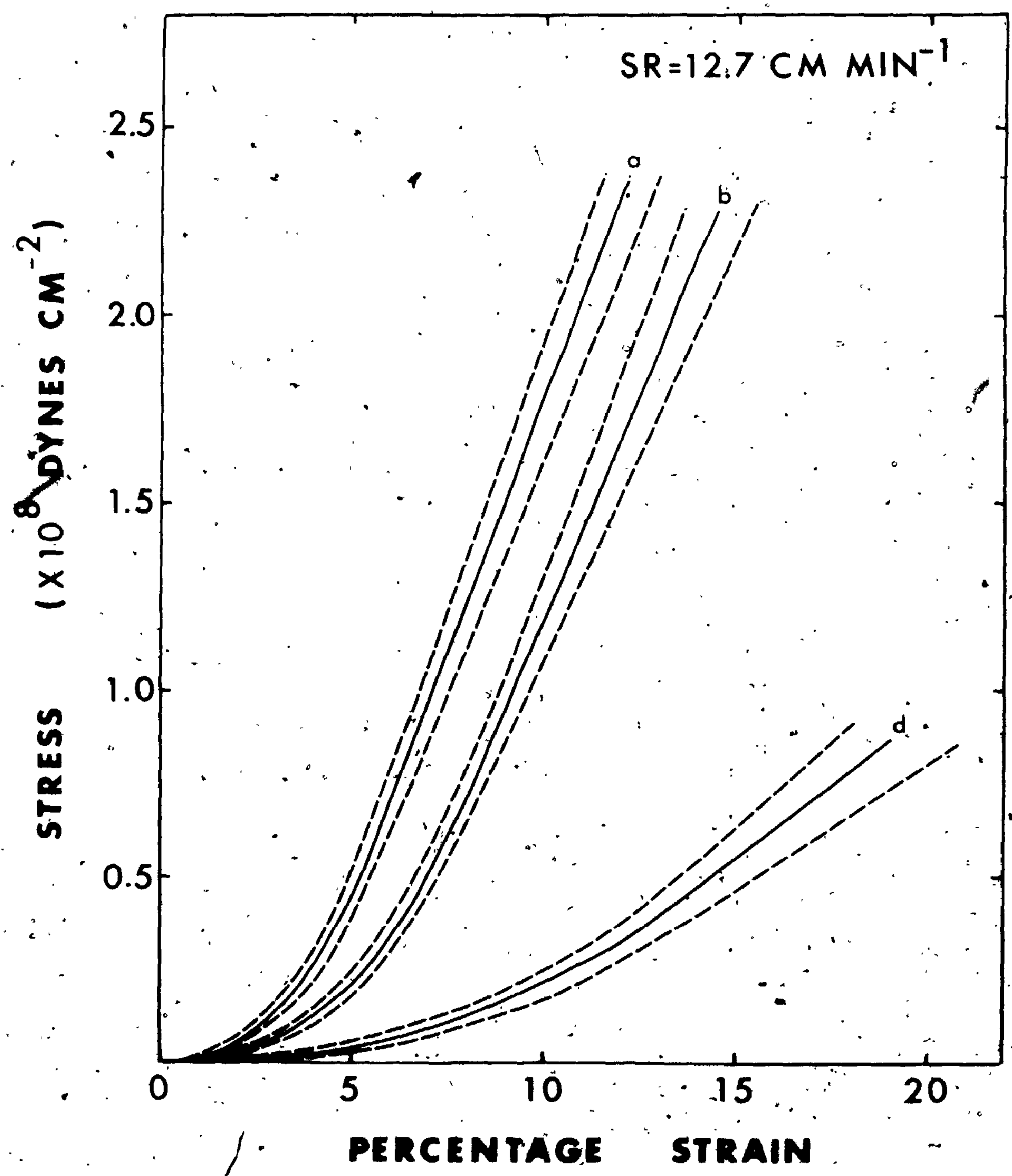
SR=12.7 CM MIN^{-1}
a
b
d
STRESS (X10^8 DYNES CM^{-2})
2.5
2.0
1.5
1.0
0.5
0
5
10
15
20
PERCENTAGE STRAIN

Figure 3.6(a). This and Figures 3.6(b) and 3.6(c) show the variation of stress-strain response, before the proportional limit, with strain rates for 3 groups of chordae of different cross-sectional area (AREA). The numbers after the continuous curve indicate strain rate values in cm min^{-1}. The broken lines show the standard error.

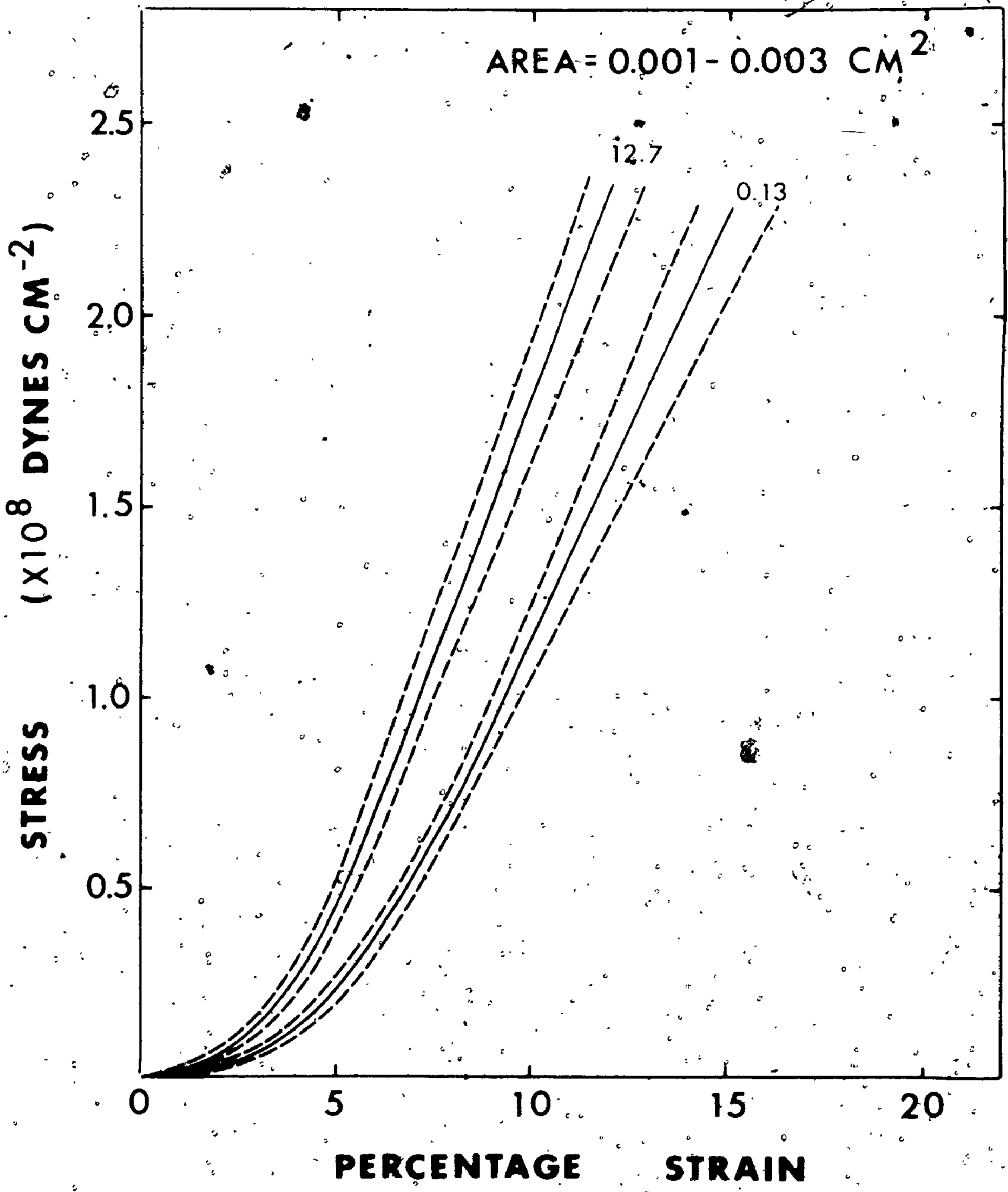
AREA = 0.001 - 0.003 CM^2
12.7
0.13
STRESS (X10^8 DYNES CM^{-2})
2.5
2.0
1.5
1.0
0.5
0
5
10
15
20
PERCENTAGE STRAIN

Figure 3.6(b). AREA = chordal cross-sectional area. Strain rates are 5.08 cm min^{-1} and 0.05 cm min^{-1}.

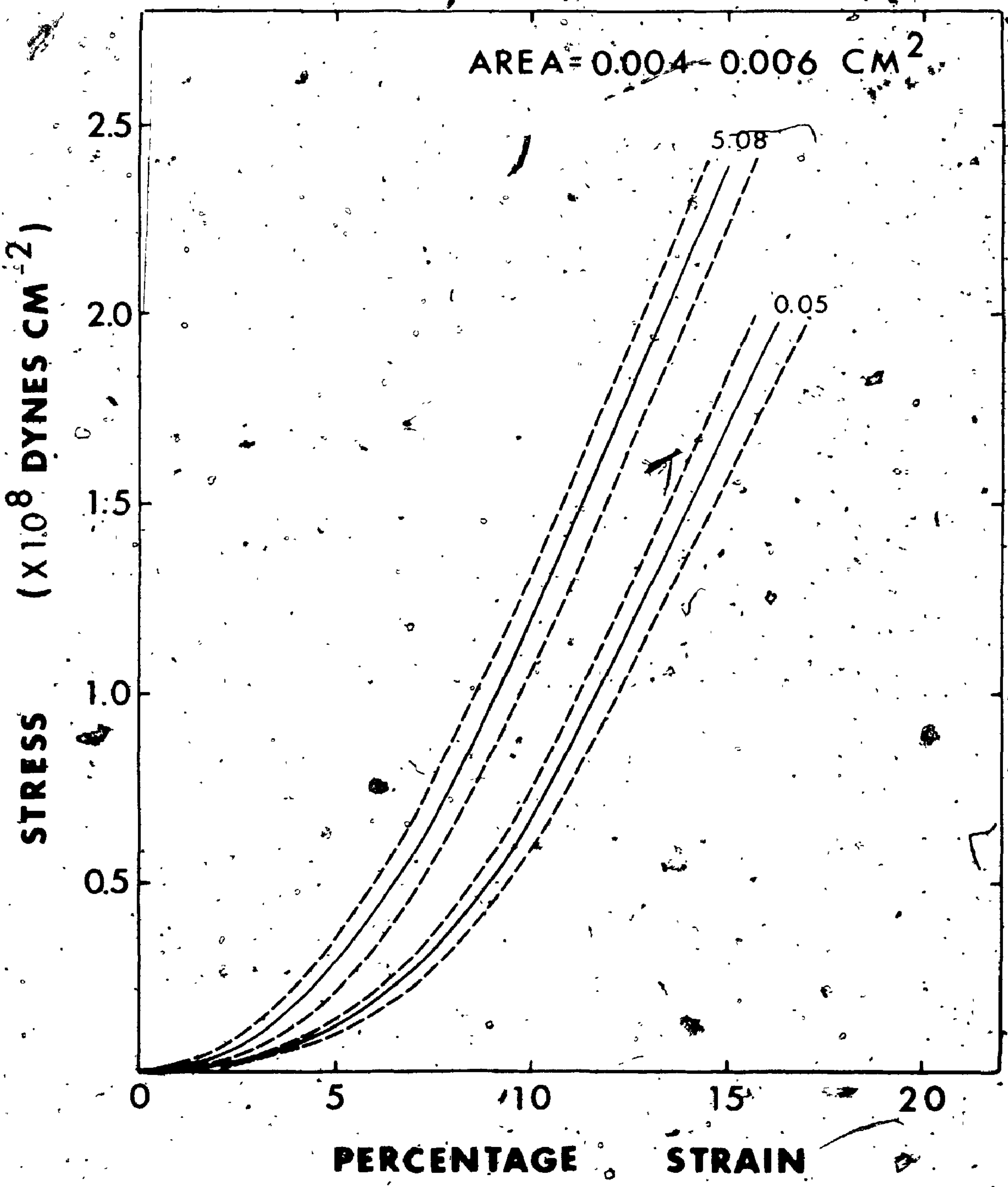
AREA = 0.004 - 0.006 CM^2
5.08
0.05
STRESS (X10^8 DYNES CM^{-2})
2.5
2.0
1.5
1.0
0.5
0
5
10
15
20
PERCENTAGE STRAIN

Figure 3.6(c). AREA = chordal cross-sectional area. Strain rates are 5.08 cm min^{-1} and 0.05 cm min^{-1}.

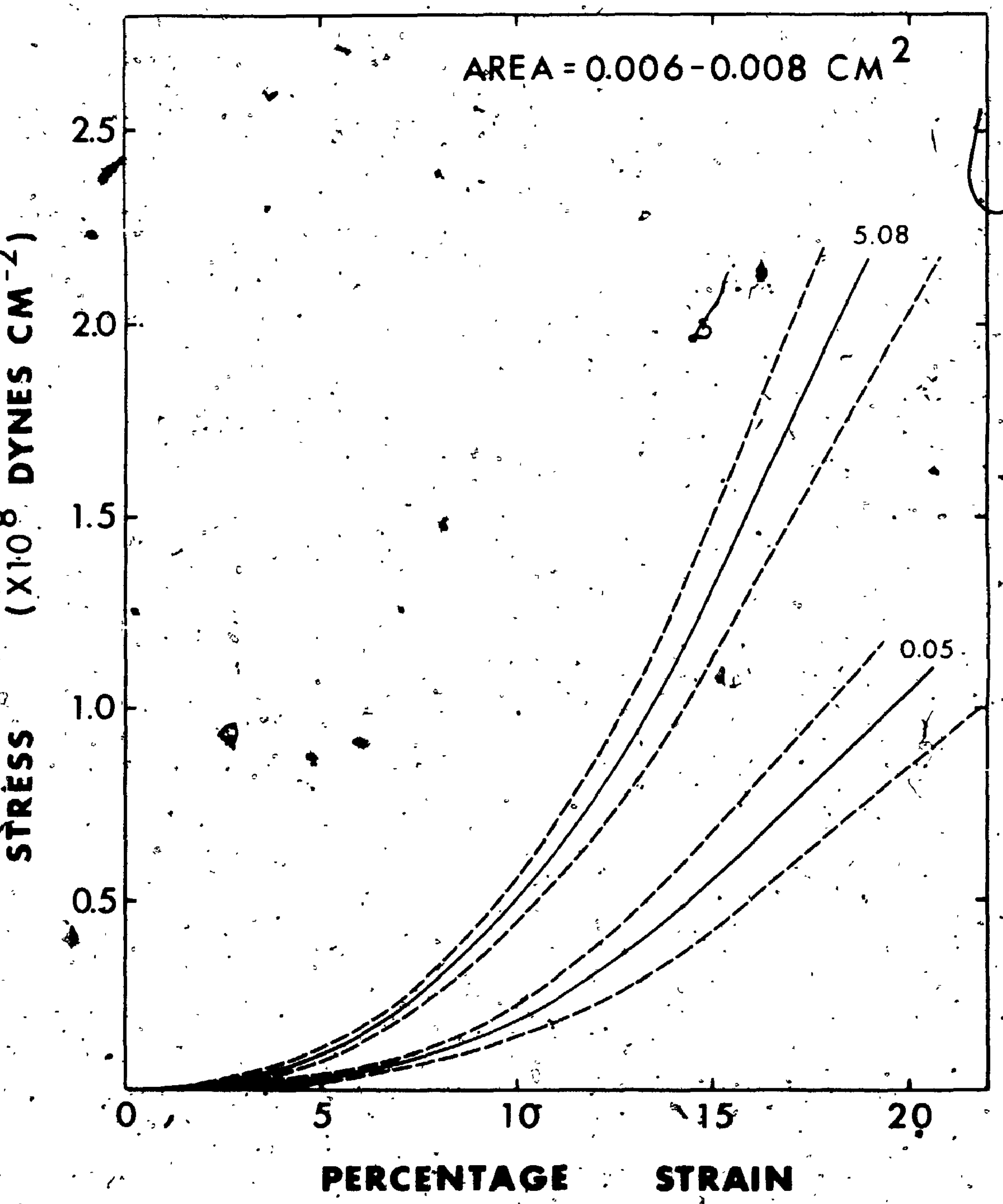
AREA = 0.006-0.008 CM^2
5.08
0.05
STRESS (X10^8 DYNES CM^{-2})
2.5
2.0
1.5
1.0
0.5
0
5
10
15
20
PERCENTAGE STRAIN

the curves was such that even a modulus at the origin was difficult to ascertain. Hence a secant modulus defined as the gradient of the straight line joining the origin to the point of transition was obtained. The secant modulus would give us a qualitative measure of the extent of the initial non-linear behaviour.

Tables 3-I and 3-II give the values of the strain and stress at the point of transition and the secant and final moduli before reaching the proportional limit. A simple statistical analysis of variance (Campbell, 1967). employed to test the significance, at the 5% level, of the variations of the final modulus with size and strain rates, showed that this modulus was independent of strain rates while it varied significantly with size. For smaller chordae, of cross-sectional area 0.001 cm^2 to 0.006 cm^2, the final modulus had a value of about 2×10^9 dynes cm^{-2} while for the larger chordae, the value was about 1×10^9 dynes cm^{-2}.

Since the uncertainty involved in the determination of the point of transition was great, the variations of the transitional strain and stress and the secant modulus with size and strain rate, could at best give a rough estimate of the extent of the initial portion of each response curve. In order to test any significant difference in the initial portion of the response curves in Figures 3.5 and 3.6. stress values for widely different sizes and

TABLE 3-I

Strain and stress values at the point of transition for different sized chordae tendineae strained at 5 different strain rates.

TABLE 3-I

Percentage Strain at Transition ± Standard Error

Strain rate (cm min^{-1})	Cross-sectional area (cm^2)			
	0.001 to 0.003	0.004 to 0.006	0.006 to 0.008	0.01 to 0.03
0.05	8.0±0.5	11.1±0.5	14.9±1.4	
0.13	8.4±0.3	10.4±0.7	10.0±1.9	
1.27		8.7±0.6	11.9±2.2	
5.08	7.9±1.0	10.0±0.7	14.3±0.8	
12.70	6.2±0.4	8.3±0.4		13.9±1.0

Stress at Transition ± Standard Error

($\times 10^7$ Dynes cm^{-2})

Strain rate (cm min^{-1})	Cross-sectional area (cm^2)			
	0.001 to 0.003	0.004 to 0.006	0.006 to 0.008	0.01 to 0.03
0.05	6.8±0.9	8.8±1.0	5.4±1.3	
0.13	8.0±0.6	7.2±1.4	5.4±1.6	
1.27		8.2±1.2	8.0±2.6	
5.08	7.8±2.2	12.0±1.3	11.6±1.6	
12.70	7.4±0.8	7.8±0.8		4.6±0.7

TABLE 3-II

The secant and final elastic moduli of the stress-strain curves of different sized chordae tendineae strained at different strain rates.

TABLE 3-II

Secant Modulus ± Standard Error (x 10^8 Dynes cm^{-2})

Strain rate (cm min^{-1})	Cross-sectional Area (cm^2)			
	0.001 to 0.003	0.004 to 0.006	0.006 to 0.008	0.01 to 0.03
0.05	8.29±1.10	7.93±0.90	3.62±0.87	
0.13	9.52±0.71	6.92±1.34	5.40±1.60	
1.27		9.43±1.38	6.72±2.19	
5.08	9.87±2.87	12.0 ±1.30	8.11±1.12	
12.70	11.94±1.29	9.40±0.96		3.31±0.50

Final Modulus ± Standard Error (x 10^9 Dynes cm^{-2})

Strain rate (cm min^{-1})	Cross-sectional Area (cm^2)			
	0.001 to 0.003	0.004 to 0.006	0.006 to 0.008	0.01 to 0.03
0.05	1.91±0.21	2.15±0.10	1.00±0.15	
0.13	2.21±0.24	2.10±0.25	1.05±0.10	
1.27		2.21±0.14	1.30±0.75	
5.08	2.29±0.50	2.41±0.04	2.15±0.30	
12.70	2.73±0.18	2.44±0.24		0.80±0.14

strain rates, at an arbitrarily chosen strain of 5% (a value below the tabulated transitional strains) are tabulated in Table 3-III for this purpose. Any significant difference between the stress values at this strain would, therefore, show a significant shift of the response curve. The probability (P) values from a two sample t-test (Campbell, 1967) at the bottom of each column of Table 3-III, show that the difference of the two stress values above them in the same column were statistically significant at the 1% level, thus indicating that the shift of the response curve towards the stress axis with increasing strain rate and decreasing size was statistically significant.

Figures 3.7(a) and 3.7(b) compare the elastic responses of chordae from a 17-year-old and a 5-year-old with the 21-66 age group. In both of these relatively young cases, the chordae again exhibited greater extensibility at lower strain rates. Though the results were from single cases, the response curves showed quite clearly that for similar sized chordae, the chordae became less extensible with age. However, within the age group of 21-66 years, no significant variation of extensibility with age was observed.

Table-IV shows the strains and stresses at rupture. The breaking strains for chordae with cross-sectional area

TABLE 3-XVI

Stress values at 5% strain. These values are tabulated to show that the stress-strain curves are dependent on chordal size and strain rate.

TABLE 3-III

Stress Values at 5% strain ± SE (x 10^7 Dynes cm^{-2})

CROSS-SECTIONAL AREA (cm^2)	STRAIN RATE ($cm\ min^{-1}$)		
	0.05	12.7	12.7
0.001 to 0.003	2.33 ± 0.36	4.55 ± 0.55	
0.004 to 0.006		2.08 ± 0.33	2.08 ± 0.33
0.006 to 0.008	0.26 ± 0.07		
0.01 to 0.03			0.45 ± 0.16
P - value by t-test	<0.01	<0.01	<0.01

STRAIN RATE ($cm\ min^{-1}$)	CROSS-SECTIONAL AREA (cm^2)	
	0.001 to 0.003	0.006 to 0.008
0.05		0.26 ± 0.07
0.13	2.46 ± 0.20	
5.08		0.95 ± 0.17
12.7	4.55 ± 0.55	
P - value by t-test	<0.01	<0.01

Figure 3.7(a). This and Figure 3.7(b) show the stress-strain response of approximately similar sized chordae for different ages. The numbers after each curve give the strain rate values in cm $\min^{-1}$. The traces show the response before reaching the proportional limit.

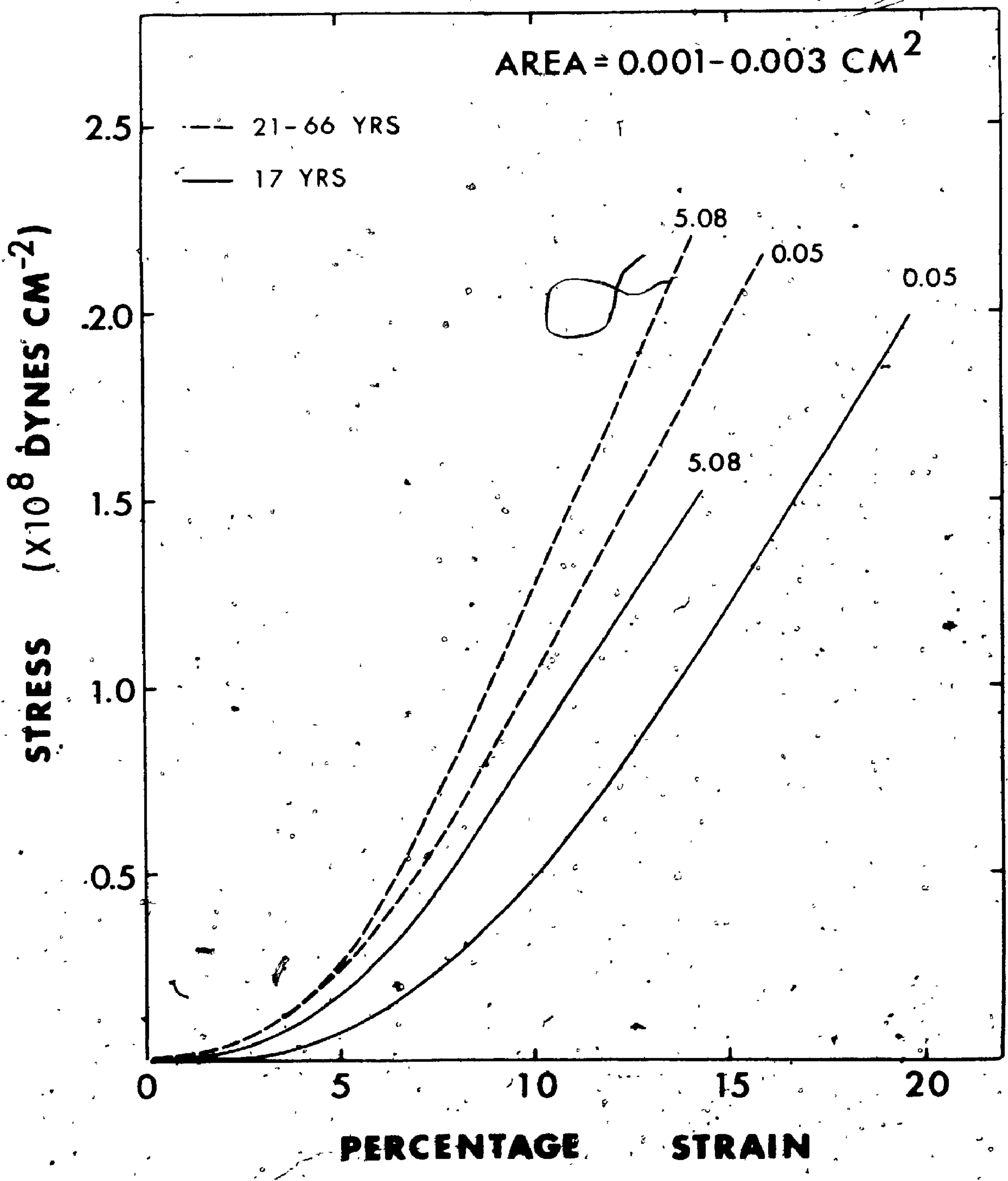
AREA = 0.001-0.003 CM^2
21-66 YRS
17 YRS
5.08
0.05
0.05
5.08
STRESS (X10^8 DYNES CM^{-2})
2.5
2.0
1.5
1.0
0.5
0
5
10
15
20
PERCENTAGE STRAIN

Figure 3.7(b). AREA = chordal cross-sectional area. Strain rates shown after each curve are in cm $\min^{-1}$.

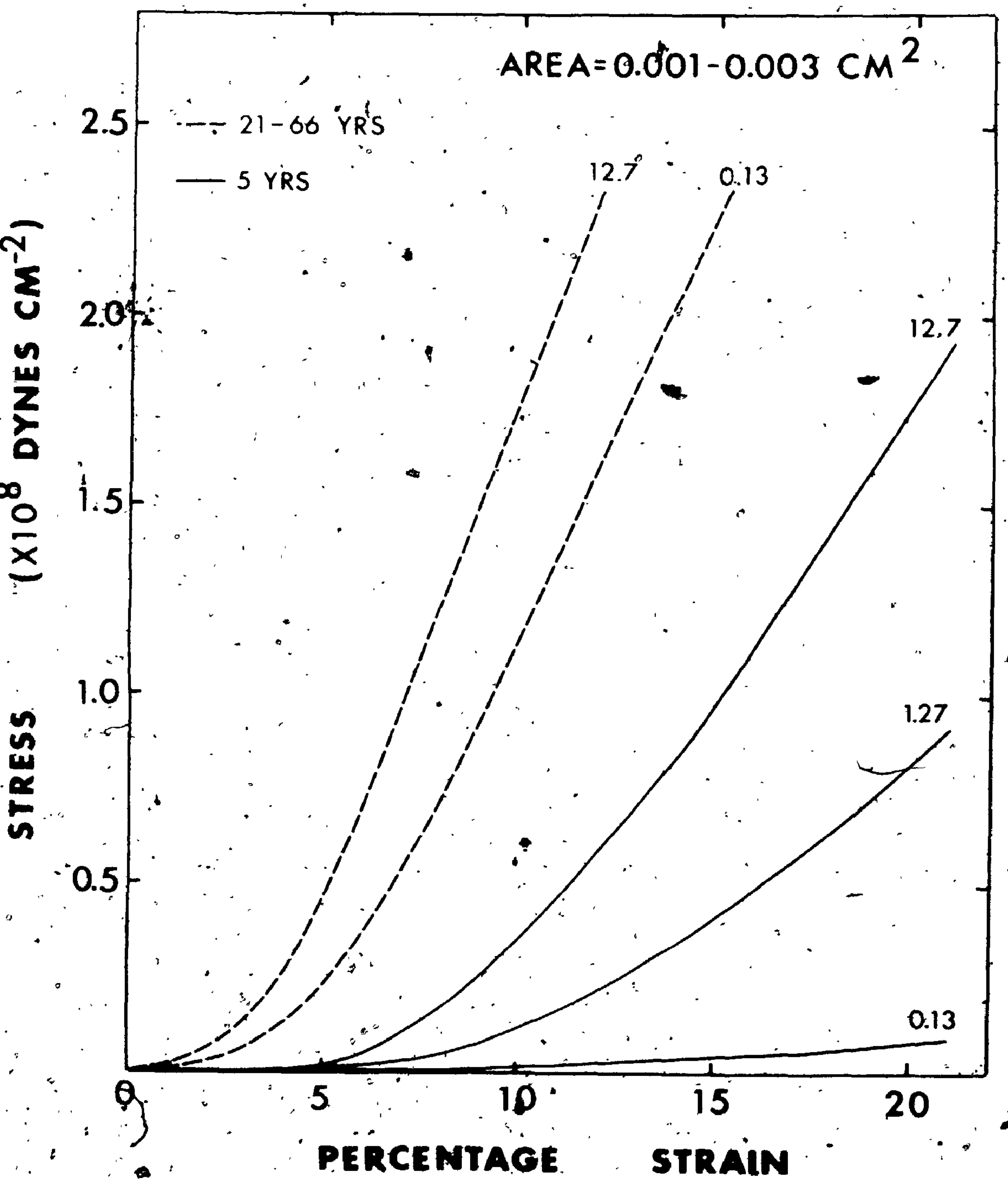
AREA=0.001-0.003 CM^2
21-66 YRS
5 YRS
12.7
0.13
12.7
1.27
0.13
2.5
2.0
1.5
1.0
0.5
STRESS (X10^8 DYNES CM^{-2})
0
5
10
15
20
PERCENTAGE STRAIN

TABLE 3-IV

Values of breaking strain as a function of strain rate and breaking stress as a function of chordal size. Though breaking strain appears to decrease with an increase in strain rate, the variation was found to be statistically insignificant. The breaking stress, however, decreased with an increase in chordal size.

TABLE 3-IV

Strain rate (cm min^{-1})	Sample Size	Breaking strain (in % ± SE)
0.05	15	22.97±0.93
0.13	13	22.16±0.76
1.27	14	21.83±0.62
5.08	13	21.07±0.78
12.70	13	20.31±0.71

CHORDAL CROSS-SECTIONAL AREA (cm^2)		Breaking stress (x 10^8 dynes cm^{-2} ± SE)
0.001-0.003	29	3.65±0.26
0.004-0.005	13	3.51±0.13
0.005-0.006	9	2.89±0.25
0.006-0.007	6	2.77±0.41
0.007-0.008	9	2.63±0.33
0.01 -0.03	5	1.30±0.35

0.001 to 0.008 cm^2 (ages 21-66 yrs) were found to be independent of chordal size and strain rate ($P > 0.05$) though there appeared to be a slight decrease with increase in strain rate. An average value of 21.4 (SE = 0.5) % was found. The breaking stress, however, decreased significantly with increase in chordal size ($P < 0.01$) but was found to be independent of strain rate.

Toughness, defined as energy required to rupture the chordae, was found to increase with chordal size. This is shown in Figure 3.8.

Chordae are under tension during ventricular systole. An attempt was, therefore, made to estimate the rate at which the chordae are being stretched during mitral valve closure. Echocardiograms give traces of the motion of the valve tissue. Figure 3.9 is one such trace for the mitral valve. The segment of the lower curve from A to C of the traces corresponds to the final motion of the valve leaflet when the valve snaps shut, and point C indicates the complete closure of the valve. Hence, a maximum slope to the curve AC at point C will give the velocity of the leaflet the moment it snaps completely shut, and since at this instant, the chordae are being stretched, the velocity of final valvular closure will give us an estimate of the initial maximum rate at which the chordae are being stretched in vivo. Since the angle of attachment of the chordae to the valve leaflet varies

Figure 3.8. Graph showing the variation of chordal toughness with chordal size. Toughness, defined as the total energy required to stretch the chordae to rupture, is seen to increase with chordal size.

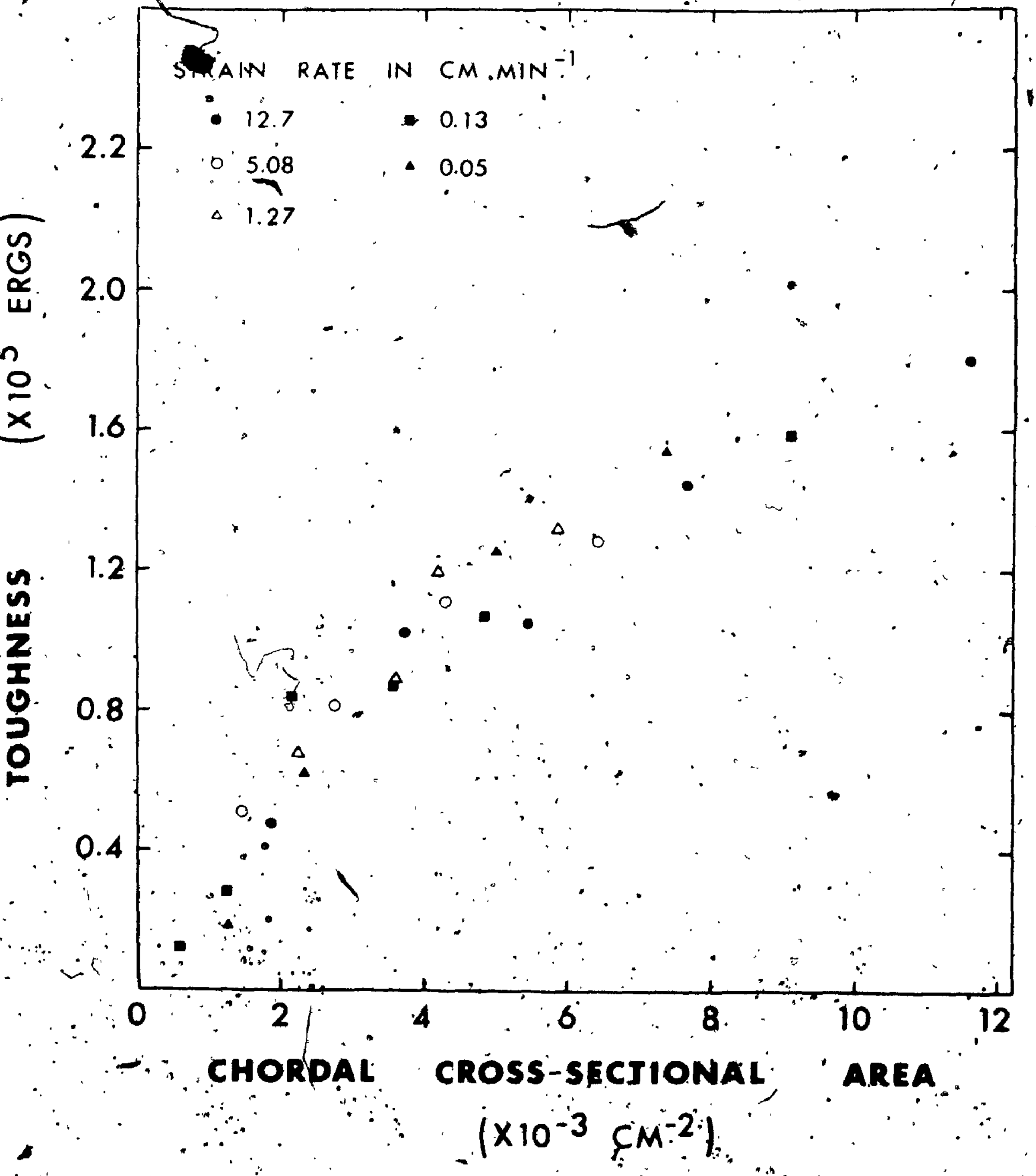
STRAIN RATE IN CM.MIN⁻¹
● 12.7
○ 5.08
△ 1.27
■ 0.13
▲ 0.05
TOUGHNESS (X10⁵ ERGS)
2.2
2.0
1.6
1.2
0.8
0.4
0
2
4
6
8
10
12
CHORDAL CROSS-SECTIONAL AREA
(X10⁻³ CM⁻²)

Figure 3.9. A typical echocardiographic record, tracing the motion of the mitral valve leaflet. The maximum gradient to the curve AC at C gives the approximate maximum rate that chordae are being stretched in vivo.

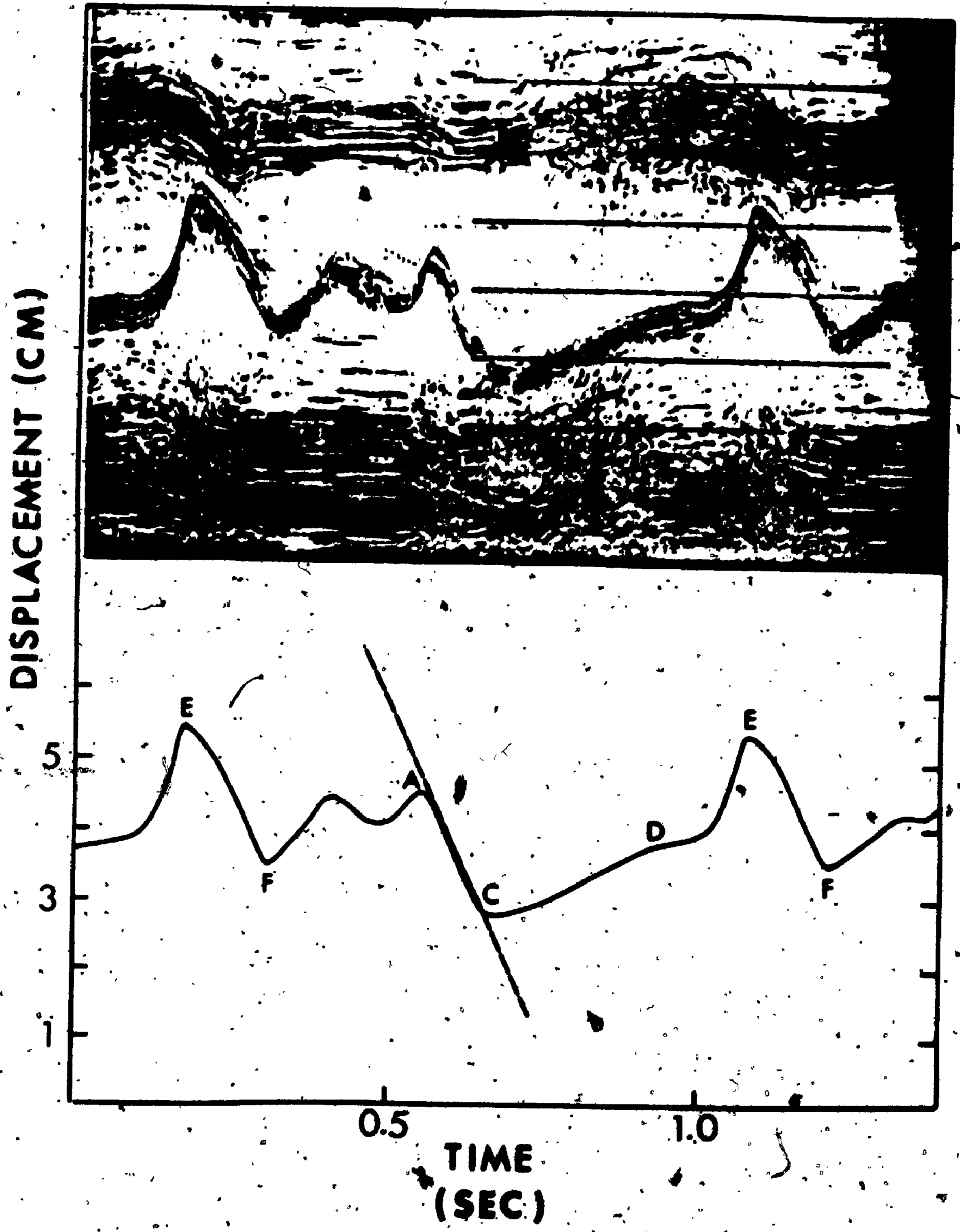
DISPLACEMENT (CM)
E
A
F
C
D
E
F
5
3
1
0.5
1.0
TIME
(SEC)

with the site of attachment to the leaflet and also from individual to individual, this estimate would give, at best a rough idea of the strain rate. Forty-three records (27 male, 16 female, ages 10 to 73) from patients with normal hearts were examined. The results in the form of a histogram are shown in Figure 3.10, and an average value of 29(SD =9) cm sec^{-1} was found. Taking the average length of a chordae at about 1.5 cm, this rate would correspond to a strain rate of about 2000% sec^{-1}. However, this is the maximum rate that the chordae would be stretched. Careful examination of the echocardiographic trace at C shows that lower rates are possible. Hence, the higher rates of in vitro testing could well be near the physiological conditions.

4. DISCUSSION

Studies of the chordal response under stress at varying strain rates show that the chordae exhibit visco-elastic properties, in that they are less extensible with increasing strain rates and their viscous properties become more pronounced at lower rates of strain.

The non-linear stress-strain response could be due to the structural composition of the chordae. Caulfield et al (1971), Silverman and Hurst (1968), Fenoglio et al (1972) showed that chordae tendineae are made up primarily of collagen with some elastin fibres. Roach and Burton

Figure 3.10. Histogram of the distribution of the maximum mitral leaflet closure rate, estimated from echocardiographic tracings.

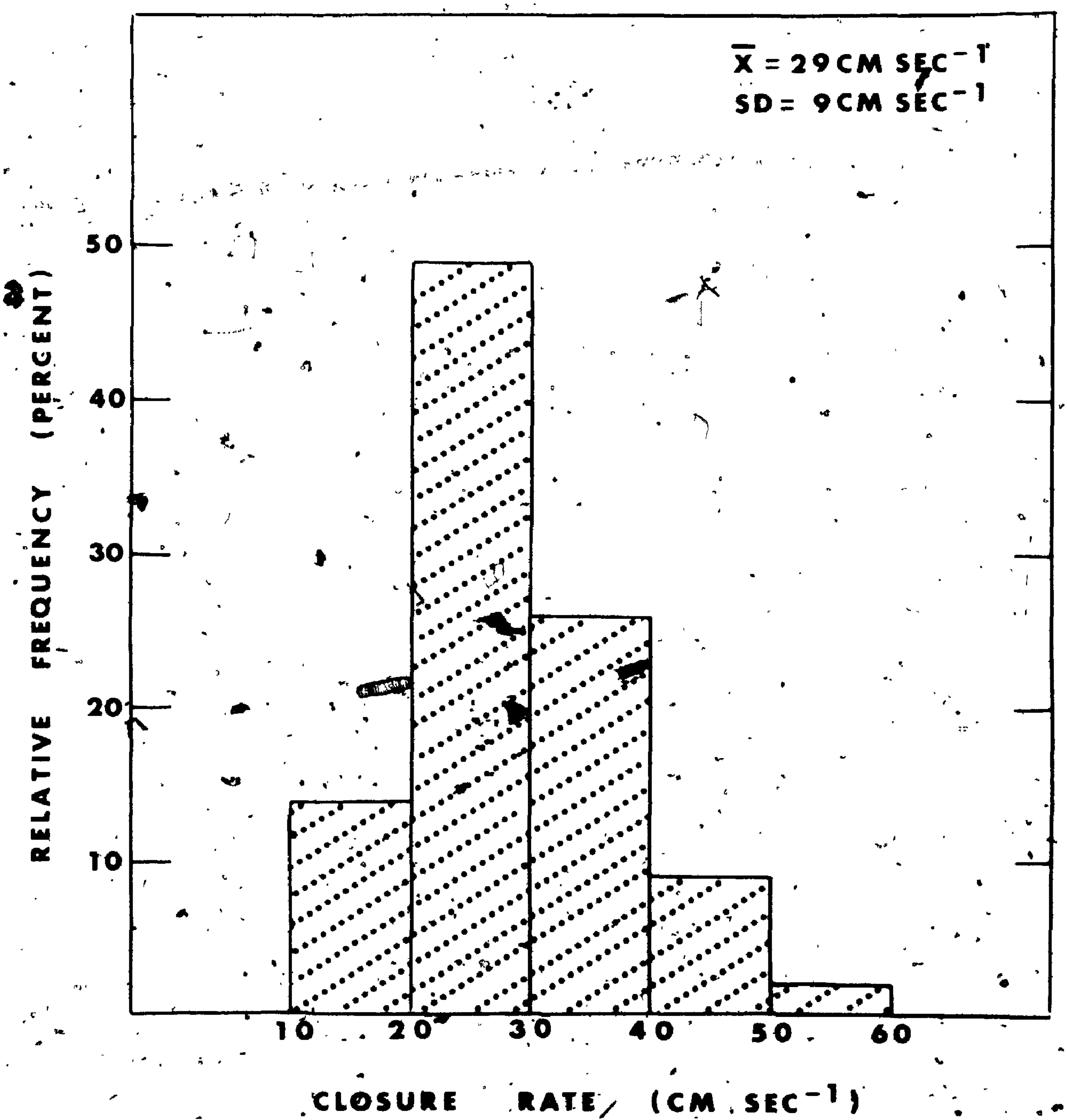
$\bar{X}$ = 29 CM SEC^{-1}
SD = 9 CM SEC^{-1}
50
40
30
20
10
RELATIVE FREQUENCY (PERCENT)
10
20
30
40
50
60
CLOSURE RATE (CM SEC^{-1})

(1957) showed that a similar non-linear response for arteries could be accounted for by its composition of elastin and collagen fibres. They showed that the initial segment of the stress-strain curve is due to the elastin while the final slope of the curve is due to the stretching of the collagen. Since the chordae are also of elastin and collagen, the non-linear response could be due to this structural composition. The transitional point would then correspond to the instant where, on further straining, the resistance to stretch is governed primarily by the collagen.

However, the structural arrangement of elastin and collagen fibres in arteries is rather different from that of the chordae. In arteries, there is a network of elastin lamellae interlaced with interlamellar collagen fibres (Wolinsky and Glagov, 1964). Such an arrangement makes arterial walls behave as a two-phase material (Glagov and Wolinsky, 1963). In the canine chordae, however, there is an outermost layer of single flattened endocardial cells, and beneath this is an area of loosely meshed collagen and elastin fibres, with the latter predominating. The large central core of the chordae is of dense wavy collagen bundles interspersed with scattered fibroblasts and elastin fibres (Fenoglio et al, 1972). If the canine chordal structure is applicable to humans, then when such a parallel arrangement of two different types of fibres is stretched the response will be governed by the relative stiffness of the individual components.

If the stiffness of elastin is greater than that of straightening the wavy collagen, the initial portion of the response curve would be due to the stretching of the elastin alone, as in arteries. If the reverse if the case then the initial resistance to stretch would be due to simply a straightening of the wavy collagen fibres. However, if both have comparable stiffness then the initial response would be due to a simultaneous stretching of the elastin and a straightening of the wavy collagen fibres. Whatever the reason, the final modulus before reaching the proportional limit will be the modulus of collagen. The value in the order of 10^9 dynes cm^{-2} observed in this study is comparable to that reported by Burton (1954) for collagen fibres.

The observed breaking strain of 21.4 (standard error = 0.5)% is quite typical of collagen fibres (Hall, 1951; Morgan and Mitton, 1960). This observation, differs from that reported by Yamada (1970) on human chordae tendineae where strains up to 40% were reached. However, the values for the breaking stress are comparable.

If the finding that chordae from isolated young patients are more extensible is typical, then the decrease of extensibility with age up to a certain level, (and not necessarily at 21 years) is in agreement with observations on tendonous tissues that the collagen content increases with age. However, in the 21-66 age group, the results do not show any further significant variation. It could be that the chordae tendineae have reached full maturity in adults.

The observations that the larger chordae are initially more extensible could be a design to enable the mitral valve to maintain an even surface on closure. Brock (1952) and Lam et al (1970) reported that the larger chordae are found at the centre of the free edges of the valve leaflets and, hence are more centrally placed with respect to the mitral orifice (figure 3.11). Brock called these areas the critical areas of insertion. In this position the thick chordae should be more extensible so that under similar forces exerted along each chordae they could be made to extend by a similar or even greater amount than the thin ones (figure 3.11). This observed property of an inverse relation between stiffness and size thus ensures that an even and regular valve surface can be maintained during valve closure. This would not be possible if all chordae had identical mechanical properties.

5. SUMMARY

A knowledge of the mechanical properties of valve tissue is a necessary prerequisite for a better understanding of valvular behaviour and the design of prosthetic

Figure 3.11. (A) Diagrams of a heart dissected in 2 different planes showing the attachments, to the anterior leaflet (AL) of the mitral valve, of some small and large chordae. Posterior leaflet (PL), papillary muscles (PM).

(B) For materials with the same property and under the same force the thicker specimen will extend by a smaller amount.

(C) Under the same force but with different elastic properties, specimens of 2 different sizes could be stretched by the same amount.

2 OF/DE 3

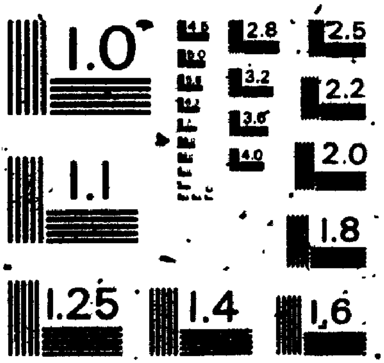
1.0
2.8
2.5
3.2
2.2
3.6
4.0
2.0
1.1
1.8
1.25
1.4
1.6

MICROCOPY RESOLUTION TEST CHART
NATIONAL BUREAU OF STANDARDS - 1963 A

ARC # 324

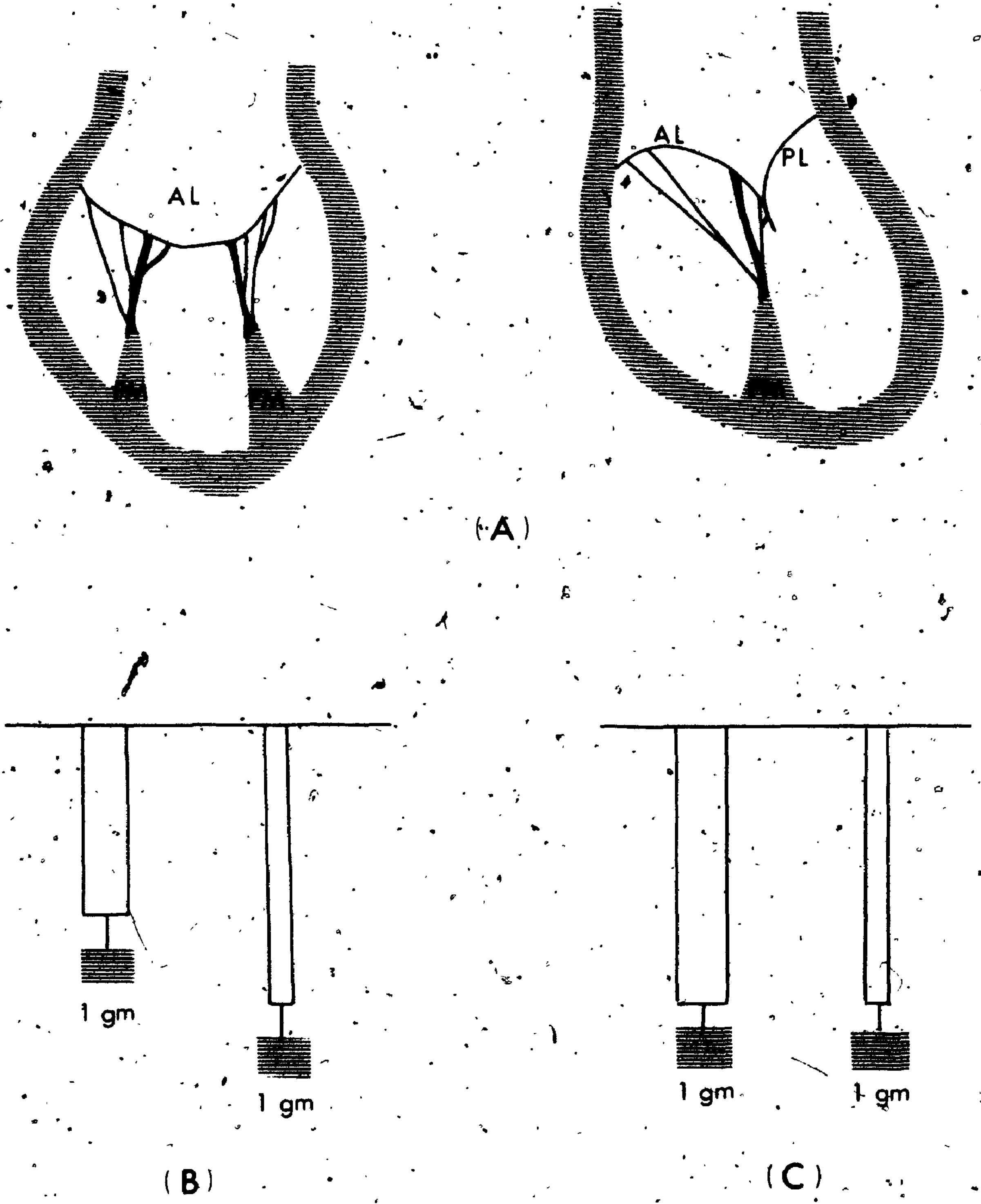
AL
AL
PL
(A)
1 gm
1 gm
(B)
1 gm
1 gm
(C)

heart valves. Elastic response of chordae tendineae under strain rates of 0.05 cm min^{-1} (6.25% min^{-1}) to 12.7 cm min^{-1} (1600% min^{-1}) were obtained by the application of an uniaxial tensile stress using an Instron Machine. The chordae exhibited viscoelastic properties in that extensibility decreased with increasing strain rates. The approximate maximum physiological strain rate of the chordae was estimated from echocardiographic traces at the instant of valve closure, and a high value of 29 (SD = 9) cm sec^{-1} (2000% sec^{-1}) was found. The breaking strains which were independent of strain rate were found to have an average value of 21.4 (± 0.5)%, while the breaking stresses which were also independent of strain rate varied from 1.30 (± 0.35) x 10^8 dynes cm^{-2} to 3.65 (± 0.26) x 10^8 dynes cm^{-2}, depending on chordal size. These values are typical of collagen fibres. The final modulus, before the proportional limit, was found to be about 10^9 dynes cm^{-2}, which is again typical of collagen fibres. In addition, smaller diameter chordae exhibited less extensibility than the larger diameter chordae. This behaviour could be due to structural and functional differences and allows the more centrally inserted chordae to maintain an even valve surface during valve closure.

CHAPTER 4.

MORPHOLOGY OF CHORDAE TENDINEAE AND ITS RELATION TO THEIR EXTENSIBILITY CURVES

1. INTRODUCTION

Human mitral ~~valve~~ chordae tendineae, like many other biological tissues such as skin (Gibson, Stark and Evans, 1969), rat tail tendons (Rigby et al, 1959) and arteries (Roach and Burton, 1957), have also been observed to exhibit non-linear quasi-static elastic response (see Chapter 3; Yamada, 1970; Clark, 1973). In the case of rat tail tendons, which are mostly collagen, the initial segment of the non-linear stress-strain curve was attributed to a straightening of the wavy collagen fibre bundles (Rigby et al, 1959) and for skin it was suggested that the behaviour was due to an initial re-alignment of the randomly coiled collagen fibres (Gibson et al, 1969). Roach and Burton (1957) showed that for arteries, made up of elastin and collagen, the initial response to mechanical stress was due to the response of the elastin and the final slope of the stress-strain curve corresponded to the stretching of the collagen.

For chordae tendineae, none of the investigators provided an explanation for the observed non-linear behaviour though it was pointed out in chapter 3 that the relative stiffness in the various tissue structural components could possibly be involved. In addition, it was also found in chapter 3, that the larger the chordae the greater the extensibility, as shown in figure 3.5, and that adult chordal tissues were less extensible than younger specimens (Figure 3.7). In this chapter, I set out to provide evidence for the possible cause of the non-linear stress-strain response and also the reason for the dependence of extensibility on chordal size and age.

Chordae tendineae are made up primarily of two major components, an outer elastin sheath with scattered collagen and an inner core of collagen with traces of elastin . (Fenoglio et al, 1972). Since it is the microstructural arrangement of the protein fibres that determines the mechanical behaviour of a given tissue, the contribution to the elastic properties from these two major components in the chordae was examined. The techniques of selective enzymatic digestion and electron microscopy, both scanning and transmission, were employed in this study.

2. METHOD

Ninety chordae from 19 mitral valves (ages 18-79, 10 males, 9 females) were studied. The chordae were selected from patients with no clinical record of mitral valve disease and whose valves appeared normal at autopsy. The valves were removed as soon as possible and not more than 12 hours after death. They were kept, if necessary, in 0.01% merthiolate, 0.9% saline at a temperature of 6°C until tests could be performed.

a) Selective Enzymatic Digestion

To determine the role of each of the two major components, elastin and collagen, in the elastic response of chordae tendineae, the technique of selective enzymatic digestion was used to remove the outer elastin sheath. Thirty seven chordae from 9 mitral valves (ages 45-76, 5 males, 4 females) were divided into two size groups of chordal cross-sectional area 0.001 to 0.003 cm^2 and 0.004 -0.006 cm^2, and assigned randomly to act as controls or test specimens. The test specimens were digested in a solution of 0.1 M $NH_4 HCO_3$ buffer containing 1.5 mg α-chymotrypsin (Sigma, C4129 Type II) per ml of buffer, 2.5 mg trypsin (Sigma, T8253 Type III) per 2 ml of buffer and 20 μl elastase (Worthington ES34E747) per 100 ml buffer, at a temperature of 37°C for 10 hours with occasional agitation. The pH of the buffer solution was 7.8. The control specimens were similarly incubated in the buffer solution of 0.1 M $NH_4 HCO_3$ without the enzymes. This digestion procedure removed both the amorphous and fibrillar components of the elastin (Newman and Low, 1973). Figure 4.1 shows the

Figure 4.1(a). Longitudinal section of chordae before enzymatic digestion. The chordae has an outer sheath of elastin (the 2 dark lines at the edge of the specimen). The darker patches within the chordae are cardiac muscles. Gomori-trichome stain.

Figure 4.1(b). Longitudinal section of chordae showing the absence of the outer elastin sheath after treatment with elastase, trypsin and α- chymotrypsin. The darker patches within the specimen are cardiac muscles. Gomori trichome stain.

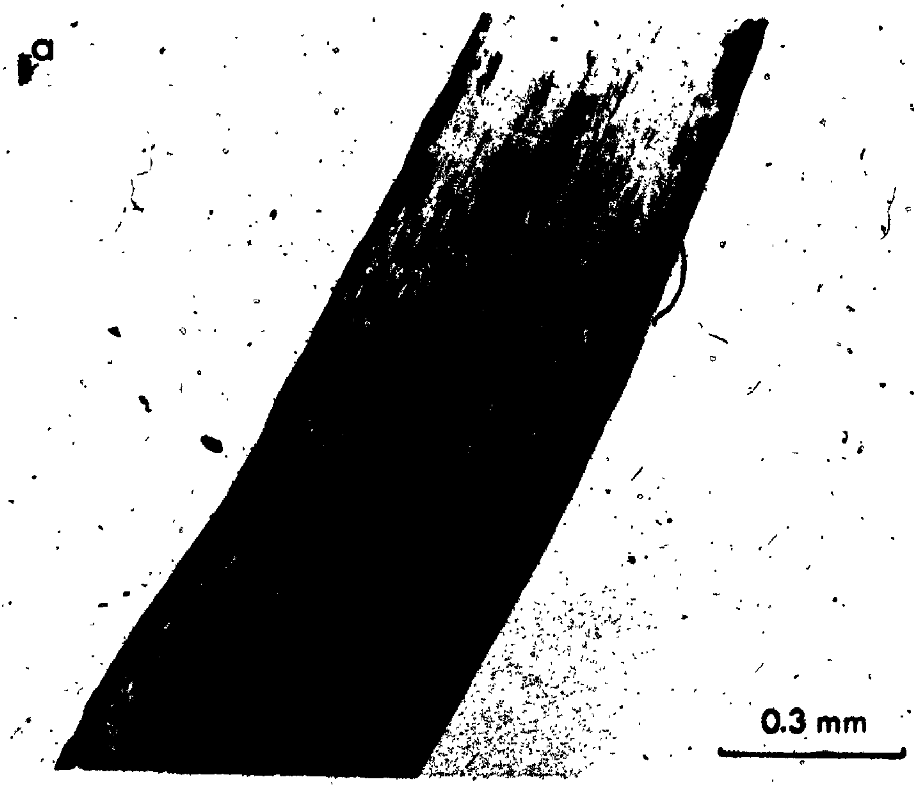
a
0.3 mm

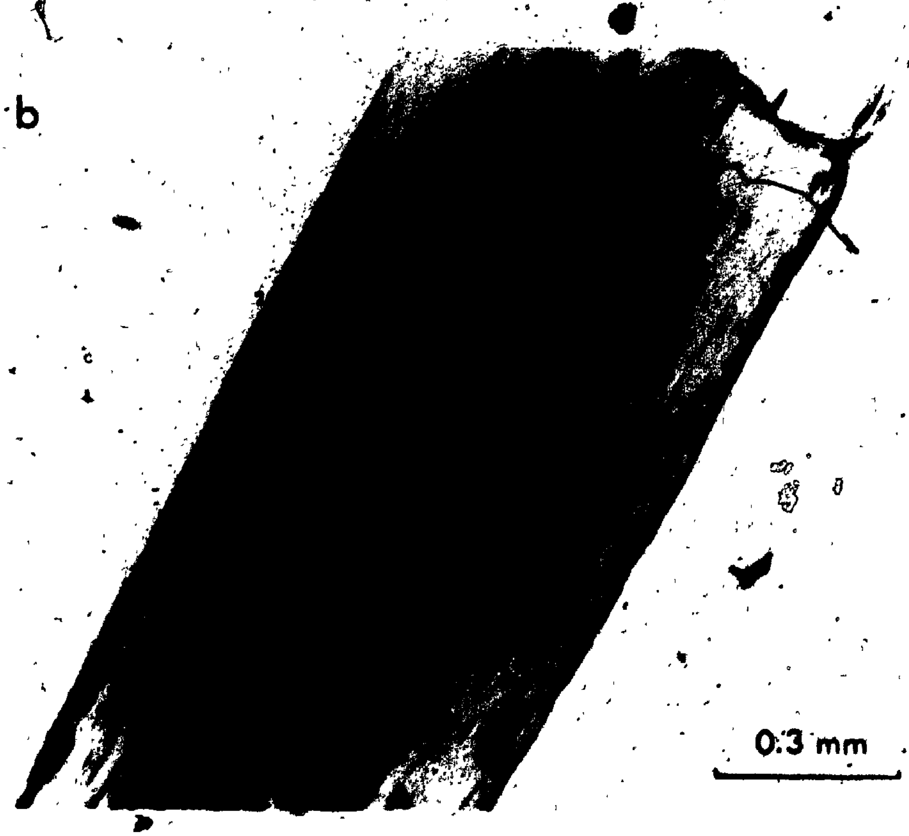
b
0.3 mm

effect on the chordae before and after this treatment. After the digestion and incubation periods test specimens and controls were removed, washed, and kept in 0.01% merthiolate, 0.9% saline solution at 6°C until further testing. To examine the effect of removal of the elastin on the mechanical response, the treated specimens and the control were subjected to an uniaxial tensile stress. A floor model of an Instron tensile testing machine (Model TT-C) was used for this purpose. The details of this procedure have been described in chapter 3. Strain rates of 0.13 cm min^{-1} and 1.27 cm min^{-1} were used and the chordae were all stretched at an initial length of 0.8 cm. The amount of force exerted on the specimens and the corresponding stretch were recorded continuously and simultaneously on a chart recorder.

b) Scanning Electron Microscopic Studies

Scanning electron microscopy was used to examine the internal structure of the chordae tendineae and in particular, the micro-architectural arrangement of the collagen fibres in the central core. Forty chordae from 10 mitral valves (ages 18-79, 5 males, 5 females) were examined. The technique used in preparing the specimens for study was essentially that of Watters and Buck (1971). The specimens, after removal, from the heart were washed in saline, identified according to size and then fixed for 2 hours in 5% glutaraldehyde in 0.1 M Sorensen's phosphate buffer at a pH of 7.1. The specimens were then transferred to a 5.4% sucrose in 0.1 M phosphate buffered solution, and stored overnight at a temperature of 6°C, after which they were gently ripped apart to expose the internal structure. The specimens were further treated in a solution of 1% osmium tetroxide in phosphate buffer. The tissue remained here for a further 2 hours after which they were washed twice with demineralised water. Dehydration was done by a series of 15 minute changes in solutions containing 30%, 50%, 70%, 90%, 95% ethanol and 100% acetone. The specimens were further treated with benzene, then a solution with equal parts benzene and propylene oxide and then with 100% propylene oxide. After this they were transferred to 50% camphene in propylene oxide and finally to melted camphene. The last two steps took 20 minutes each. The camphene treated specimens were then left overnight in a fume chamber to allow the camphene to sublime. The specimens were then coated with gold and examined under a scanning electron microscope (Hitachi HHS-2R). In addition, a few specimens, fixed under tension, were also studied.

c) Transmission Electron Microscopic Studies

This part of the investigation was used to determine the density and size distribution of the collagen fibrils in the different sized chordae. Transverse sections of 14 chordae from 4 mitral valves were studied. The specimens, after removal from the heart, were immediately fixed in 2.5% glutaraldehyde in 0.1M cacodylate solution at a pH of 7.3 for 10 minutes. After the initial fixation, the tissues were minced into 1 mm^3 with the aid of a dissecting microscope and then returned to the fixative for a further 2 hours. The tissues were then washed in 3 changes, of 10 minutes each, in 5.4% sucrose in 0.1 M cacodylate buffer at pH 7.3. Post fixation of 1 hour duration was done in 1% osmium tetroxide in the same buffer containing 5.4% sucrose. The specimens were then dehydrated with 3 washes, in each of solutions containing 50%, 70%, and 95% ethyl alcohol. This was then followed by a further wash in a solution containing equal parts of ethanol and acetone. Each of the above washings took 5 minutes. The dehydrated tissues were then stained "en bloc" in lead acetate and uranyl nitrate for 1½ hours after which they were washed 3 times, each for 10 minutes in a solution of 50% alcohol and 50% acetone. Infiltration of the tissue was done initially with a solution of 25% alcohol, 25% acetone and 50% spurr for 1 hour, then followed by pure spurr overnight. All the processing was done on a rotator. The specimens were then embedded with Beem capsules (Ladd Research Industry Incorp. #2365) with fresh spurr and left overnight in an oven at 70°C. The embedded blocks were then sectioned into specimens of 800 Å - 900 Å thickness in either a LKB ultramicrotome 3 or a LKB - Huxley ultramicrotome. The thin transverse sections of the chordae were then mounted on 150 mesh formvar coated copper grids and stained with uranyl acetate and Reynolds lead citrate. The sections were then examined with a Zeiss Electron microscope EM9S, and micrographs taken. From these electron micrographs the density per unit transverse sectional area and the size distribution of the collagen fibrils were determined with a Particle Size Analyzer (Carl Zeiss TGZ3).

3. RESULTS

a) Selective Enzymatic Digestion

Figures 4.2(a) and 4.2(b) show the elastic response of chordae tendineae after treatment with a solution containing elastase, trypsin and α-chymotrypsin in 0.1 M NH_4HCO_3 buffer at a pH of 7.8. The elastic response of controls is also shown. Figure 4.2(a) shows the behaviour of chordae of cross-sectional area 0.001 to 0.003 cm^2 when strained at 0.13 cm min^{-1} and Figure 4.2(b) shows the results for chordae of cross-sectional area 0.004 to 0.006 cm^2 and strained at 1.27 cm min^{-1}. The stress-strain curves in both the figures indicate that the response to mechanical stress of both the test specimens, whose elastin sheath had been removed, and the controls were similar. This implied that the more readily extensible elastin layer cannot contribute

Figure 4.2(a). The elastic response of chordae whose outer elastin sheath had been removed. The response of the treated specimens was similar to the controls. The specimens have cross-sectional areas of 0.001 to 0.003 cm^2 and were strained at 0.13 $cm \cdot min^{-1}$. The 2 dotted lines denote the standard error. The sample size for each of the curves in this and the next figure ranges from 6 to 13.

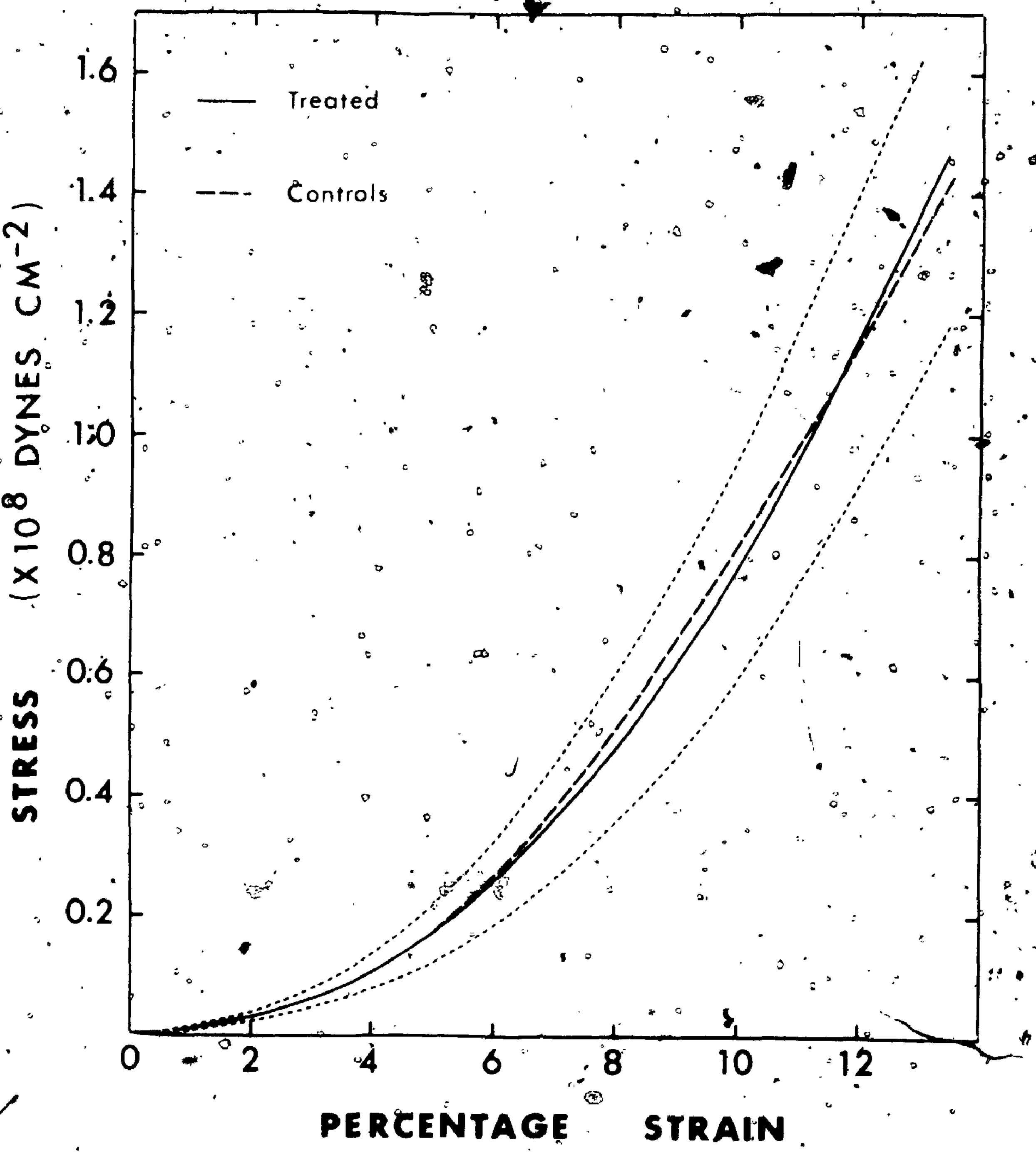
Treated
Controls
STRESS (X10^8 DYNES CM^{-2})
1.6
1.4
1.2
1.0
0.8
0.6
0.4
0.2
0
2
4
6
8
10
12
PERCENTAGE STRAIN

Figure 4.2(b). Similar to Figure 4.2(a) but the chordal cross-sectional areas were 0.004 to 0.006 cm^2 and the strain rate was 1.27 cm min^{-1}.

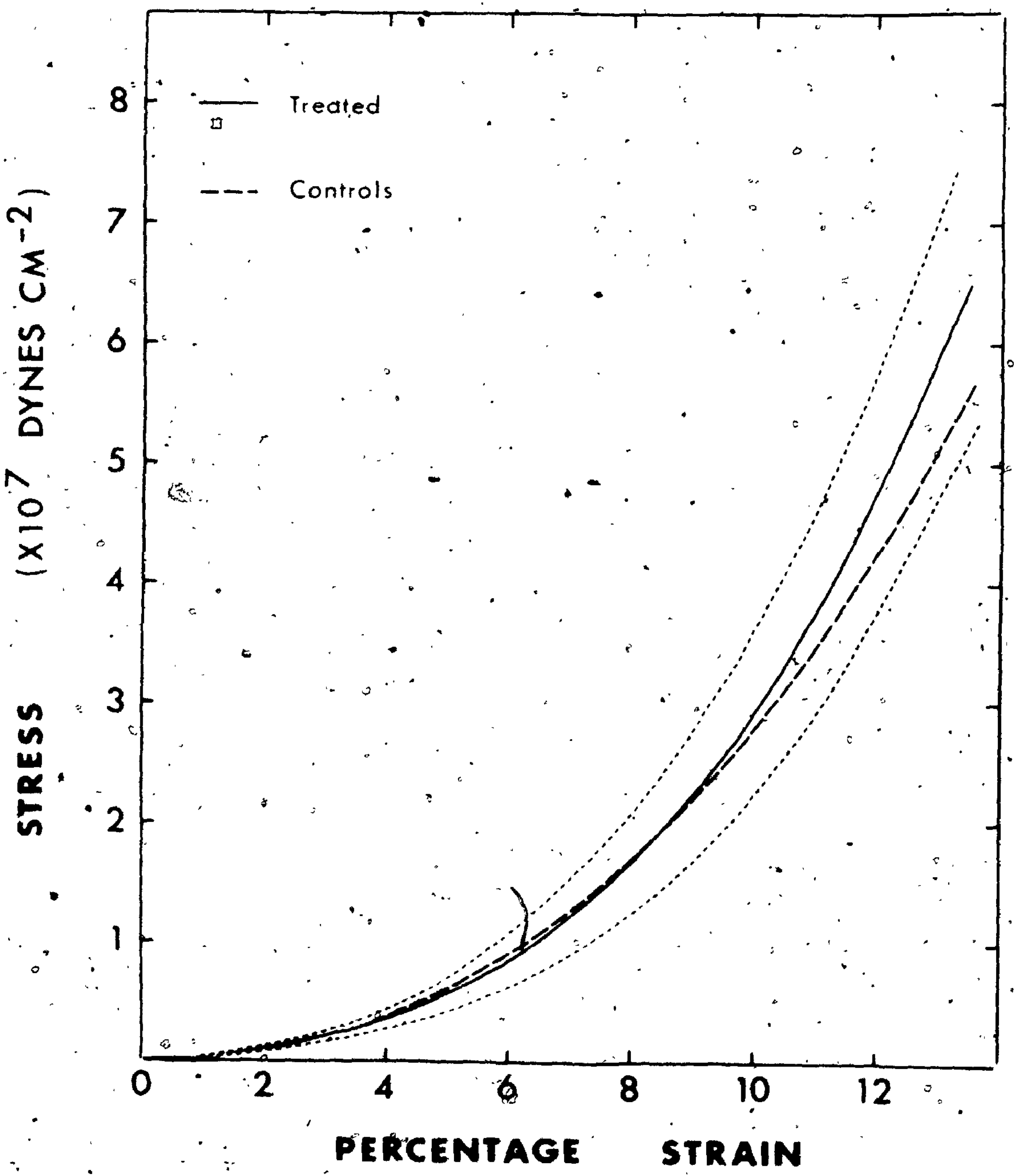
Treated
Controls
STRESS (X10^7 DYNES CM^-2)
8
7
6
5
4
3
2
1
0
2
4
6
8
10
12
PERCENTAGE STRAIN

to the non-linear elastic behaviour of chordae tendineae, hence, the mechanical properties of this tissue are governed primarily by the behaviour of the inner collagen core.

b) Scanning Electron Microscopic Studies

The internal structure of the collagen fibres in an adult chordae tendineae as revealed by scanning electron microscopy is shown in Figures 4.3(a) and 4.3(b). In Figure 4.3(a) the collagen fibres in the chordal core were observed to be aligned parallel to the axis of the chordae and were rather straight, with only a few specimens showing a very slight wavy pattern. This was in contrast to the very wavy patterns observed in rat tail tendons by Rigby et al (1959) and in canine chordae (Fenoglio et al, 1972).

Figure 4.3(b) shows the enlargement of one of these fibres. It was found that at the micro-structural level the collagen fibre was made up of a network of collagen fibrils, aligned in a direction generally parallel to the chordal long axis. This network arrangement was also observed at this high magnification for the collagen fibres in chordae from a young patient (an 18 year old male). However, at a lower magnification the young specimens exhibited a much more wavy pattern compared to their older counterparts as shown in Figure 4.4.

Figure 4.3(a). Scanning electron micrograph of the central collagen core of an adult chordae (a 70 year old female). The collagen fibres in this region were found to be relatively straight.

60 µ

Figure 4.3(b). Scanning electron micrograph showing the presence of a network of collagen fibrils in the collagen fibres of Figure 4.3(a).

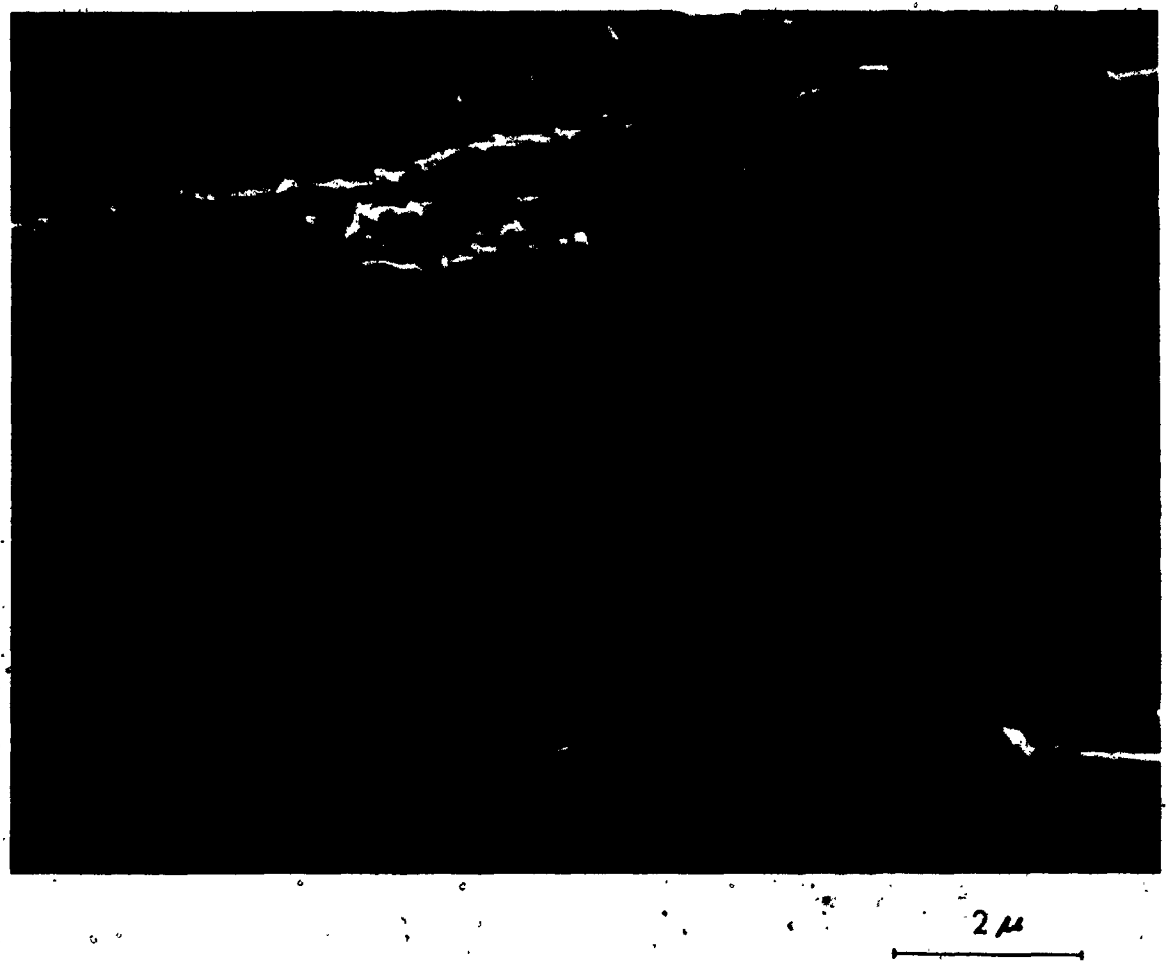
2 µ

Figure 4.4. Scanning electron micrograph of the central collagen core of a chordae from a 18 year old male. In contrast to Figure 4.3(a) the fibres here exhibit a much more wavy pattern.

60 μ

If we characterise this wavy pattern by a waviness index (WI) defined as

$$WI = \frac{\text{length of wavy fibre}}{\text{straight length between end points of fibre}}$$ (Wolinsky and Glagov, 1964).

WI would have a value of 1.0 for a straight fibre such as those for older chordae. For the 18-year-old specimens WI was found to be 1.072 (SE = 0.002), implying that the wavy fibres were 7.2% (SE = 0.4%) longer than a straight fibre with similar fibre end points.

Figure 4.5 shows the effect of fixing an adult chordae under tension. It was observed here that the network of fibrils was more collapsed in many regions along the specimen.

(c) Transmission Electron Microscopic Studies

Figures 4.6(a) and 4.6(b) are transmission electron micrographs of transverse sections of the chordae. The collagen fibrils in the scanning electron micrographs appeared as circular dots in these pictures. Figure 4.6(a) shows the central core of a typical small chordae and Figure 4.6(b) that of a much larger specimen. These micrographs show that the density of collagen fibrils was greater for the smaller chordae. The fibril density of the central core for 3 different chordal size groups is listed in Table 4-I and the average fibril diameters are also presented. An analysis of variance showed that the fibril density decreased significantly as chordal size increased ($P<0.01$).

Figure 4.5. Scanning electron micrograph showing the effect on the fibrillar network when the specimen was fixed under tension. The network of collagen fibrils was seen to be more collapsed in this micrograph. This more collapsed network was found in several regions along the chordae.

Figure 4.6(a). Transmission electron micrograph of a transverse section of the central core of a thin chordae. The dots correspond to the collagen fibrils. Greyish patches show the presence of elastin.

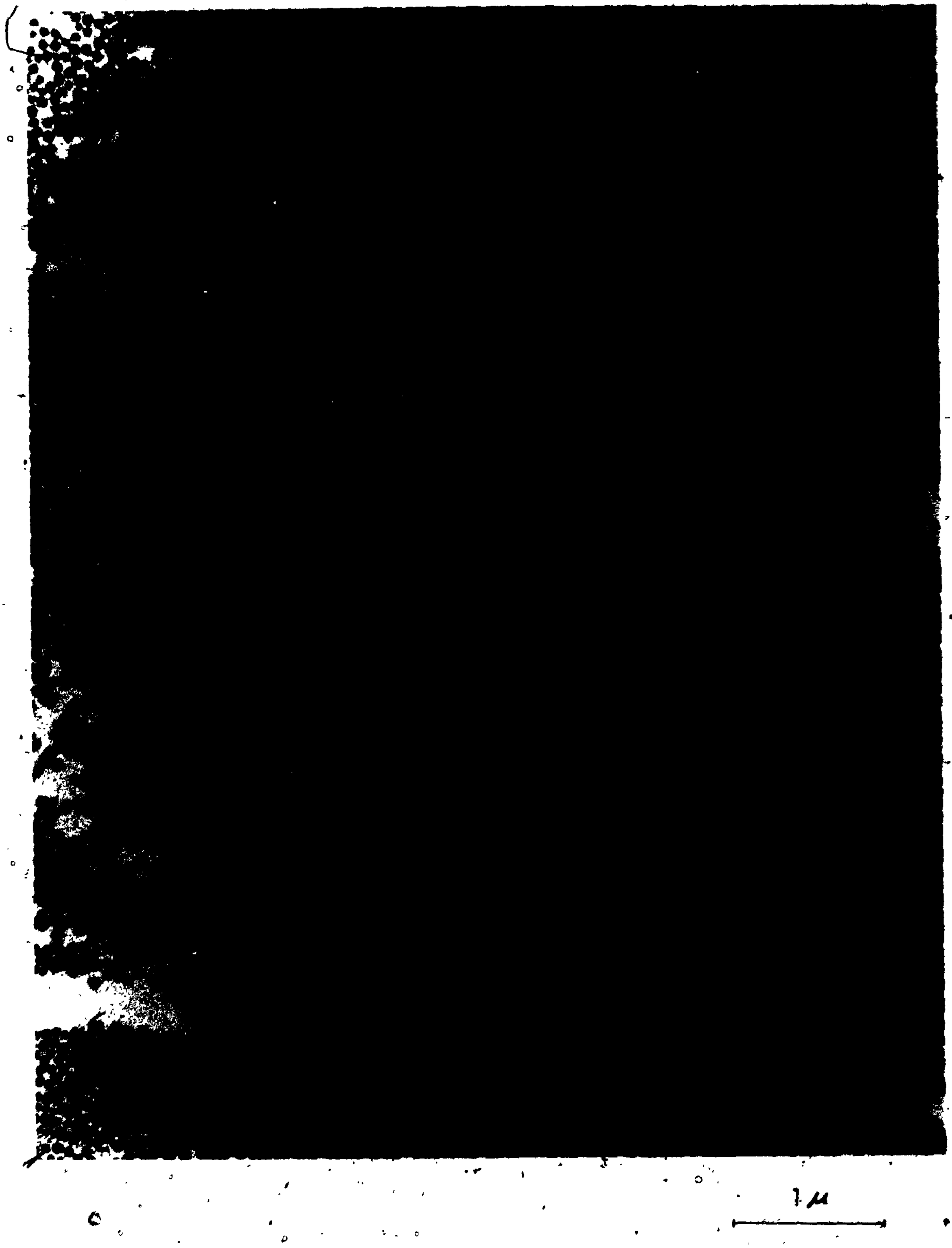
1 μ

Figure 4.6(b). Transmission electron micrograph of a transverse section of the central core of a thick chordae. Note that the fibril density in this micrograph is less than that shown in Figure 4.6(a).

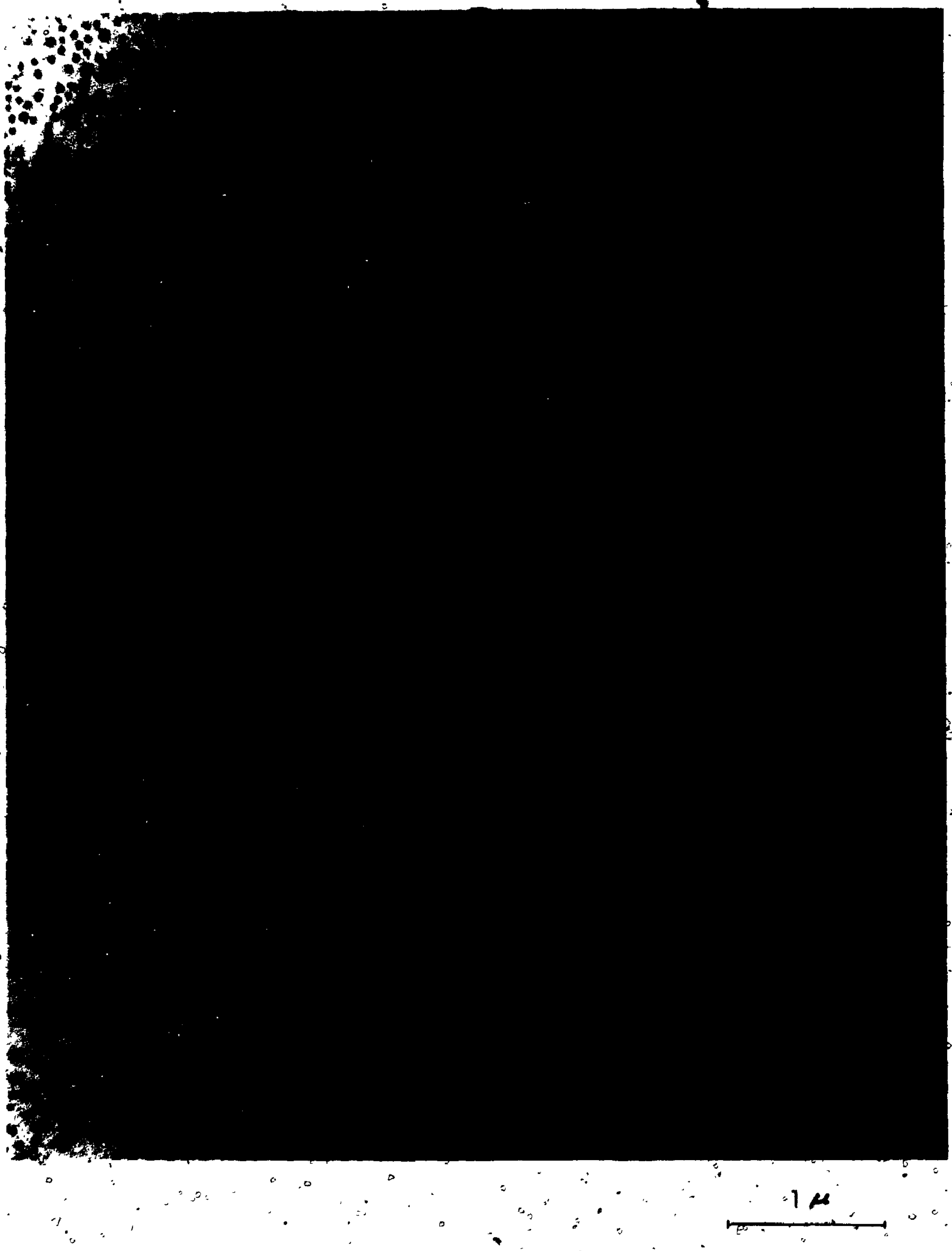
1 μ

TABLE 4-I

Average collagen fibril size and fibril density as a function of chordal size. The fibril density was found to decrease with an increase in chordal size and the group of chordae with the largest diameter has fibril size that were significantly smaller than the other 2 groups of smaller sized chordae tendineae.

TABLE 4-P

Chordal cross-sectional area (cm^2)	Average diameter (in Å) of collagen fibrils (± standard error)	Number of collagen fibrils per 10^{-8} cm^2 (± standard error)
0.0013-0.0019	545 ± 2 (1309)	182.4 ± 1.3 (30)
0.0072-0.0074	552 ± 3 (815)	163.6 ± 1.7 (29)
0.0260-0.0280	516 ± 2 (843)	131.2 ± 1.6 (36)

Numbers within brackets denote sample size.

The average fibril sizes between the first two groups of smaller diameter chordae were not significantly different (t-test, $P>0.01$), but the diameter in the third group was found to be smaller. This smaller average fibril size in the large chordae would further decrease the force supporting areas in them. The distribution of fibril size for the third group of thick chordae and those of the first and second group of smaller chordae are shown in figures 4.7(a) and 4.7(b)

4. DISCUSSION

The enzymatic digestion studies showed that the removal of the outer sheath of elastin from human mitral valve chordae tendineae did not significantly affect the elastic response of this tissue under mechanical stress. Thus, the initial segment of the non-linear stress-strain curve cannot be attributed to the presence of the more extensible elastin. This is in contrast to observations in arteries. For that tissue, it had been shown that the initial segment of the non-linear stress-strain curve was due to the extension of the elastin and the final slope of the curve was attributed to the collagen response (Roach and Burton, 1957). My findings, therefore, indicate that although both arteries and chordae contain essentially the same 2 structural components the reason for their elastic response cannot be explained by the same theory. This points

Figure 4.7(a). Collagen fibril size distribution in chordae tendineae of cross-sectional area 0.001 to 0.008 cm^2.

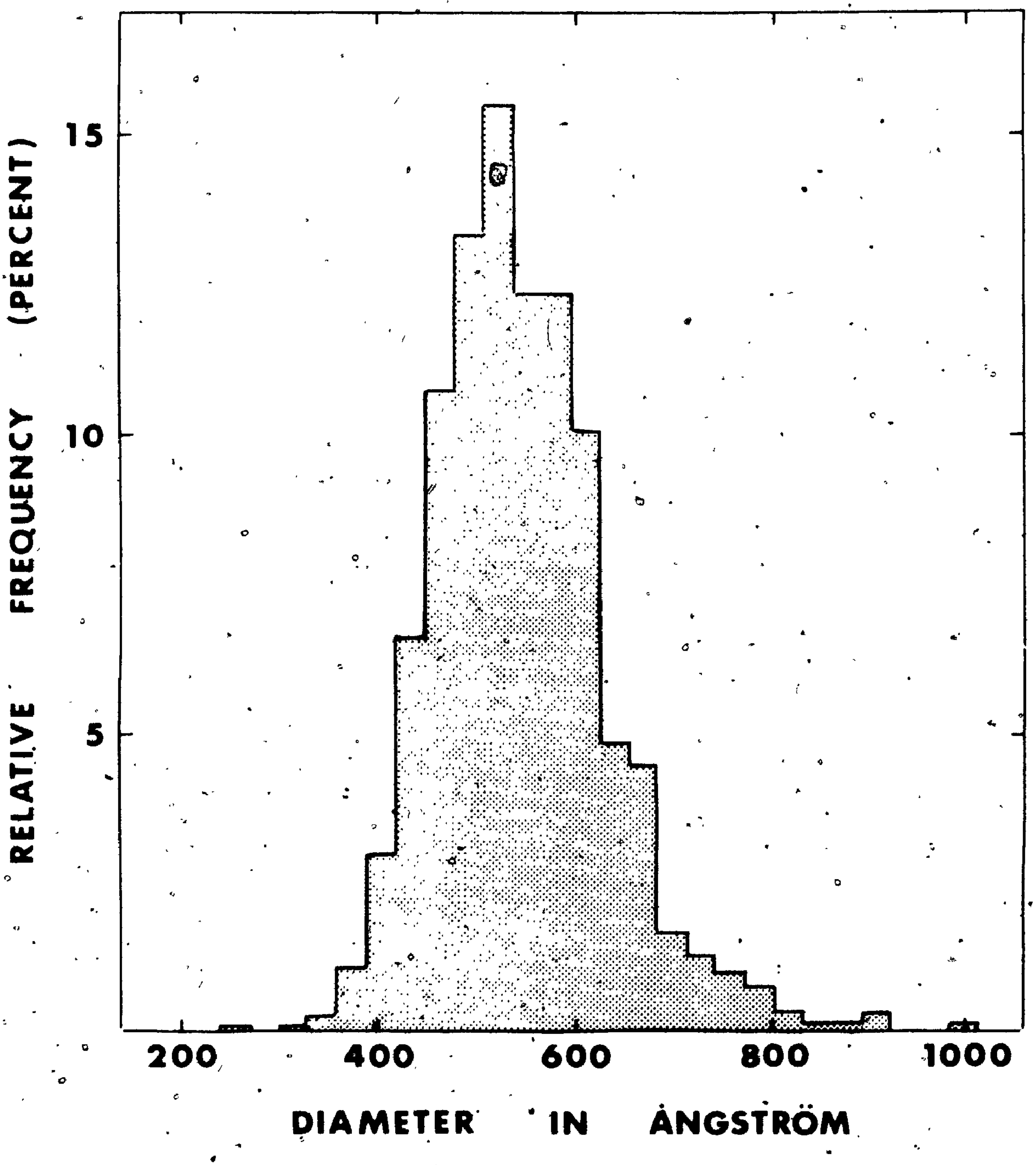

RELATIVE FREQUENCY (PERCENT)
15
10
5
200
400
600
800
1000
DIAMETER IN ÅNGSTRÖM

Figure 4.7(b). Collagen fibril size distribution in chordae tendineae of cross-sectional area 0.02 to 0.03 cm^2.

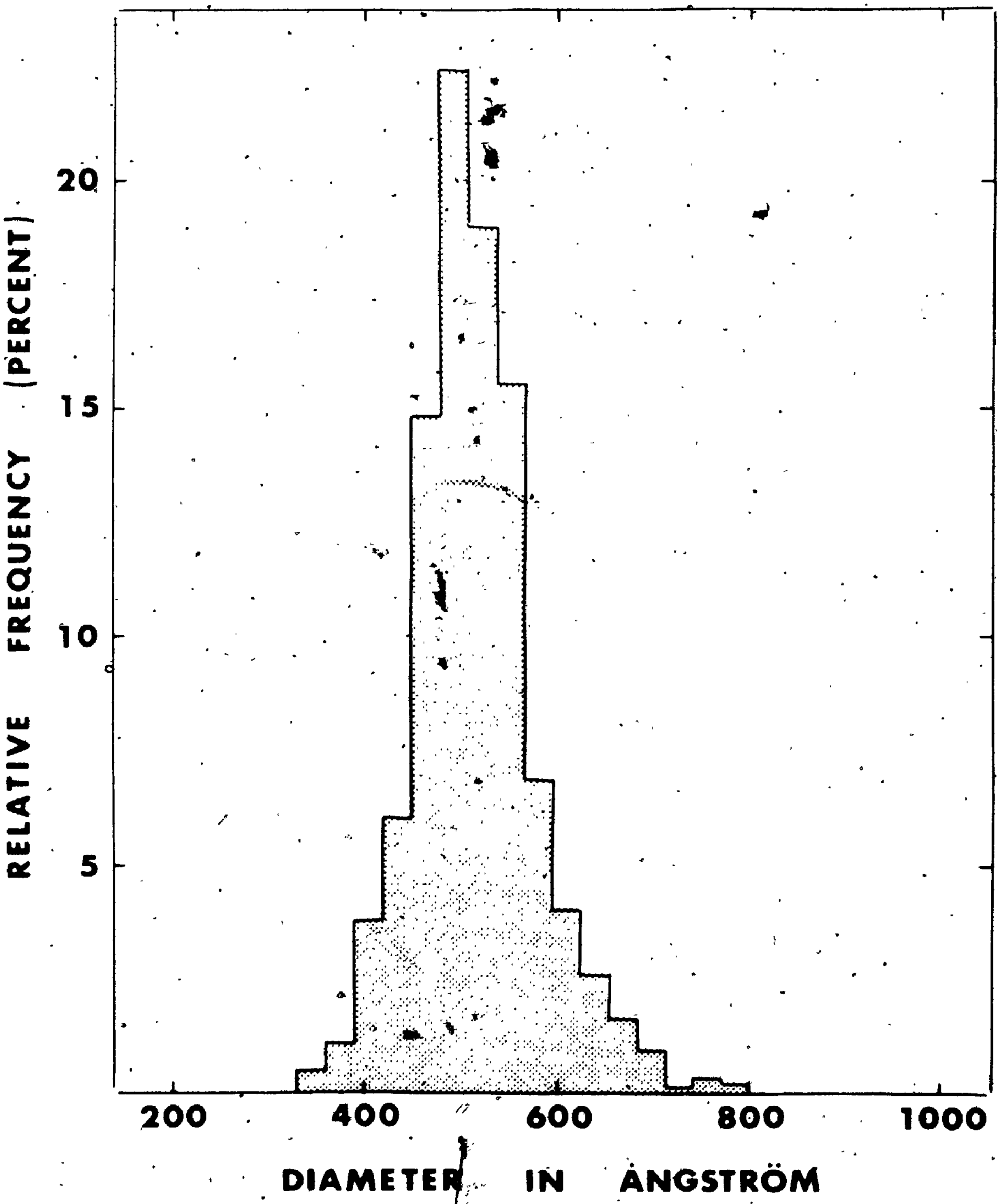
RELATIVE FREQUENCY (PERCENT)
20
15
10
5
200
400
600
800
1000
DIAMETER IN ÅNGSTRÖM

to the importance of the differences in the architectural arrangement of the structural components of these two tissues in determining their elastic properties. For arteries, there is a network of elastin lamellae interlaced with interlamellar collagen fibres (Wolinsky and Glagov, 1964). Such an arrangement makes the arterial wall behave as a two-phase material (Glagov and Wolinsky, 1963). In the chordae, however, there is an outer sheath of loosely meshed collagen and elastin fibres with the latter predominating, and the large central core is of dense collagen bundles with scattered elastin fibres.

The scanning electron microscopic studies showed that, at the microstructural level, the collagen fibres were in fact a network of fibrils. For such a system, when a force is applied, the response is to initially straighten any wavy pattern that may be present. This is followed by the stretching and collapsing of the fibrillar network, as shown in Figure 4.5 which illustrates the structure for a chorda fixed under tension. On further stretching, a force greater than that applied initially is needed to strain the tissue as this will now involve the straining of the bonds and bond angles within the fibrils. This response will, therefore, give rise to the observed non-linear stress-strain curves. This network also ensures that the individual fibrils are not excessively strained.

If the observation that the collagen fibres in the younger chordae were much more wavy than the essentially straight fibres in older specimens is typical, then this finding would explain the greater extensibility exhibited by these younger chordae. The waviness index found for the 18 year old chordae (2 specimens) showed that these specimens would extend by a further 7.2% before the fibres were straightened. From the results in Figure 3.7(a) which is reproduced here as figure 4.8, it is observed that the transitional strain (i.e. the strain level when the elastic curve becomes linear), occurs at 8.0% for the mature chordae and at 15% for a 17 year old specimen. Since this difference of 7% is comparable to the waviness index of 1.072 , it thus appears to indicate that the initial portion of the stress-strain curve of young chordae is attributed primarily to the straightening of the wavy collagen fibres and that the contribution arising from the fibril network arrangement is small in these young specimens.

Fibril size and distribution could not be determined accurately from scanning electron microscopy as this involved the coating of the specimen with gold. Hence transverse sections of the chordae were studied by transmission electron microscopy. The transmission electron

Figure 4.8. A comparison of the elastic response of chordae of different ages. In the 21-66 age group, most specimens were from patients over 35 years except one which was from a 21 year old male. Strain rate was 0.05 cm min^{-1} and the chordae have cross-sectional areas of 0.001 to 0.003 cm^2.

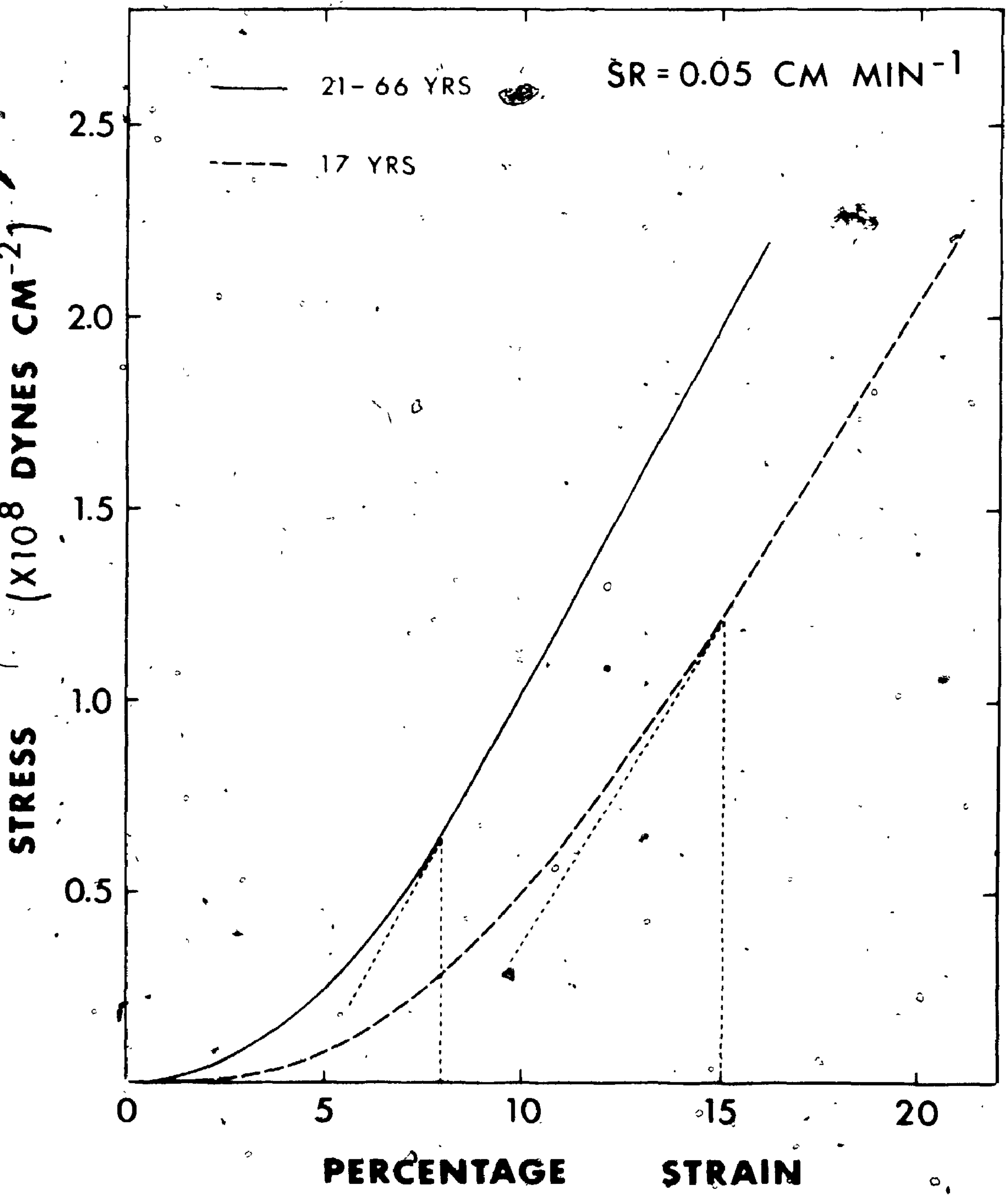
21- 66 YRS
17 YRS
SR = 0.05 CM MIN^{-1}
STRESS (X10^8 DYNES CM^{-2})
2.5
2.0
1.5
1.0
0.5
0
5
10
15
20
PERCENTAGE STRAIN

micrographs (Figure 4.6) showed the presence of the fibrils in the central core of the chordae thus confirming the observations of the scanning pictures. Results summarized in Table 4-I show the fibrils in the smaller chordae to be more closely packed compared to the larger size specimens, thus implying that a greater force per unit area would be necessary to stretch the more dense network of fibrils in thin specimens. This explains the greater extensibility exhibited by the larger size chordae. The average size of the collagen fibrils observed in this investigation was also found to be comparable to values reported for collagen fibrils (Viidik, 1973).

In conclusion, this study provided an explanation for the greater stiffness observed in adult human mitral valve chordae and the greater extensibility exhibited by the larger size chordae. It also showed that the non-linearity of the elastic response of mature chordae was due to the architectural arrangement of the collagen fibrils of this tissue.

5. SUMMARY

Human mitral valve chordae tendineae whose elastic response curves are non-linear have also been found to exhibit extensibility that increases with an increase in chordal size and decreased with an increase in chordal age. The techniques of selective enzymatic digestion and scanning and transmission electron microscopy were employed to provide explanations for these observations. It was found that the removal of the outer elastin sheath by enzymatic digestion did not significantly affect the elastic response of this tissue. Scanning electron microscopy revealed that for young chordae the collagen fibres in the central core exhibited a very wavy pattern but in adult specimens relatively straight fibres were observed. The increased waviness accounts for the greater extensibility shown by the young specimens. At high magnification, the collagen fibres from both young and old chordae were found to consist of a network of collagen fibrils that became more collapsed when the tissue was fixed under tension. This network arrangement of the fibrils explains the non-linearity in the elastic response of the tissue, and ensures that the individual collagen fibrils are not excessively strained. Transmission electron micrographs showed that the density of collagen fibrils decreased as chordal size increased. The number of fibrils per 10^{-8} cm^{2} of the central core decreased from 182.4 (SE = 1.3) to 131.3 (SE = 1.6) as average chordal cross-sectional area increased from 0.0016 cm^{2} to 0.0268 cm^{2}. This difference in fibril density provides an explanation for the greater extensibility shown by the thicker chordae. The collagen fibril diameters were found to show an approximately normal distribution and values, depending on chordal size ranged from 516 Å to 552 Å.

CHAPTER 5

DYNAMIC ELASTICITY OF CHORDAE TENDINEAE

1. INTRODUCTION

The uniaxial tensile tests on chordae tendineae reported in chapter 3 do not fully characterize the manner in which this tissue responds under the normal conditions of dynamic stress. This chapter therefore sets out to examine the dynamic elastic properties of human mitral valve chordae tendineae by subjecting the tissue to sinusoidal stress variations over a frequency range of 0.42 Hz to 6.68 Hz.

2. METHOD

a) Theory

When a linear viscoelastic material is subjected to a sinusoidal mechanical stress (σ), deformation is resisted by both an elastic restoring force and a viscous resistance. In the steady state condition the resulting strain (ε) is also sinusoidal but will be out of phase with the stress as shown in Figure 5.1. In view of this phase shift ϕ (radians), the stress can, therefore, be resolved vectorially into a component in phase with the

Figure 5.1. Diagram showing phase shift ϕ between the sinusoidal stress imposed on the chordae tendineae and the resulting sinusoidal strain.

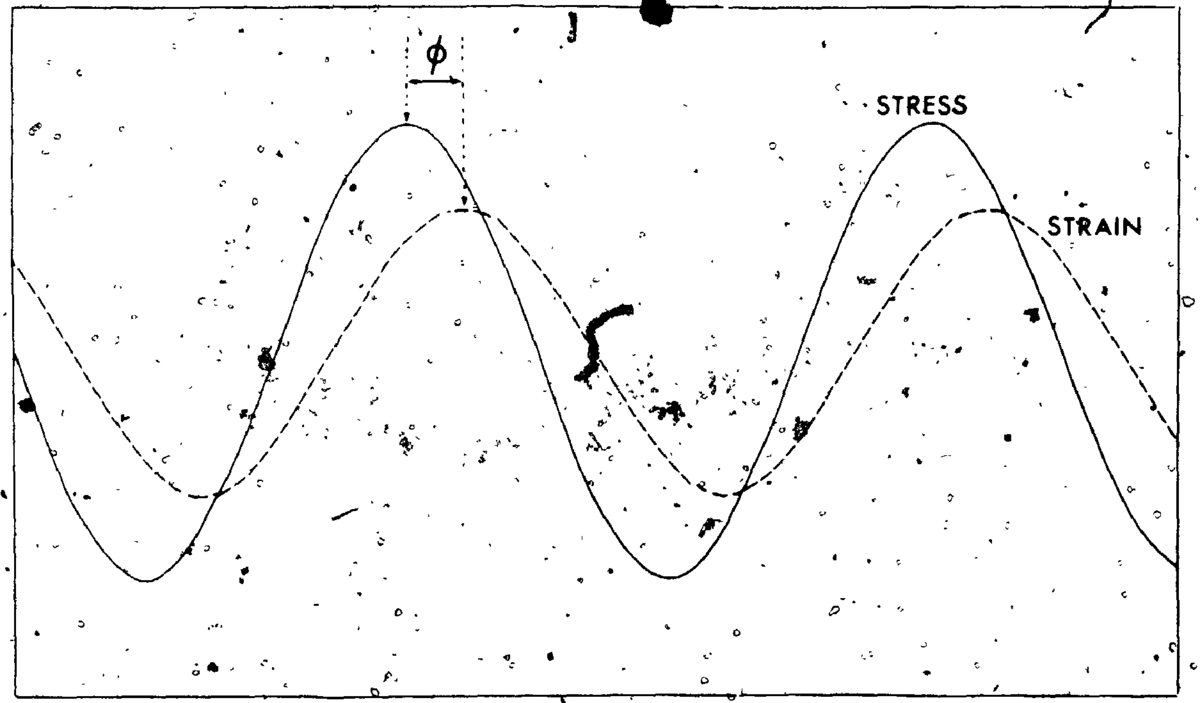

ϕ
STRESS
STRAIN

strain and a component 90° out of phase with the strain. These stress components when divided by the strain will, therefore, give an in phase (real) and an out of phase (imaginary) component of the dynamic elastic modulus, E*. Thus, E* can be written as a complex ratio.

$$E^* = \frac{\sigma}{\varepsilon} = E' + iE'' \qquad (5-1)$$

where E' will be the in phase or storage modulus, E" the out of phase or loss modulus and $i = \sqrt{-1}$. E' and E" are related to the phase shift ϕ and the magnitude of E* by

$$E' = \frac{\sigma_0}{\varepsilon_0} \cos \phi \qquad (5-2)$$

$$E'' = \frac{\sigma_0}{\varepsilon_0} \sin \phi \qquad (5-3)$$

where σ_0 and ε_0 are the respective maximum stress and strain values at a given frequency. In general, E*, E', E" and ϕ are frequency dependent. If ε_0, σ_0 and ϕ can be determined experimentally both E', the storage modulus, and E", the loss modulus can be found at each frequency of the stressing function.

b) Apparatus and Experimental Procedure

The apparatus used for subjecting the chordae to uniaxial sinusoidal tensile stress variations is shown in figure 5.2. Essentially it consisted of a motor coupled to a system of gears which drove a connector rod attached

Figure 5.2. Diagram of the apparatus used for the uniaxial and sinusoidal stretching of chordae tendineae.

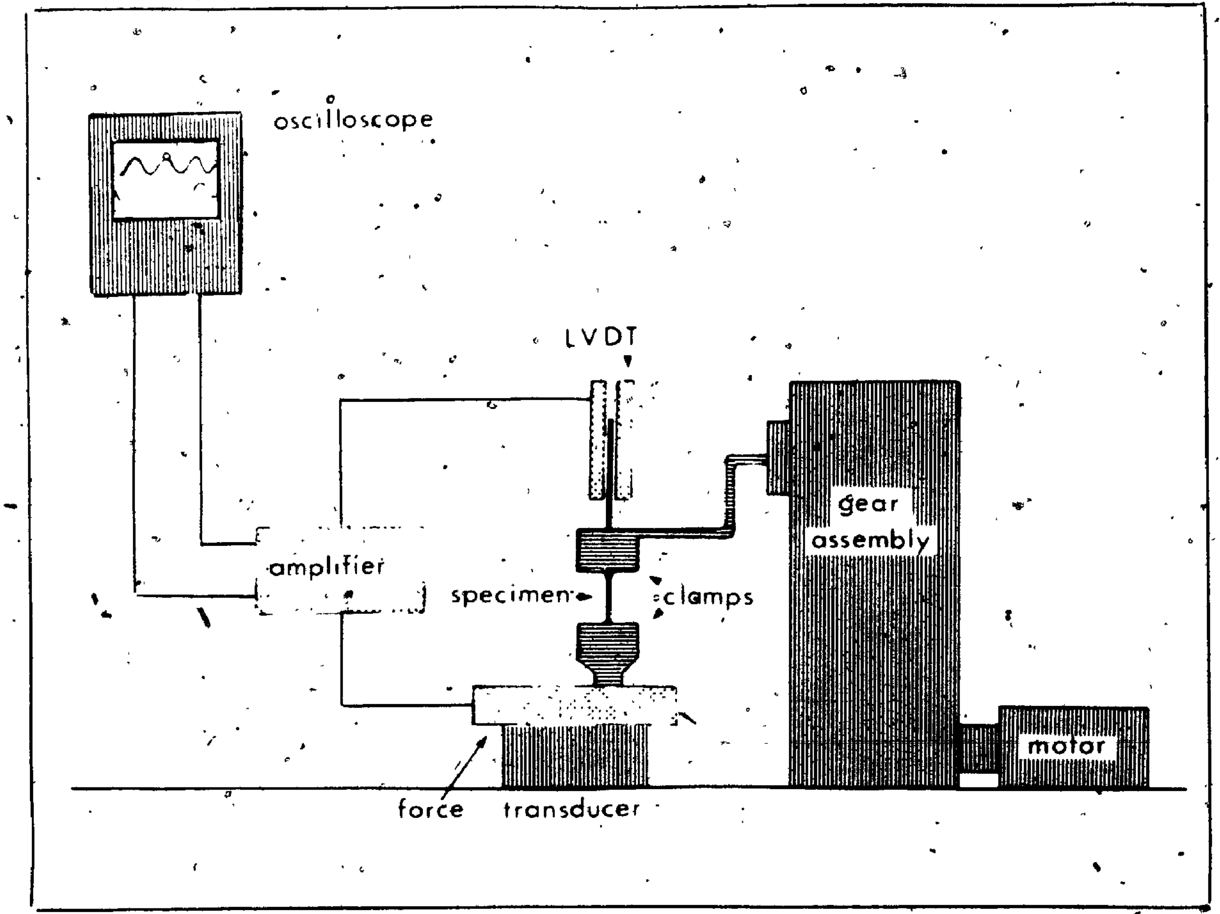
oscilloscope
LVDT
gear assembly
amplifier
specimen
clamps
motor
force transducer

to a parallel-plate clamping device, at 5 different preset frequencies. Attached to the clamp and resting vertically on it was the core of a linear variable differential transformer (LVDT, Schaevitz, type 100 MHR), which according to the manufacturer's specifications, offered negligible friction during use. The LVDT measured the movement of the clamp and hence the stretch on the tissue. The force exerted on the stretched tissue was measured by a force-displacement transducer (Grass, model FT.03C with black spring, displacement rate = 0.5 mm/kg), which also carried a second parallel-plate clamping device. These clamps were found to hold the specimens firmly without slipping (see chapter 3). To stretch the chordae sinusoidally, the specimen under study was held vertically between the clamps as shown in figure 5.2. A slight initial tension of about 7 gms was applied. This produced an initial strain in the order of 1% on the specimens. The tissue was then subjected to repeated stretches by the sinusoidal upward and downward motion of the upper clamps. Signals from the LVDT and the force transducer were connected to the amplifier assembly of the Beckman Dynograph recorder (type RM). The amplified signals were then connected to a storage oscilloscope (Tektronix 5103N). As the tissue was sinusoidally stretched, two sinusoidal traces of applied stretch and the resulting force were displayed on the oscilloscope. Any phase shift between the applied stretch and the resulting force would appear as a phase shift between the peaks of these 2 traces. When a steady-state condition was reached, permanent photographic records of these traces were taken.

Seventy-two chordae from 19 mitral valves (11 males, 8 females, ages 31-76) were tested. The specimens were selected from patients with no clinical record of mitral valve disease and whose valves appeared normal at autopsy. The valves were removed not more than 12 hours after death and stored in 0.01% merthiolate, 0.9% saline solution, at 6°C until testing. Only chordae whose cross-sectional area were nearly uniform were selected for testing and the mean cross-sectional area of each chorda was obtained with a travelling microscope. Since the mechanical properties had previously been shown to be dependent on the thickness of the chordae (chapter 3), the specimens were classified into 4 size groups and tested at three different levels of strain at a room temperature of 22 ± 1°C and not more than 3 days after removal from the heart. During this period of storage no observable changes in mechanical response was detected.

Throughout each experiment, the specimen was kept moist by wrapping it with a piece of tissue paper soaked in saline. Each specimen was stretched to one selected level of strain at the 5 different stressing frequencies. The initial lengths of all specimens were kept constant at 0.8 cm, and care was taken to ensure that the specimens were vertically mounted.

From the peaks of the sinusoidal force and stretch traces and knowing the cross-sectional area, and the initial length, values of the maximum stress, σ_0, and the maximum strain, ε_0, were evaluated. Any motion of the force transducer was corrected accordingly. The phase lag ϕ measured in radians was calculated from

$$\phi = 2\pi f \Delta t \tag{5-4}$$

where f was the frequency of the forcing function and Δt was the time difference between the occurrence of the peaks of the force and stretch curves. Any phase shift due to the equipment itself was also corrected accordingly. Equations (5-2) and (5-3) were then used to evaluate E', the storage modulus, and E", the loss modulus.

3. RESULTS

Figure 5.3(A) shows typical oscilloscope tracings of the imposed sinusoidal stretch and the corresponding sinusoidal force on the tissue. In order to determine the phase shift between these 2 traces with greater accuracy the peaks of the traces were enlarged and sweep rate on

Figure 5.3. A typical response trace taken from the oscilloscope. Chordae tendineae were stretched sinusoidally about mean strains of 3.25%, 4.75% and 5.0%.

(A) Lower trace shows the sinusoidally applied stretch and the top trace the corresponding sinusoidal force on the chordae.

(B) Peaks of the force and stretch traces enlarged and sweep rate increased for measurement of phase shift.

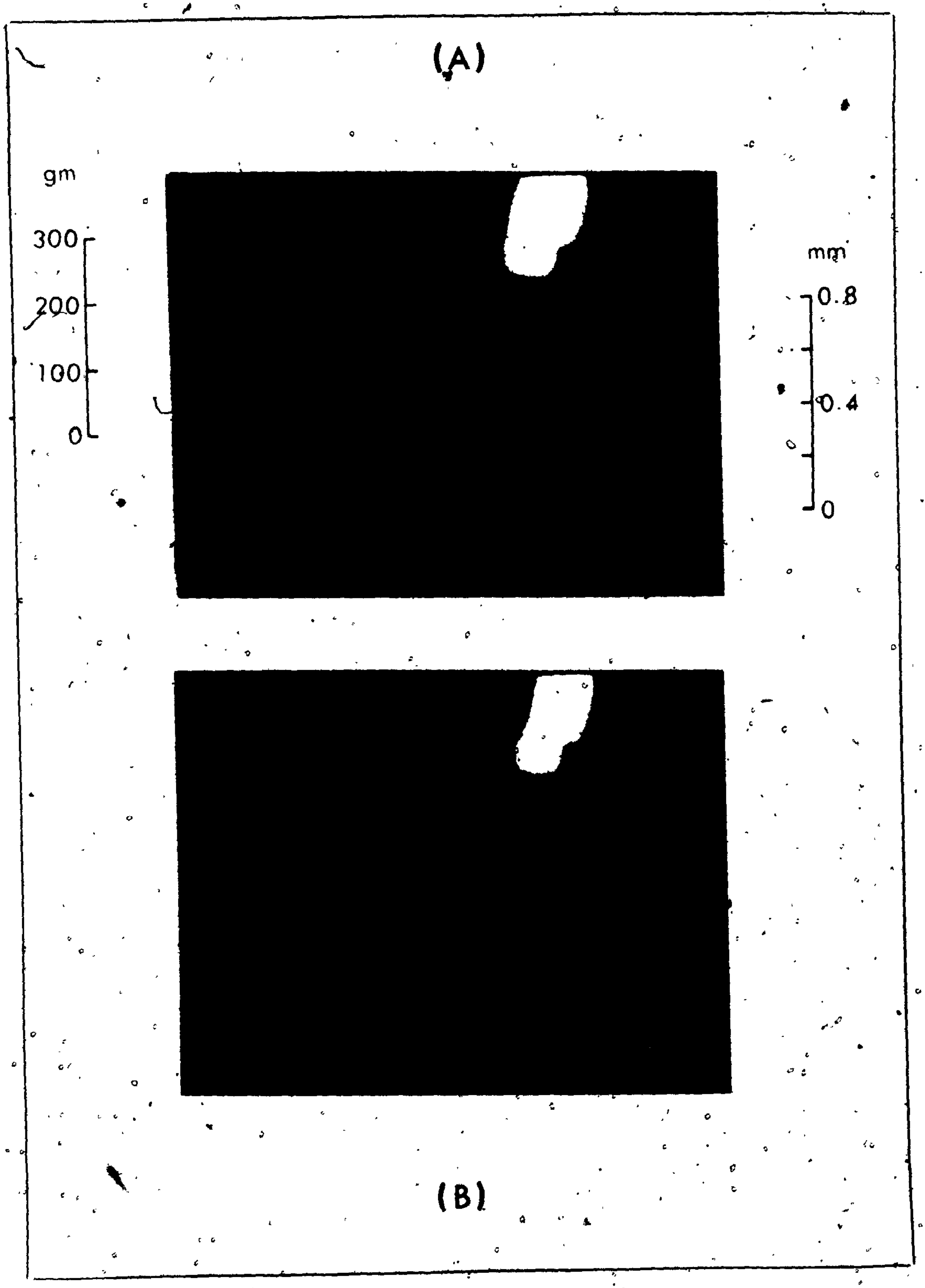
(A)
gm
300
200
100
0
mm
0.8
0.4
0
(B)

the oscilloscope increased. For both the pictures the lower trace was for the sinusoidal applied stretch and the upper trace the corresponding sinusoidal force.

Since the results in figure 5.3(A) show that the force and stretch traces were good approximations to sine waves, (in that when the traces were subjected to Fourier analysis, the variance of the fundamental harmonic accounts for more than 95% of the total variance of the series), the use of equations 5-2 and 5-3 for the evaluation of E' and E" was justified.

Table 5-I shows the average stress levels at the various strains. It was found that the stress developed was independent of the applied frequency and that the thinner the chordae the larger the stress for the same amount of strain. This finding was in agreement with my previous study on quasi-static properties (see chapter 3).

Figures 5.4 and 5.5 present the storage modulus E' for the various frequencies applied. As expected, since stress was independent of frequency, the corresponding E' values were found to behave in a similar manner. An inverse relation between chordal thickness and E' was again observed. The average values of the storage modulus for the different sized chordae at the different strain levels are also shown in Table 5-I.

Figure 5.6 shows the variation of the phase lag, with frequency. The ϕ values appeared to decrease with increasing frequency. A straight line fit to the data points gave a regression coefficient of -0.0042 which was

TABLE 5-I

Stress and storage modulus values for different sized chordae strained to different levels. E' and σ_o were found to decrease with an increase in chordal size and to increase with strain level. The sample size for each of the entries ranges from 5 to 11.

TABLE 5-I

Stress values, σ_0 ± SE (x 10^7 dyn cm^{-2})

Cross-sectional area (cm^2)	Percentage strain		
	6.5	9.5	10.0
0.001-0.003	8.85±0.28		18.51±0.64
0.004-0.006	4.30±0.22		
0.006-0.008	2.82±0.11	5.56±0.37	
0.01 -0.0[illegible]	1.23±0.04		

Storage modulus, E' ± SE (x 10^8 dyn cm^{-2})

Cross-sectional area (cm^2)	Percentage strain		
	6.5	9.5	10.0
0.001-0.003	13.63±0.49		18.55±0.60
0.004-0.006	6.79±0.41		
0.006-0.008	4.45±0.18	5.89±0.41	
0.01 -0.02	1.84±0.05		

Figure 5.4. Graph shows the storage modulus, E', versus frequency at 6.5% strain. "Area" in this and subsequent figures in this chapter is used to denote cross-sectional area of the chordae. The vertical bars indicate one standard error of the mean. The sample size for each of the points in this figure and figures 5.5 to 5.8 ranges from 5 to 11.

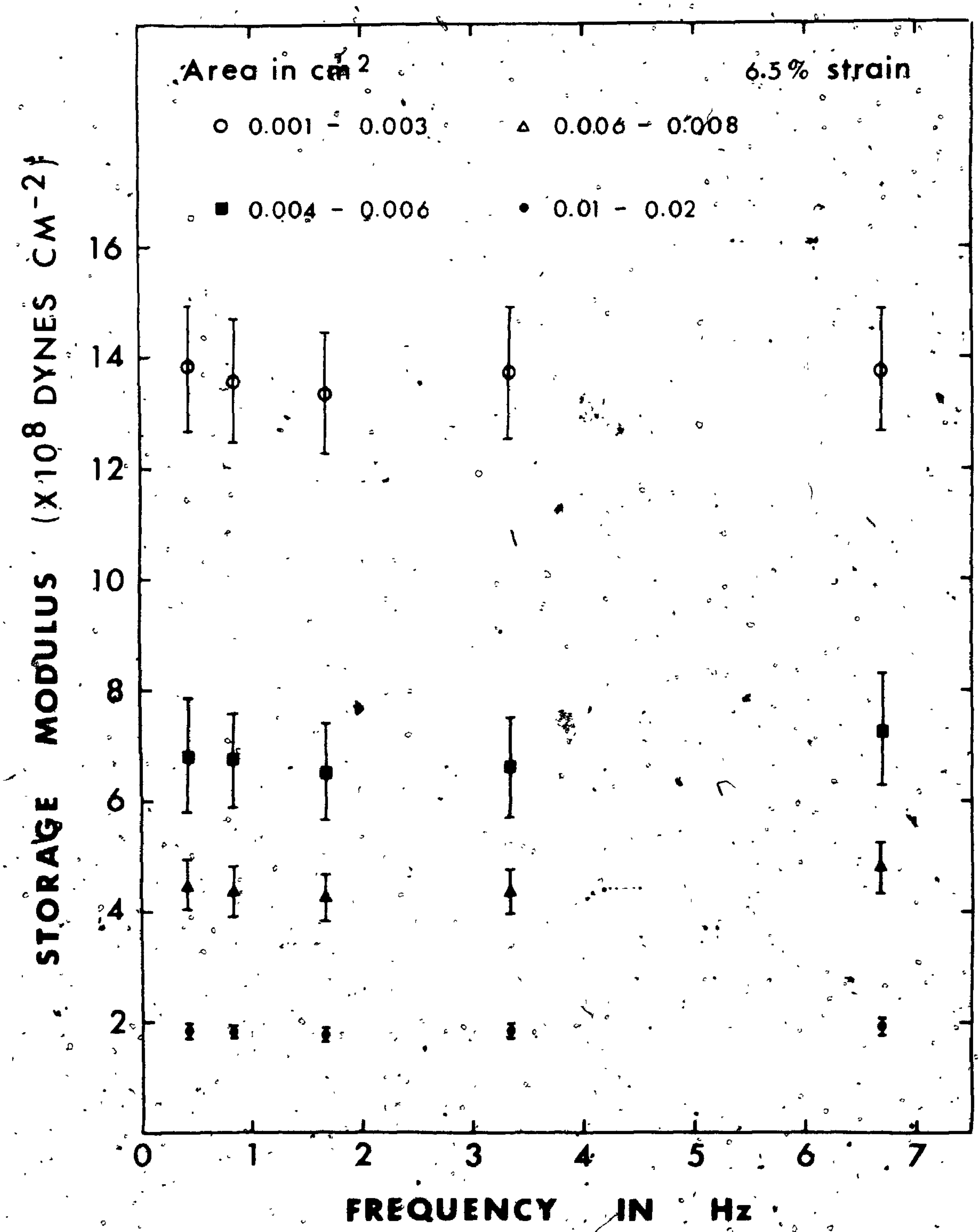
Area in cm^2
6.5% strain
○ 0.001 - 0.003
△ 0.006 - 0.008
■ 0.004 - 0.006
● 0.01 - 0.02
STORAGE MODULUS (X10^8 DYNES CM^{-2})
16
14
12
10
8
6
4
2
0
1
2
3
4
5
6
7
FREQUENCY IN Hz

Figure 5.5. Storage modulus, E', versus frequency at 10.0% and 9.5% strain. Vertical bars denote the standard error.

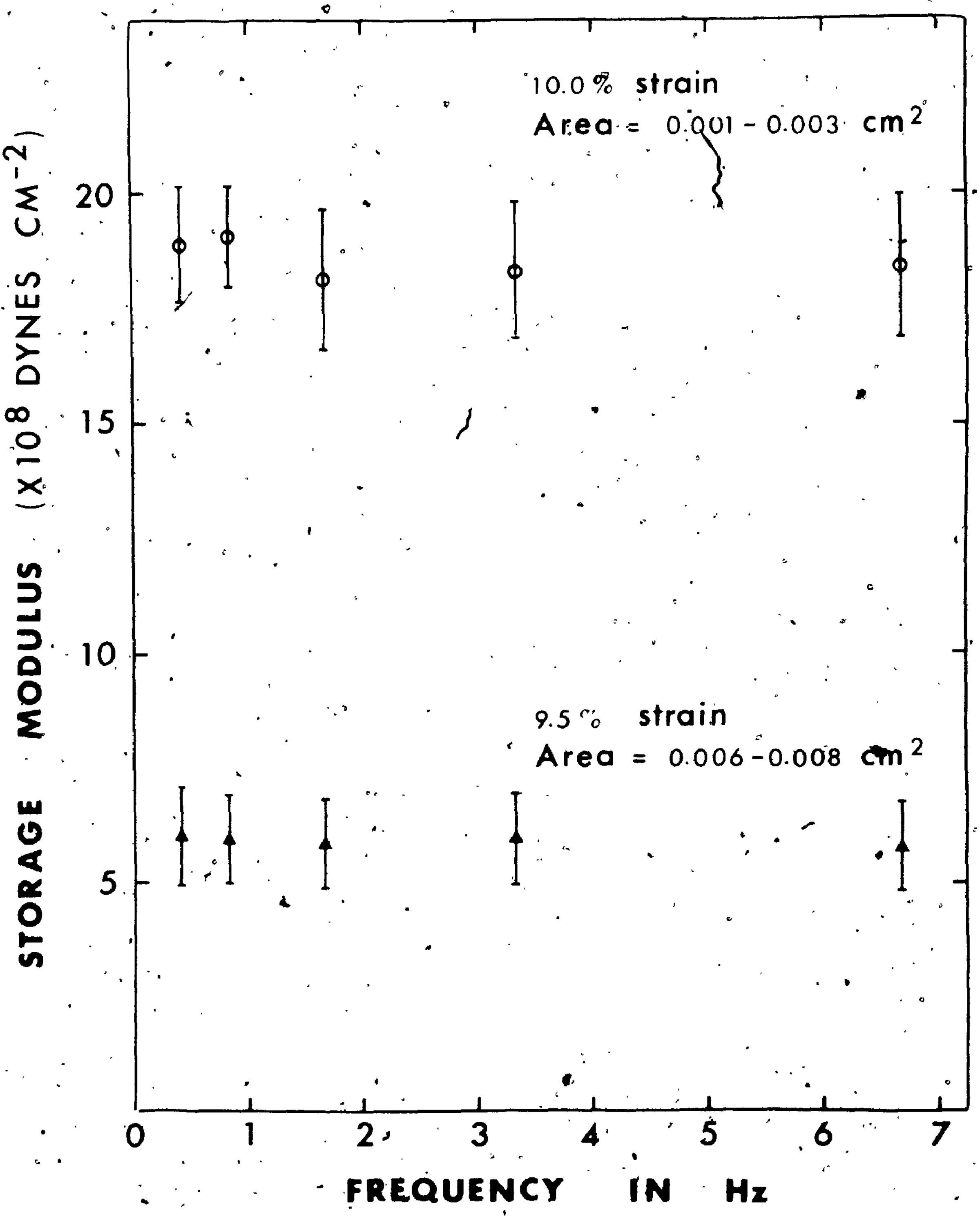
10.0 % strain
Area = 0.001 - 0.003 cm²
9.5 % strain
Area = 0.006 - 0.008 cm²
STORAGE MODULUS (X10⁸ DYNES CM⁻²)
20
15
10
5
0
1
2
3
4
5
6
7
FREQUENCY IN Hz

Figure 5.6. Graph showing the variation of phase lag, ψ, between stress and strain, with frequency.

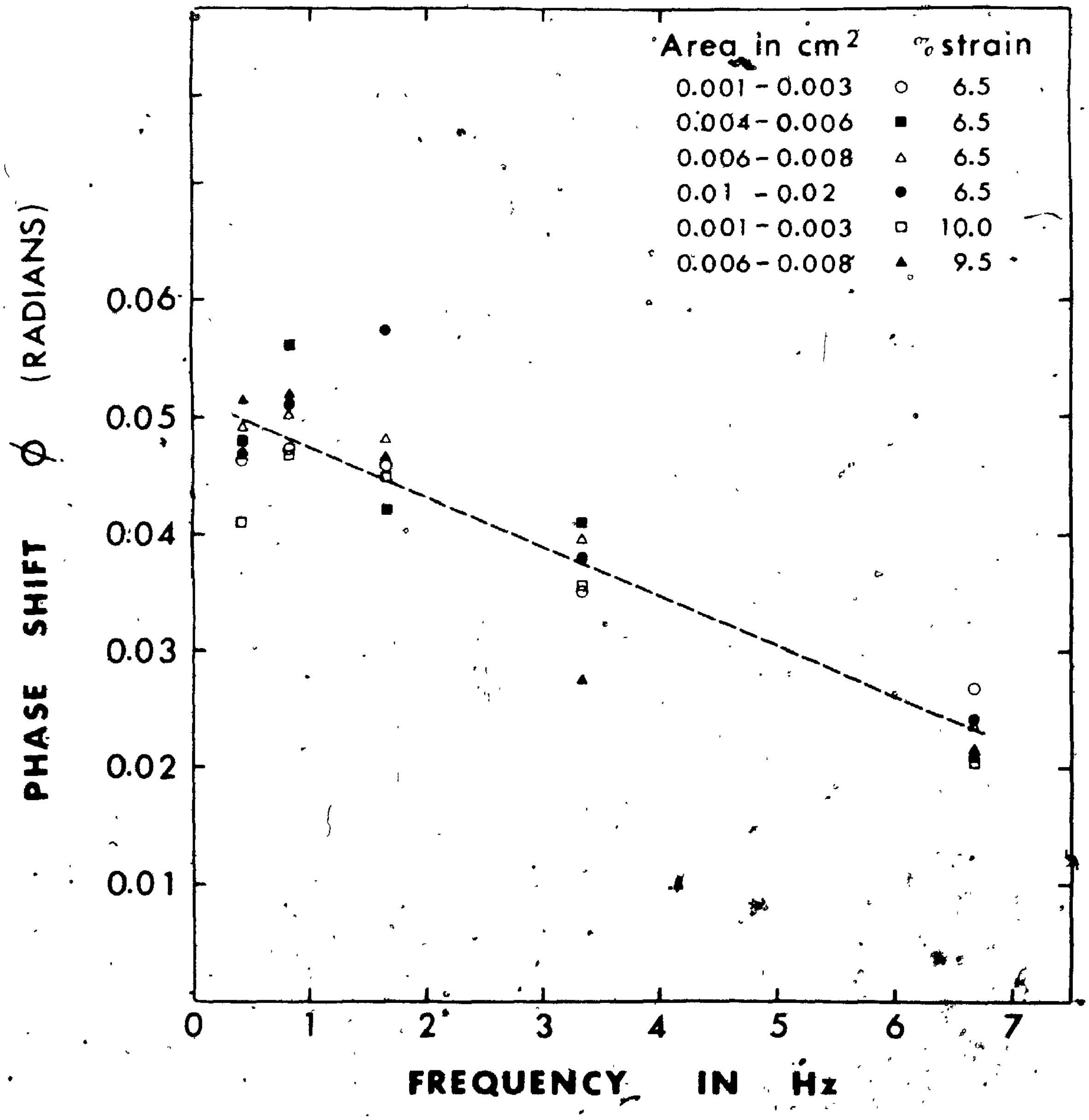
Area in cm²
% strain
0.001 - 0.003 ○ 6.5
0.004 - 0.006 ■ 6.5
0.006 - 0.008 △ 6.5
0.01 - 0.02 ● 6.5
0.001 - 0.003 □ 10.0
0.006 - 0.008 ▲ 9.5
PHASE SHIFT φ (RADIANS)
0.06
0.05
0.04
0.03
0.02
0.01
0
1
2
3
4
5
6
7
FREQUENCY IN Hz

found to be significantly different from zero (P <0.001). The phase lag at each frequency was found to be independent of chordal size and strain level. Since ϕ decreased with frequency so would the loss modulus. The behaviour of E" with frequency is presented in Figures 5.7 and 5.8. Since ϕ was independent of chordal size but stress decreased with chordal size E" was also seen to behave in like manner. The regression coefficients from straight line fits show that the slopes of the various E" plots were significantly different from zero and their values are shown in Table 5-II.

As with my previous study (chapter 3) with single uniaxial tensile stretches, the results in this investigation did not appear to vary with either sex or age (31-76 years).

4. DISCUSSION

Since chordae tendineae of the mitral valve (and also of the tricuspid valve) are repeatedly stretched throughout the entire life of an individual, the tissue was subjected to similar stress variations to elicit its viscoelastic properties. The frequency range employed included the physiological rates that the tissue would likely experience during normal function. Due to the limitations of the experimental technique, response at

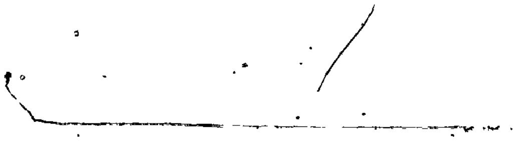

Figure 5.7. Plot of the loss modulus, E", versus frequency at 6.5% strain. Vertical bars denote one standard error.

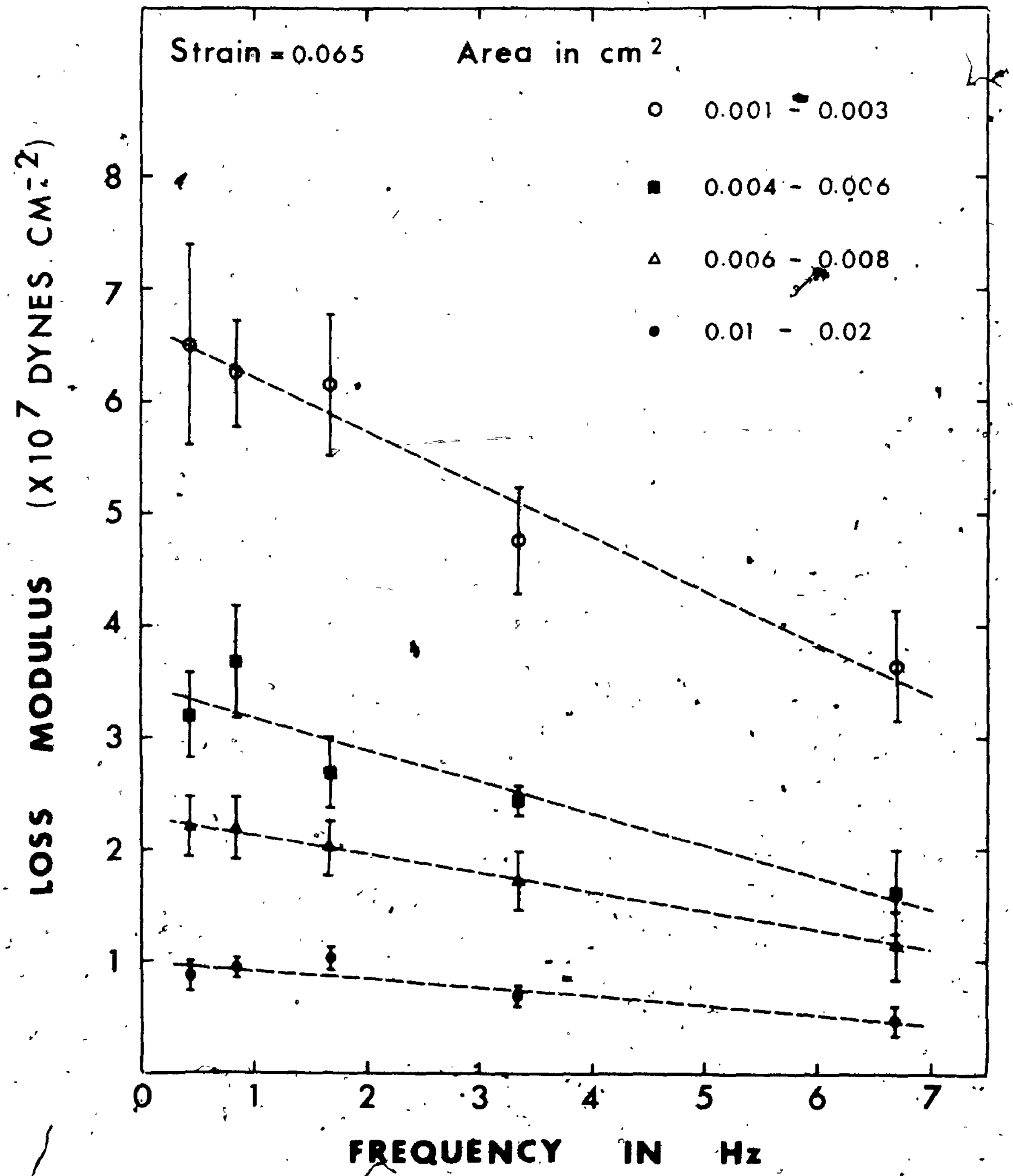
Strain = 0.065
Area in cm^2
○ 0.001 - 0.003
■ 0.004 - 0.006
△ 0.006 - 0.008
● 0.01 - 0.02
LOSS MODULUS ($\times 10^7$ DYNES CM^{-2})
1
2
3
4
5
6
7
8
0
1
2
3
4
5
6
7
FREQUENCY IN Hz

Figure 5.8. Loss modulus, E", versus frequency at 10.0% and 9.5% strain. Vertical bars denote one standard error.

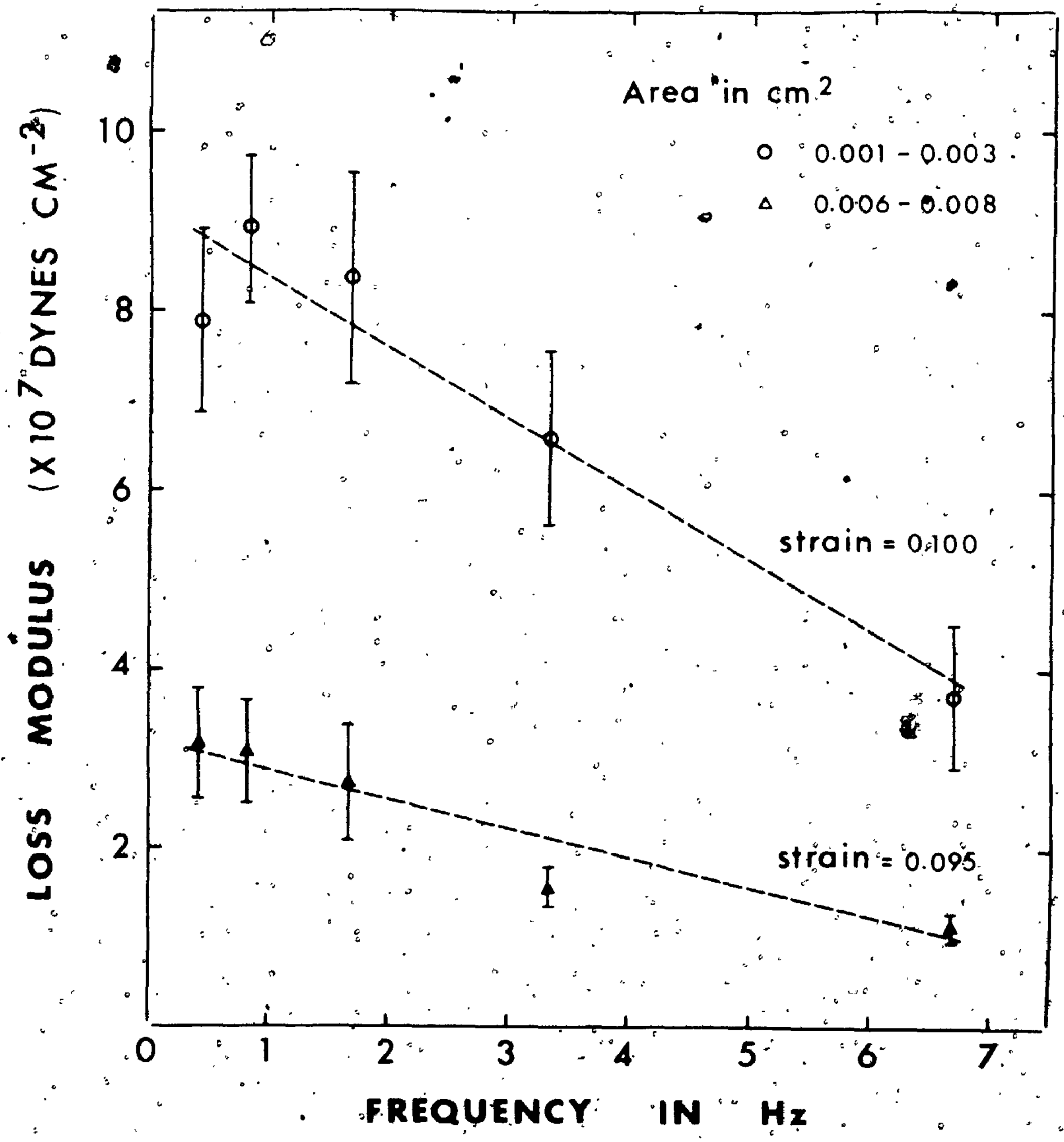
Area in cm^2
○ 0.001 - 0.003
△ 0.006 - 0.008
strain = 0.100
strain = 0.095
LOSS MODULUS (X 10^7 DYNES CM^{-2})
10
8
6
4
2
0
1
2
3
4
5
6
7
FREQUENCY IN Hz

TABLE 5-II

Regression coefficients of the loss modulus versus frequency graphs for different sized chordae tendineae and for different levels of strain. All the regression coefficients were found to be significantly different from zero.

TABLE 5-II

Regression coefficients for E" plots

Cross-sectional area (cm^2)	Coefficient (x 10^7 dyn cm^{-2} Hz^{-1})	P values	Strain level
0.001-0.003	-0.471	<0.001	6.5%
0.004-0.006	-0.285	<0.001	6.5%
0.006-0.008	-0.176	<0.01	6.5%
0.01 -0.02	-0.081	<0.01	6.5%
0.001-0.003	-0.789	<0.001	10.0%
0.006-0.008	-0.336	<0.001	9.5%

lower strains, though desirable, could not be accurately studied and hence was not performed.

The independence of stress and; hence storage modulus, at a particular strain, with frequency is an advantageous feature. This would ensure that the chordae are not overstressed with an increase in heart rate.

The low ϕ values indicate that the chordae would return very rapidly and almost completely to their original length when the stress on them is removed. This is in agreement with the studies of Clark (1973) where he reported that the elastic recovery was greater than 98%. This would be a necessary property for a structure that is stretched about 2×10^9 times during a normal lifespan.

The independence of phase lag with chordal size and strain level would enable a smooth and even closure of the valve. When the valve closes, the different sized chordae on any single valve would be stretched by different amounts. Should the phase lag between stress and response be dependent on the size of chordae and strain level, it would imply that certain chordae would attain their maximum strain before others, thus upsetting the smooth and even closure.

The finding that both phase lag and loss modulus decreased with frequency shows that the chordae do not behave like an 'orthodox' viscoelastic substance.

However, this property is both advantageous and desirable in that it would allow the chordae to respond more quickly than linear material at increased heart rates. If the reverse were to be true then complete closure of the valve might be so out of phase with ventricular systole as to render the proper functioning of the valve impossible at elevated heart rates.

The results reported in this investigation indicate that chordae tendineae possess properties that are pertinent and advantageous for the proper and coordinated functioning of the mitral valve.

5. SUMMARY

Chordae tendineae are under constant dynamic stress and, therefore, measurements of static properties alone cannot provide a complete analysis of their mechanical response under stress. This study investigated the dynamic viscoelastic properties of human mitral valve chordae tendineae. The tissue was subjected to sinusoidal stress variations over a frequency range of 0.42 to 6.68 Hz. At a fixed strain, the storage modulus, E' was found to be independent of applied frequency but varied inversely with chordal thickness. Values in the order of 10^8 to 10^9 dynes cm^{-2} were found. E' also increased with strain level. The phase lag, ϕ, between stressing function and response was found to be small

(0.02 to 0.058 radians) and decreased with frequency, thus allowing a more rapid response (than a linear viscoelastic material) at elevated heart rates. Phi values at each frequency were found to be independent of chordal size and strain level. This property would enable a smooth and even closure of the mitral valve. The loss modulus, E", was found to be 18 to 50 times smaller than E'. This implied an almost complete recovery on removal of any stress on the tissue. E', which also decreased with frequency, was found to be smaller for the larger chordae.

CHAPTER 6

THE LOW FREQUENCY DYNAMIC VISCOELASTICITY OF THE ANTERIOR LEAFLET OF THE HUMAN MITRAL VALVE

1. INTRODUCTION

The mitral valve is in a dynamic state of stress in vivo; therefore, in this study the dynamic viscoelasticity of human mitral valve leaflets for low stressing frequencies was investigated. Membranous samples were used, instead of strips of the valve tissue for, owing to the arrangement of the connective fibres, cut edges of strips could possibly weaken the tissue and, hence, lead to incorrect information on its mechanical response.

2. METHOD

a) Theory

When a linear viscoelastic material is subjected to sinusoidal mechanical stress, σ , the resulting, ε , is also sinusoidal but will be ϕ radians out of phase with the stress. The dynamic elastic modulus E* can then be written as a complex ratio.

$$E^* = \frac{\sigma}{\varepsilon} = E' + iE'' \qquad (6\text{-}1)$$

where E', the storage modulus is given by

$$E' = \frac{\sigma_o}{\varepsilon_o} \cos \phi \qquad (6-2)$$

and E", the loss modulus is given by

$$E'' = \frac{\sigma_o}{\varepsilon_o} \sin \phi \qquad (6-3)$$

where σ_o, and ε_o are the maximum stress and strain and they have to be determined experimentally. (see chapter 5 for a more detailed discussion).

b) Apparatus and Experimental Procedures

Figure 6-1 shows the apparatus used to investigate the dynamic viscoelasticity (i.e. to experimentally determine σ_o, the maximum stress, ε_o, the maximum strain and ϕ, the phase shift) of membranous samples of human mitral valve tissue. An acrylic plexiglass cylinder of internal diameter 1 cm had a circular opening of diameter 1 cm at one end and carried a piston at the other. The piston was operated by an AC-DC Universal gear motor (Bodine Type NSE-11R Model 108) connected to a frequency control built in our laboratory. Connected between the motor and the piston was an electromagnetic clutch with spring brake (Precision Instruments DX-9) and a micro-switch. This assembly allows half-cycle operations to be performed with greater accuracy at higher frequencies.

Figure 6.1. Diagram of the apparatus used to stretch membranous samples of the mitral and aortic valve leaflets.

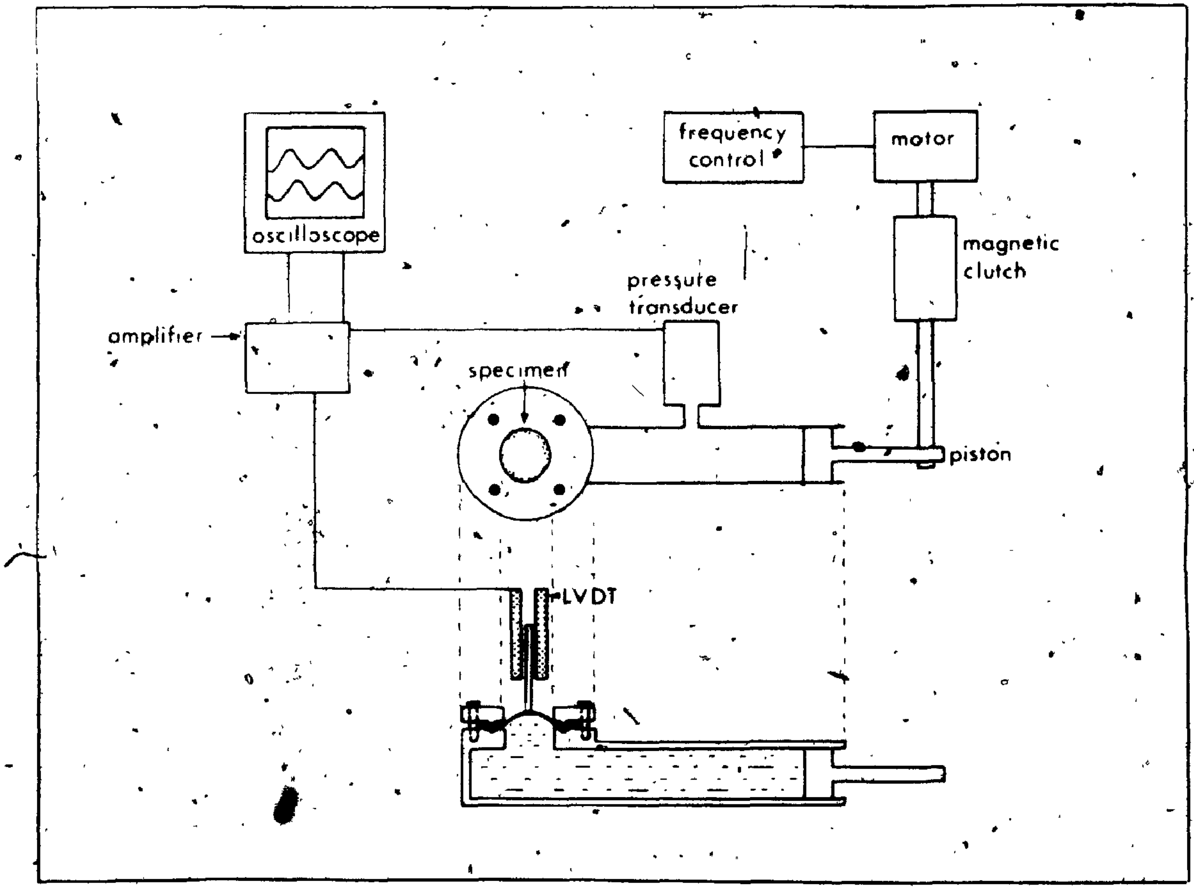
oscilloscope
frequency control
motor
magnetic clutch
pressure transducer
amplifier
specimen
piston
LVDT

Mounted on the 1 cm diameter opening of the cylinder were 2 annular rings of acrylic plexiglass which served as clamps. The rings had internal diameters of 1 cm and were constructed such that the lower ring had a groove running around its orifice and placed 1 mm away from it. At this same position, the upper removable ring had an elevated circular structure so that the rings fitted closely when a piece of material was sandwiched between them. This design of the clamps held the material firmly preventing slippage.

The cylinder was completely filled with 0.9% saline solution and when pressure was applied by moving the piston inwards, any material mounted on the clamps would be stretched and, hence, would bulge upwards. The applied pressure was measured by a pressure transducer (Statham P23DEc) connected to the side of the cylinder and the height of the bulge was measured by a light-weight core (0.52 gms) linear variable differential transformer (LVDT, Schaevitz, type 100 MHR, which according to the manufacturer's specifications, offered negligible friction during use). The core of the LVDT was attached to one end of a small, very light wooden splint whose other end rested on the top surface of the tissue (see figure 6.1). Contact between the extended core and the tissue was found to be maintained at all times for all the experiments. Signals from both the transducers were fed into the amplifier assembly of a Beckman Dynograph recorder (type RM) and the amplified signals were displayed on a storage oscilloscope (Tektronix 5103N). If the piston was made to move in a sinusoidal fashion, sinusoidal pressure variations would be sent down the cylinder and these would cause a sinusoidal bulging of whatever material that was clamped to the opening. Hence, the oscilloscope would display 2 sinusoidal traces of pressure (P) and bulge height (h) of the same frequency. Any phase shift (ϕ) between the applied sinusoidal stress and the resulting sinusoidal strain would be displayed as a phase shift between the pressure and bulge height traces.

Eighteen human mitral valves (ages 26-78, 7 females, 11 males) from patients who had no clinical record of mitral valve disease and which appeared normal at autopsy were used. The valves were removed not more than 12 hours after death and kept in 0.9% saline, 0.01% merthiolate solution at a temperature of 6°C until testing. Since the anterior leaflet of the mitral valve has the largest surface area and covers most of the left atrioventricular orifice, it was used in the experiments and pieces of diameter greater than 1 cm were cut from a region with as uniform a thickness as possible. A piece of the tissue was then placed over the opening of the saline filled cylinder and clamped. During the filling of the cylinder and the fastening of tissues, care was taken to ensure that no air bubbles were trapped. As the ventricular aspect of the mitral valve is the surface where pressure is applied in the in vivo state, the tissues were mounted with the ventricular aspect down. The mounted tissue was then subjected to sinusoidal pressure variations and the resulting pressure applied (P) and the bulge height (h) were simultaneously recorded when a steady state was achieved. Throughout the experiment the upper exposed surface of the tissue was kept moist. Permanent records in the form of photographs were taken of these traces, and from them, values of stress and strain could be calculated. In order to increase the accuracy in the determination of the phase shift, traces at high sweep rates and with the peak regions enlarged were als[illegible]ecorded. Each membranous sample was subjected to sinusoidal stress at 5 different frequencies ranging from 0.5 Hz to 5 Hz and all the experiments were performed at a room temperature of $22 \pm 1^{\circ}$C and not more than 5 days after removal from the heart. For the stresses applied, it was observed that the bulge appeared as spherical caps. To obtain stress values from the measured pressure values, the average thickness of the almost uniform sample was required, and this was obtained with a travelling microscope.

c) Analysis

Since σ_0, the maximum stress and ε_0, the maximum strain were required they had to be calculated from the measured pressure (P) and bulge height (h) values.

For a segment of a sphere cut by a single plane of radius r, the area A of the convex surface is given by

$$A = \pi(r^2 + h^2) \qquad (6\text{-}4)$$

where h is the height of the cut segment of the sphere. For a thin piece of tissue stretched to form part of a sphere from a plane configuration, h would be the height of the bulge and r the radius of the original circular unstretched tissue. Hence, the initial surface area of the unstretched tissue was

$$A_0 = \pi r^2 \qquad (6\text{-}5)$$

Therefore, the increase in area was $\Delta A = A - A_0 = \pi h^2$. Hence, the areal strain

$$\varepsilon = \frac{\Delta A}{A_0} = \frac{h^2}{r^2} \qquad (6\text{-}6)$$

Therefore ε_0, the maximum strain could be calculated from equation (6-6) when the bulge height h was maximum.

If we neglect the small edge effects and the low bending stresses, the Law of Laplace can be applied to deduce the stress on the tissues. For a membrane forming part of a sphere the Law of Laplace states that

$$P = \frac{2T}{R} \qquad (6\text{-}7)$$

where P is the pressure difference applied across the membrane, T the tensile force per unit length on the membrane and R the radius of curvature of the spherical surface. Simple calculations show that R is related to the bulge height h by

$$R = \frac{r^2 + h^2}{2h} \tag{6-8}$$

Hence,

$$T = \frac{P(r^2 + h^2)}{4h} \tag{6-9}$$

In this study P was the measured gauge pressure and if d was the thickness of the membrane, then the stress σ on the membrane is

$$\sigma = \frac{T}{d} = \frac{P(r^2 + h^2)}{4hd} \tag{6-10}$$

The maximum stress, σ_0 was calculated from equation (6-10) when P was maximum, and r in this study was 0.5 cm.

Hence from the maximum P and h values from each trace, and knowing r and d, σ_0, and ϵ_0 and, therefore the storage modulus E' and the loss modulus E" could be calculated for each frequency.

In the above analysis several assumptions were made, namely, the bending stresses and edge effects due to clamping of the specimen were negligible and that the spherical cap formed was thin walled. These assumptions have to be justified.

In engineering practice, it is customary to consider a surface as thin walled if the $\frac{R}{d}$ ratio is approximately 10 or larger. In my experiments, the bulge height was typically of the order of 0.1 cm and this gives a R value of about 1.3 cm. Since d was also of the order of 0.1 cm the $\frac{R}{d}$ ratio is about 13. Hence, the assumption of a thin walled spherical cap is justified.

As is known in the theory of plates and shells (Flugge, 1960) the bending rigidity of a thin isotropic plate or a thin shell is proportional to the third power of the wall thickness whereas the extensional rigidity is proportional to the wall thickness. Since the thickness of the specimens was mostly of the order of 0.1 cm or less the bending stresses would be small compared to the extensional stresses.

To show that the edge effects were negligible, experiments were performed with a piece of rubber using 2 different openings of the cylinder of diameter 0.6 cm and 1.0 cm. At the same strain, the results obtained with the piece of rubber were comparable, differing by less than 5%, thus indicating that the edge effects can be ignored.

To show further that the experimental technique and the analysis with its approximations were valid, pieces of thoracic aorta from dogs were tested. The results obtained were comparable in magnitude to those reported by Bergel (1961) and Patel et al (1970).

3. RESULTS

Figure 6.2(A) shows a typical oscilloscope trace of the imposed sinusoidal pressure (top trace) and the corresponding resulting sinusoidal bulging of the tissue (bottom trace). It was observed from such traces that at low sweep rates the phase shift between the 2 traces was hardly discernable and in order to visualize a possible phase shift with any degree of accuracy, the peaks of the 2 traces were enlarged and the sweep rate increased. Figure 6.2(B) shows such an enlarged trace (top, pressure; bottom, bulge height) where the phase shift can now be quite readily seen, and the response (bulging height trace) was observed to lag behind the forcing function (pressure trace). Since these traces were obtained as a variation with time on the oscilloscope the phase shift ϕ (radians) was obtained from the following formula

$$\phi = 2\pi f \Delta t \qquad (6\text{-}11)$$

where f was the imposed frequency in hertz and Δt in seconds was the time difference observed between the occurrence of the 2 peaks.

The results of Figures 6.3 to 6.6 cover a small range of areal strain of 1.5% to 5%. Figure 6.3 is a plot of the observed phase lag ϕ for 5 different frequency values. There appeared to be a gradual increase of ϕ as frequency increased and a straight line fit to the experimental points showed

Figure 6.2. An actual typical response curve taken from the oscilloscope. (A) Top curve shows the imposed sinusoidal pressure variations and the lower trace the resulting sinusoidal bulging of the mitral leaflet.

(B) Peaks of the pressure and bulge height traces enlarged and the sweep rate increased.

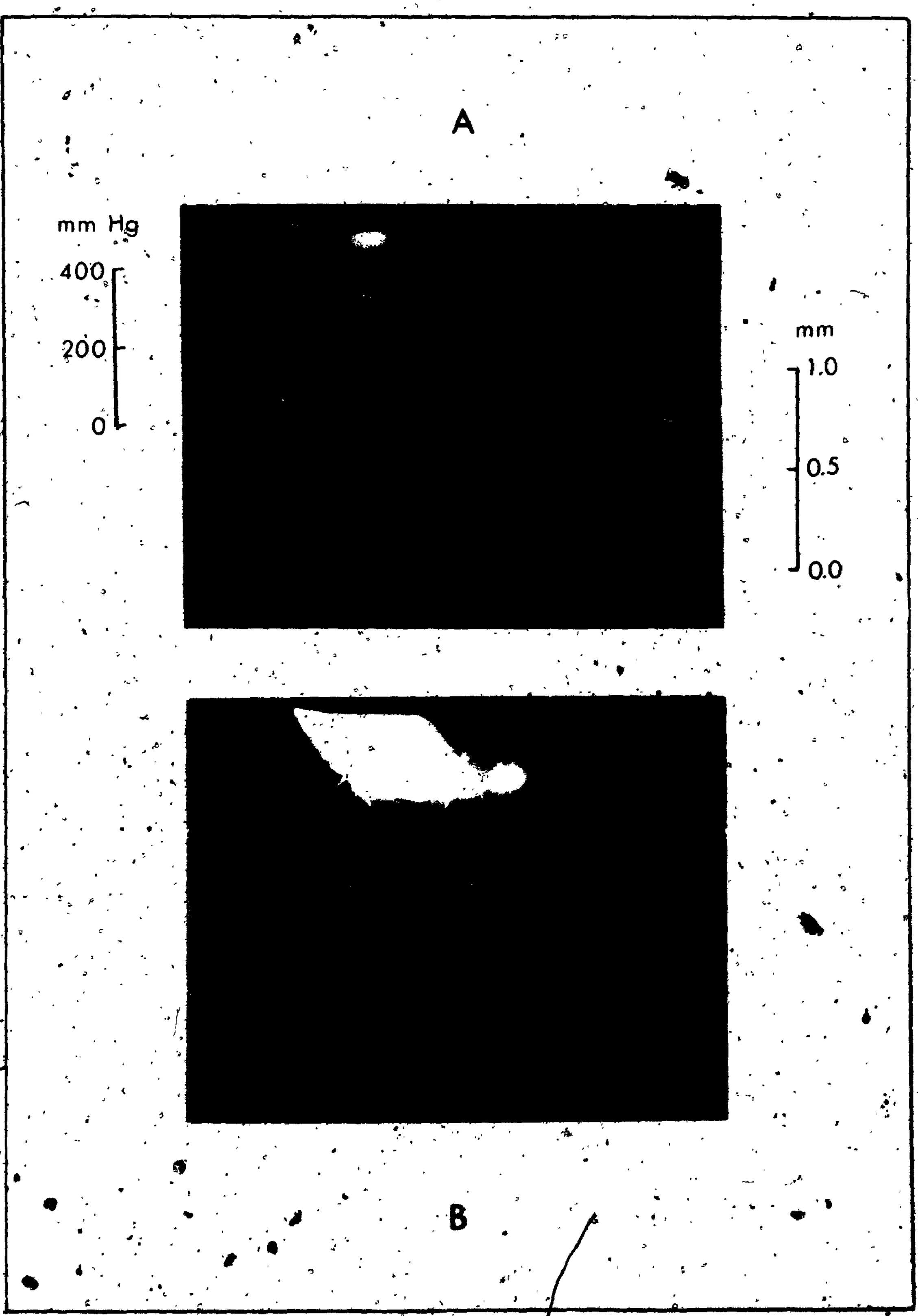
A
mm Hg
400
200
0
mm
1.0
0.5
0.0
B

Figure 6.3. Phase lag ϕ, between the stressing function and the response, plotted against frequency. The vertical bars show the standard error and the dotted lines indicate the 95% confidence interval for the true regression line.

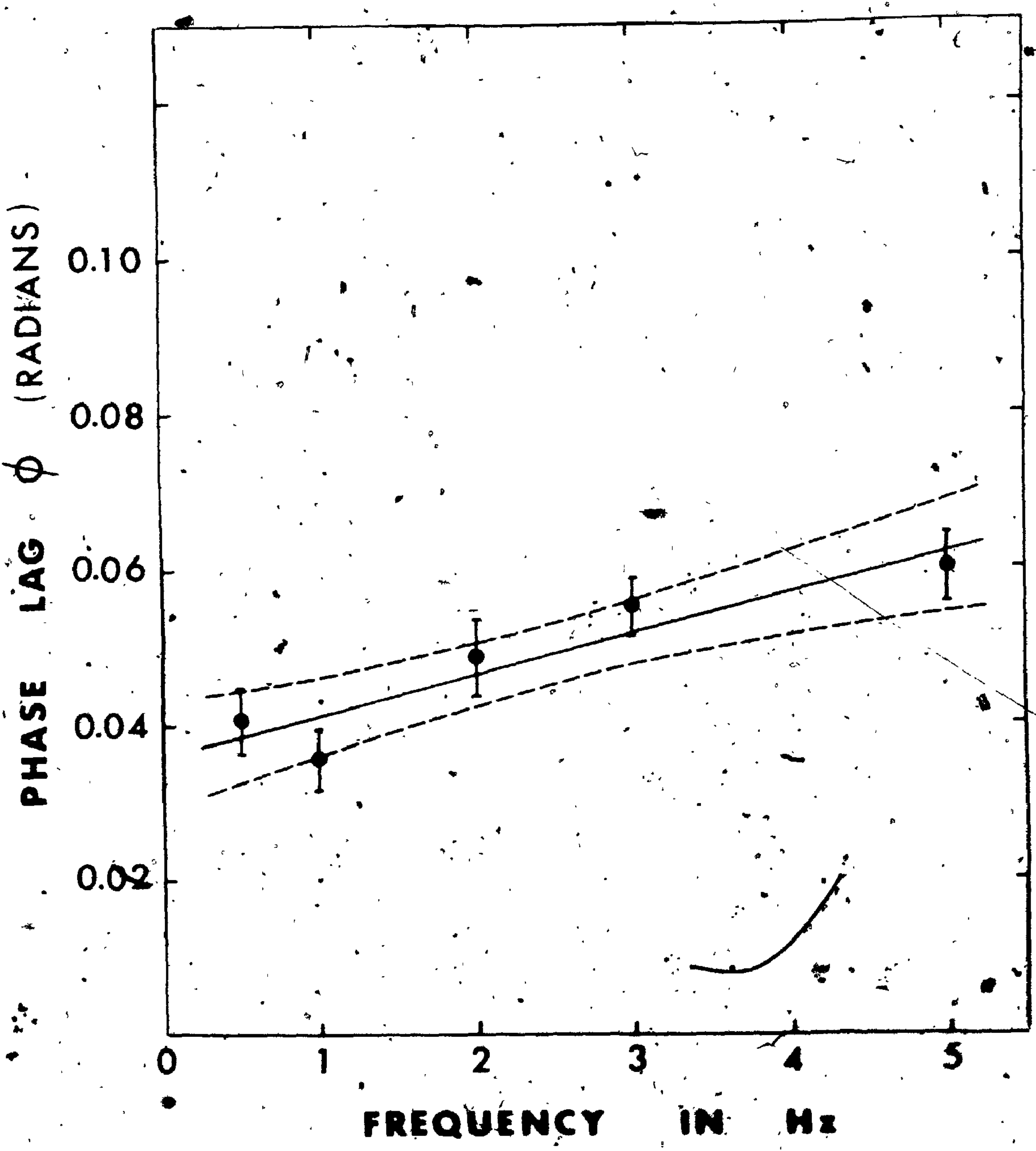
PHASE LAG ϕ (RADIANS)
0.10
0.08
0.06
0.04
0.02
0
1
2
3
4
5
FREQUENCY IN Hz

that the slope was significantly different from zero ($P < 0.001$), with a regression coefficient of 0.0052 (SE = 0.0012), thus there was an increase in phase lag with frequency. For physiological frequencies, ϕ was small. Small ϕ values indicate that the tissue has little viscous resistance and, hence, would recover very rapidly to its original state when the stress on it is removed.

Figure 6.4 shows the variations of the dynamic modulus with frequency. The top curve is a graph of the in phase or storage modulus E' versus frequency. The slope of the best straight line was found to be not significantly different from zero ($P > 0.3$). Thus, E' was quite independent of the frequency values investigated and an average value of 2.55 (SE = 0.12) $\times 10^8$ dynes cm^{-2} was found. The lower group of experimental points show the relation of the out of phase or loss modulus E" with frequency. As expected, since ϕ increased with frequency, E" was observed to behave in a similar manner, and the best straight line fit had a slope that was significantly different from zero ($P < 0.001$), with a regression coefficient of 0.015 (SE = 0.004).

The dynamic moduli were found to be similar for both sexes. Of the 18 valves studied, 3 were from patients below 40 years of age and the rest were 54 years and over. For the latter group, the moduli were found to be

Figure 6.4. Dynamic elastic moduli of the anterior leaflet of the mitral valve. Top trace shows the variation of the storage modulus, E', with frequency and the lower graph shows the variation of the loss modulus, E", with frequency. The vertical bars show the standard error and the dotted lines indicate the 95% confidence interval for the true regression line.

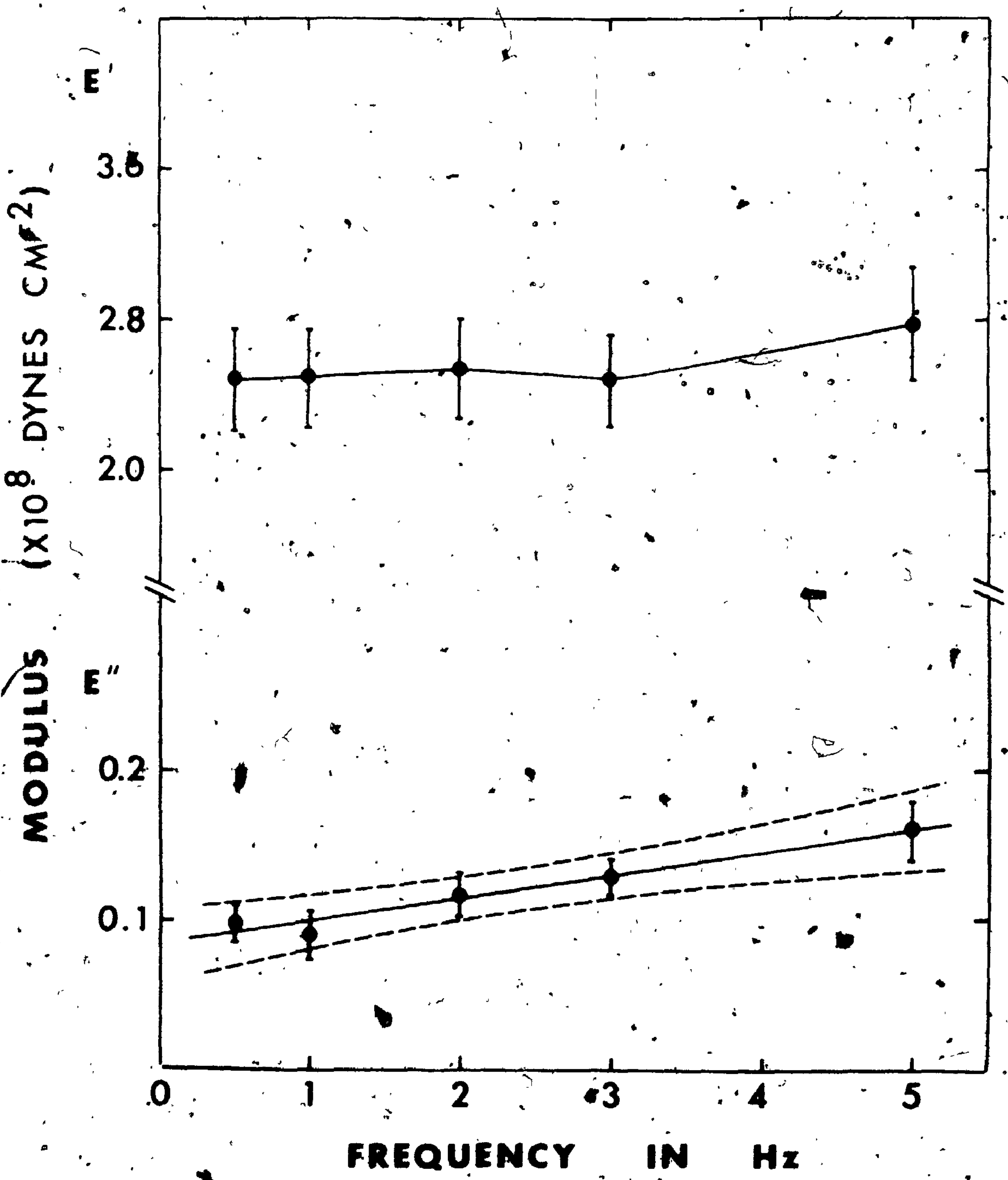
E'
3.6
2.8
2.0
E''
0.2
0.1
0
1
2
3
4
5
MODULUS (X10⁸ DYNES CM⁻²)
FREQUENCY IN Hz

quite independent of age. Though statistical analysis showed that the 3 relatively young cases were similar to the older age group, we cannot however make any definite conclusions about dependency on age for the group as a whole as the sample size was small for the younger age group.

In order to provide a clearer idea of the pressure required to strain the tissue, Figure 6.5 is presented as a graph of pressure per millimetre of tissue thickness required to produce the corresponding areal strain. Since tissue thickness was typically in the order of 1 mm, this value was chosen. The scatter of data points could be due to the use of different specimens. The best straight line fit to the data points, shows that for every increase of valve area by 1% a pressure of about 200 mm Hg was required. This is far above the normal systolic left ventricular pressure in humans. Similar values were found for all the other frequencies investigated.

4. DISCUSSION

The approach adopted in this study for investigating the viscoelastic property of the human mitral valve leaflet was designed to simulate the normal conditions under which the tissue is stressed. Sinusoidal fluid pressure was used as the imposed stressing function on the ventricular aspect

Figure 6.5. Graph showing pressure per mm tissue thickness required to produce the corresponding areal strain on the mitral leaflet. Frequency = 3 Hz. The dotted lines show the standard error of the slope.

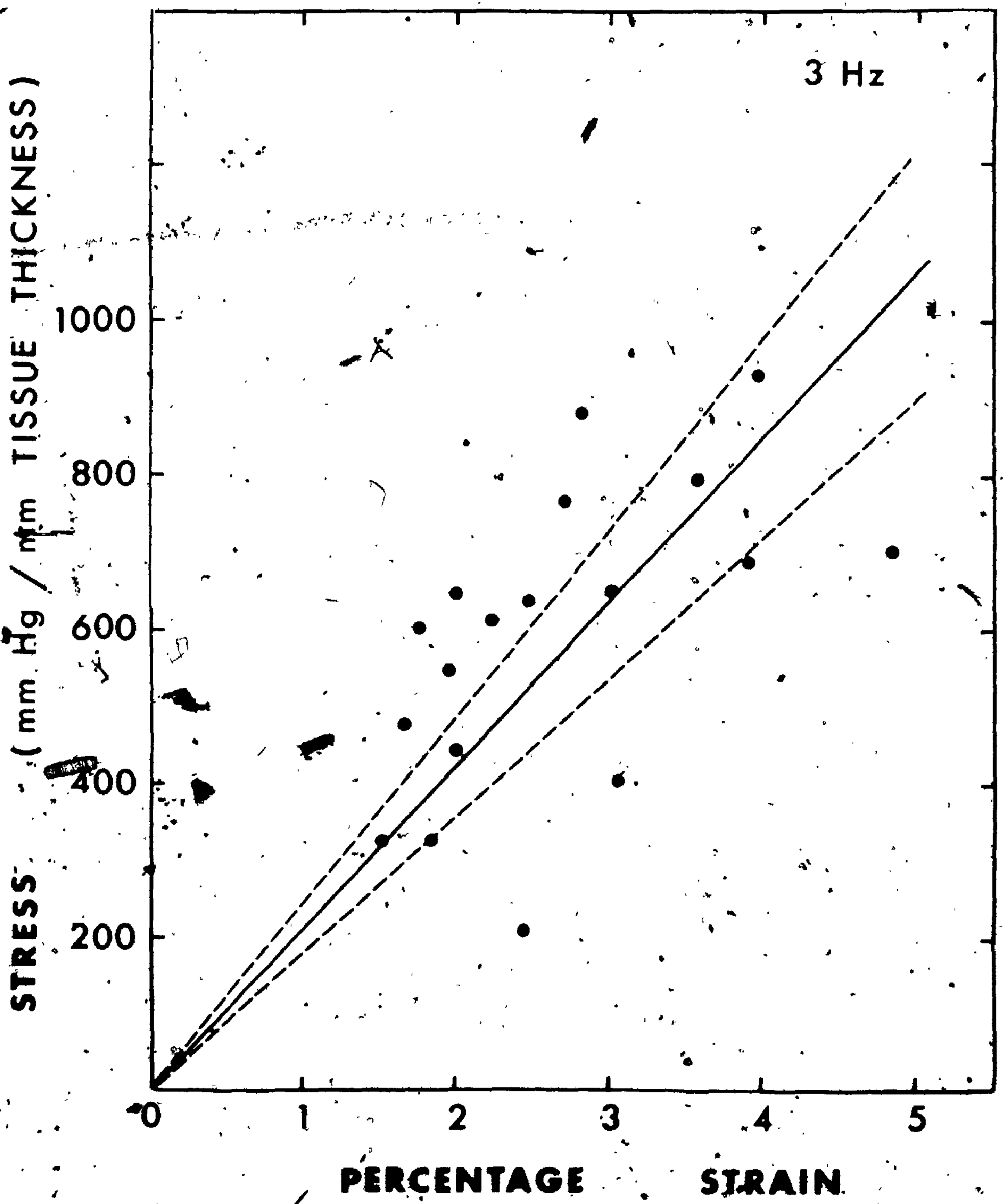
3 Hz
STRESS (mm Hg / mm TISSUE THICKNESS)
1000
800
600
400
200
0
1
2
3
4
5
PERCENTAGE STRAIN

of the valve leaflet, as in the in vivo condition. This study differs from other investigations on the same topic in that dynamic rather than static responses were investigated and membranous samples of tissue rather than strips were used. Fenoglio et al (1972) have reported that for canine anterior mitral valve leaflets, collagen fibres originating from the core of chordae tendineae criss-cross as they course towards the mitral annulus, thus producing a basket weave effect. If strips of tissue are cut from such an arrangement and then stressed, the data obtained may not be representative of the actual state, as the cut edges of such a weave could well weaken the whole structure. The frequency range in my study was designed to include the spectrum of frequency values to which a normal functioning valve might be subjected.

The results presented in Figures 6.3, 6.4 and 6.5 show that the anterior human mitral valve leaflet is a rather inextensible material with a low loss modulus (E"). This is in contrast to materials like dog aorta whose dynamic moduli reported by Patel et al (1970) are of the order of 10^6 dynes cm^{-2}, and which have a higher loss. The low loss observed is in fact advantageous to a structure that is under constant dynamic stress, in that energy loss will be low and hence heating effects minimal. The rather high storage modulus (E') value at low strain could well reflect the criss-cross arrangement of the stress bearing components of the valve tissue. The behaviour of E' and E" with frequency is somewhat similar to those observed for vulcanized rubber over the frequency range investigated (Ferry, 1961). Hence, any material used as a substitute for the mitral valve should be rather inextensible and have a low loss modulus.

In a normal cardiac cycle, pressure in the left atrium is not constant and the atrial pressure curve shows three major pressure elevations, the a, c, and v waves (see figure 1.3). The presence of the 'c' wave has been attributed to the bulging of the mitral valve (and in particular the valve leaflets) into the left atrium during ventricular systole (Guyton, 1971; Massumi et al, 1973). Since the left atrium is open to veins which have a large capacitance and low wall distensibility any increase in atrial pressure must necessarily imply a large volume displacement and hence a considerable bulging of the mitral valve. However, Rushmer et al (1956) using cine-fluorographic techniques showed that the excursion of the leaflets was small and at no time did the valve edges ascend to the plane of the mitral ring. Their study therefore suggests that the mitral valve may not bulge into the left atrium. Rushmer (1970) also pointed out that the mitral bulging observed by other investigators could be due to the fact that exposed or excised hearts tend to shrink and function at abnormally small dimensions. Under these conditions, the valves may have a great deal more slack and thus could execute wider excursions and lead to the bulging that was observed.

These differences in opinion on mitral bulging may be resolved by a consideration of the extensibility of the papillary muscles, valve leaflets and chordae tendineae, since the bulging of the valve during ventricular systole, if present, would involve the stretching of these structures.

Grimm, Lendrum and Lin (1975), using cineradiography revealed that the papillary muscles of intact dogs in fact shorten by about 22.8% during cardiac function. Their results thus show that the papillary muscles are not extended during valve closure.

It is also unlikely that the bulging could be attributed to the stretching of the valve leaflets. The results in this chapter show that the high storage modulus of the valve tissue implies that a large amount of force is necessary to stretch the material, as reflected in the graph of Figure 6.5. Since maximum systolic left ventricular pressure is typically about 120 mm Hg, my results indicate that even if all the stresses on the mitral valve were borne by the anterior leaflet, the tissue would experience strains of less than 1%. The presence of chordae tendineae would reduce this amount considerably. The possible bulging of the mitral valve cannot be explained by the stretching of the chordae tendineae either. Typically there are some 25 first order primary chordae tendineae (Roberts and Cohen, 1972) with an average cross-sectional area of 5×10^{-3} cm^2. The stress sustained by each of these, assuming a mitral ring of about 8.5 cm^2 (Brock, 1952; Burch and DePasquale, 1965), would be about 1×10^7 dynes cm^{-2}. This stress value is similar to that obtained by Salisbury et al (1963) where they attached force transducers to the chordae of mongrel dogs and measured the tension sustained in situ throughout the cardiac cycle. This stress, applied to the chordae at a strain rate of 1600% min^{-1} produces a strain of only about 4% (see chapter 3). In addition, the chordae further dissipate this force by their many branchings, thus reducing the strain. From these estimates, it can be concluded that under normal physiological conditions, the elasticity of the mitral valve and chordae tendineae permits them to withstand normal physiological stress with negligible stretching. This observation, together with the shortening of the papillary muscles, makes it unlikely that the mitral valve would bulge into the left atrium to produce the atrial 'c' wave.

3 OF/DE 3

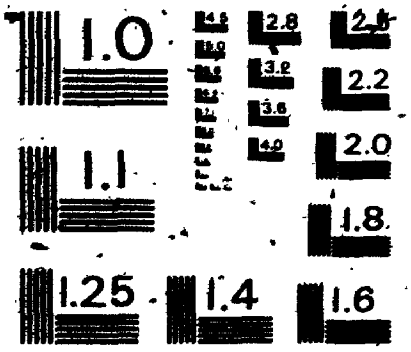
1.0
1.1
1.25
1.4
1.6
1.8
2.0
2.2
2.5
2.8
3.2
3.6
4.0

MICROCOPY RESOLUTION TEST CHART
NATIONAL BUREAU OF STANDARDS – 1963 – A

5. SUMMARY

The dynamic viscoelasticity of the anterior leaflet of human mitral valves was investigated by subjecting the ventricular aspect of membranous samples of the tissue to sinusoidal fluid pressures. The frequency range of the stressing function used was from 0.5 Hz to 5 Hz. The storage modulus of the tissue was found to be independent of the stressing frequency and an average value of 2.55 (SE = 0.12) x 10^8 dynes cm^{-2} was observed. Losses were small and the phase shift between stressing function and resulting strain and hence the loss modulus increased with frequency. For the frequency range investigated the phase shift varied from 0.04 to 0.06 radians and the loss modulus was of the order of 10^7 dynes cm^{-2}. From the observed data it was concluded that any tissue substitute used in mitral valve replacement should be rather inextensible and have a low loss modulus. Also under normal physiological conditions, the mitral valve cannot bulge into the left atrium during peak ventricular systole and hence events in the cardiac cycle, such as the presence of the atrial pressure 'c' wave, that involve the distensibility of the valve need to be re-examined.

CHAPTER 7

THE LOW FREQUENCY DYNAMIC VISCOELASTICITY OF THE HUMAN AORTIC VALVE CUSPS

1. INTRODUCTION

As with the mitral valve, the aortic valve is in a dynamic state of stress in the natural condition. This chapter therefore, investigates the dynamic elasticity of human aortic valve cusps for low stressing frequencies. Similarly, large disc shaped samples of the membranous valve cusps rather than strips of tissues were used.

2. METHOD

The theory and experimental approach used in this study were the same as those for the mitral valve leaflets. The details of these were outlined in chapter 6 and, hence a repetition here is deemed unnecessary.

In this study, 14 human aortic valves (ages 40-76, 6 females and 8 males) from patients with no clinical record of aortic valve disease and whose valves appeared normal at autopsy were used. The cusps were removed, identified according to site of attachment to the aorta and kept in 0.9% saline, 0.01% merthiolate solution at a temperature of 6°C until testing. As with the mitral valve the aortic valve cusps were all removed not more than 12 hours after death, and as far as possible all 3 cusps from each valve were tested. Pieces of diameter greater than 1 cm were cut from the central portion of each cusp, where the thickness was found to be fairly uniform. This tissue was then placed over the opening of the saline filled cylinder and clamped (see figure 6.1). During the filling of the cylinder and the fastening of tissues, care was taken to ensure that no air bubbles were trapped. As the aortic aspect of the cusp is the surface upon which most pressure is applied in the in vivo state, the tissues were mounted with this surface down. The mounted tissue was then subjected to sinusoidal pressure variations and the applied pressure (P) and the resultant bulge height (h) were simultaneously recorded when a steady state was achieved. Permanent records in the form of photographs were taken of these traces, and from them, values of stress and strain were calculated. In order to increase the accuracy in the determination of the phase shift, traces at sweep rates as high as 63.5 cm sec^{-1}, and with the peak regions enlarged were also recorded. Each membranous sample was subjected to sinusoidal stresses at 5 different frequencies ranging from 0.5 Hz to 5 Hz and all the experiments were performed as soon as possible at a room temperature of 22 ± 1°C and not more than 3 days after removal from the heart. To obtain stress values from the measured pressure values, the average thickness of the nearly uniform sample was required, and this was obtained with a travelling microscope.

The analysis used in this study was similar to that used for the mitral valve leaflets. In that analysis several assumptions were made, namely, the tissue was stretched to form part of a sphere, the bending stresses and edge effects due to clamping of the specimen were negligible and that the spherical cap formed was thin-walled. Some of these assumptions have to be justified for the aortic cusps as well.

To show that the tissue bulged to form a spherical cap, the elevations of different regions of the cap were measured. From the maximum height of the cap the expected elevations of these regions were calculated by assuming a spherical bulge. Most of the calculated and measured values were in relatively good agreement, differing on the average by 15.8% (SE = 1.9%, range 0% to 30%). This value was found by treating all overestimates and underestimates as positive differences. Hence, to a first approximation the assumption of a spherical configuration is justified.

It is customary to consider a surface as thin walled if the $\frac{R}{d}$ ratio is approximately 10 or larger.

In the experiments, the bulge height was of the order of 0.1 cm, giving a R value of about 1.3 cm. Since d was in the order of 0.06 cm the $\frac{R}{d}$ ratio was about 22. Hence, the spherical cap can be considered as thin walled.

In the theory of plates and shells the bending rigidity of a thin isotropic plate or a thin shell is proportional to d^3 whereas the extensional rigidity is proportional to d, the thickness (Flugge, 1960). For values of d less than 1, d^3 would be smaller than d. Since the thickness of the specimens was of the order of 0.06 cm, the bending stresses would be small in comparison to the extensional stresses.

3. RESULTS

The top trace of Figure 7.1(A) shows a typical oscilloscope trace of the imposed pressure while the lower trace shows the resulting sinusoidal bulging of the tissue. In order to visualize any possible phase shift with greater accuracy the peaks of the 2 traces were enlarged and the sweep rate increased. Figure 7.1(B) shows such an enlarged tracing (top for pressure, lower trace for bulge height), and the response was observed to lag behind the forcing function. Since these traces were good approximations to sine waves, (in that when subjected to Fourier analysis, the variance of the first harmonic accounts for more than 95% of the total variance of the series) the use of equations

Figure 7.1. An actual typical response trace taken from the storage oscilloscope. (A) Top trace shows the imposed sinusoidal pressure and the lower trace the resulting sinusoidal bulging of the clamped aortic tissue.

(B) Peak of the pressure and bulge height traces enlarged and, the sweep rate increased.

(A)

mm Hg
400
200
0
mm
1.5
1.0
0.5
0.0

(B)

6-2 and 6-3 for the evaluation of E' and E" was justified. The phase shift ϕ in radians was calculated from the following formula

$$\phi = 2\pi f\Delta t$$

where f is the imposed frequency in hertz and Δt in seconds was the time difference between the occurrence of the 2 peaks.

The results shown in Figures 7.2 and 7.3 cover a small range of areal strain of 2% to 4.5%. Statistical analysis showed that the response of tissues tested immediately after removal from the heart was not significantly different from those that were stored up to 3 days. The variation of phase lag ϕ with frequency is shown in figure 7.2. All values were found to be low and there appeared to be a drop in ϕ at 5 Hz. However, a simple analysis of variance indicated that the difference between the ϕ values was not significant ($P > 0.05$) and an average value of 0.033 (SE = 0.002) radians was found. The low ϕ values indicate that the tissue has little viscous resistance and, hence, would recover very rapidly to its original state on removal of any applied stress. This property is advantageous to a structure that is under constant dynamic stress.

Figure 7.3 shows the variations of the dynamic modulus with frequency. The data points on the top of the

Figure 7.2. Phase lag, ϕ , between stressing function and response, plotted against frequency. The vertical bars show the standard error. The sample size for each of the points in this and figure 7.3 is 16.

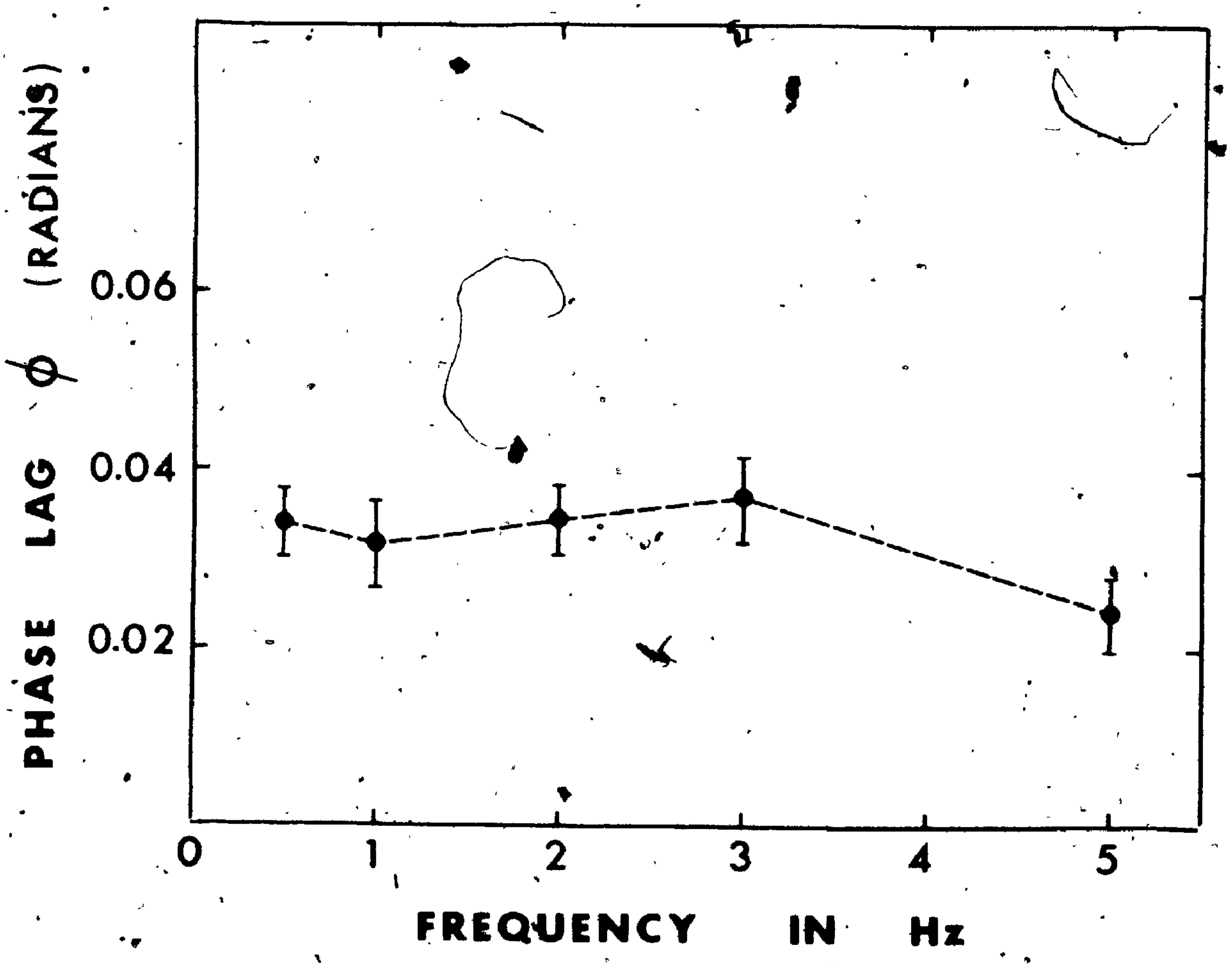
PHASE LAG ϕ (RADIANS)
0.06
0.04
0.02
0
1
2
3
4
5
FREQUENCY IN Hz

Figure7.3. Dynamic elastic moduli of aortic valve cusps. The top graph shows the variation of the storage modulus, E', with frequency and the lower graph shows the variation of the loss modulus, E", with frequency. The vertical bars indicate the standard error.

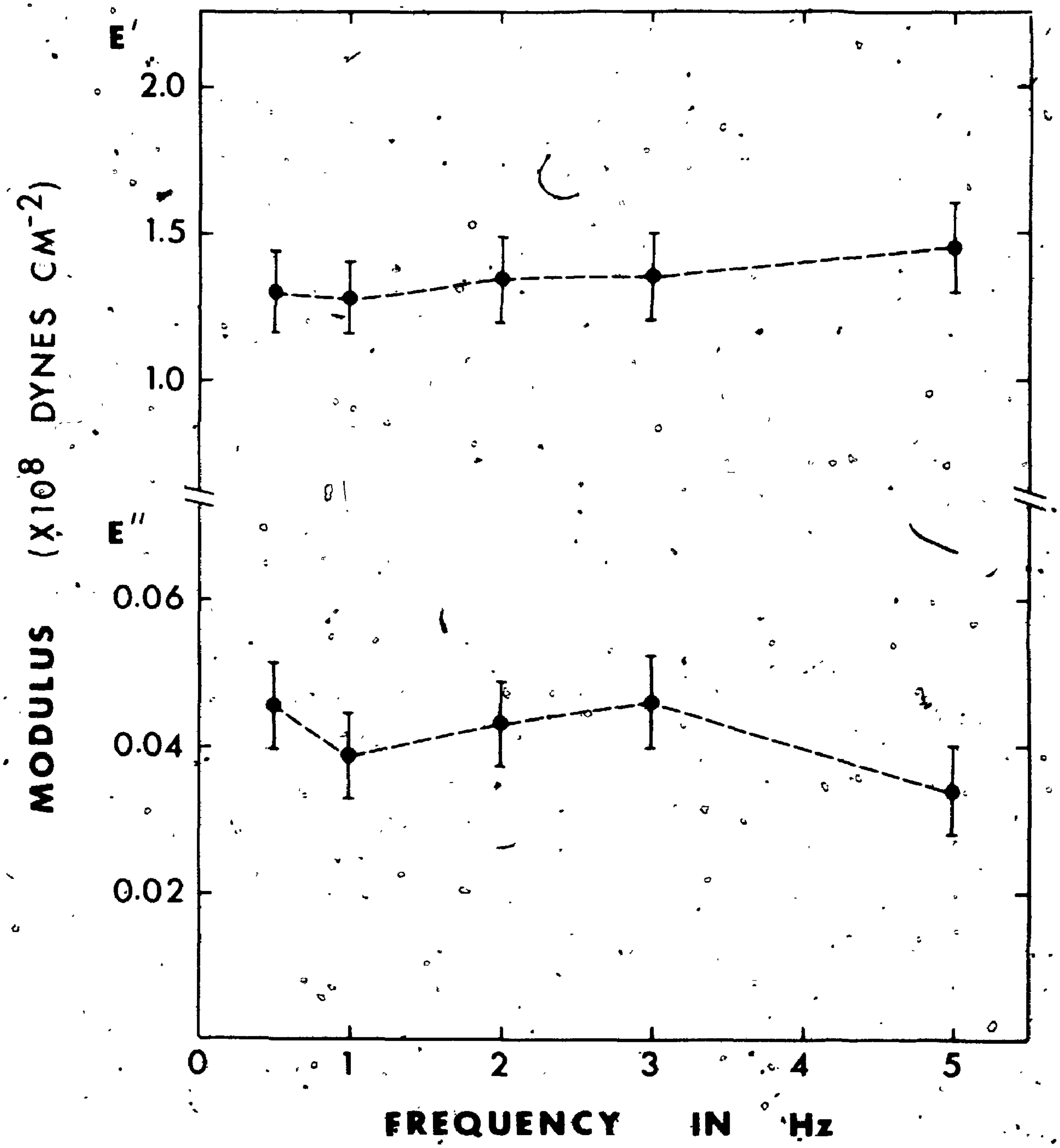
E′
E″
2.0
1.5
1.0
0.06
0.04
0.02
MODULUS (X10^8 DYNES CM^{-2})
0
1
2
3
4
5
FREQUENCY IN Hz

graph are for the storage modulus E' and those at the bottom for the loss modulus E". The slope of the best straight line through the E' values was found to be not significantly different from zero ($P > 0.3$). Thus, again E' was quite independent of the frequency values investigated, and an average value of 1.35 (SE = 0.06) x 10^8 dynes cm^{-2} was found. As both E' and ϕ were found to be independent of frequency, E" would be expected to behave in a similar manner. An average value of 4.14 (SE = 0.28) x 10^6 dynes cm^{-2} was found.

The dynamic elastic moduli and phase lag did not vary significantly between the 3 cusps of the aortic valve. This finding is in agreement with the pressure-volume studies of Wright and Ng (1974). The results were also found to be similar for both sexes and did not appear to depend on age in the group of specimens of ages 40-76 years old.

4. DISCUSSION

The experimental approach adopted for the study of the viscoelastic property of human aortic valve cusps was similar to that used for the mitral valve leaflet. It was designed to simulate the in vivo condition under which the aortic valve is stressed. This was achieved by the application of sinusoidal fluid pressures on the aortic surface of the aortic valve cusps. This investigation differs from those of other workers in that dynamic rather than static tissue responses were studied and membranous samples instead of tissue strips were employed. The frequency range was chosen to include the spectrum of frequencies in which a normal functioning valve might be subjected.

The results presented in figures 7.2 and 7.3 show that the human aortic valve cusps are relatively inextensible and the material has a very low loss value. These characteristics are worth considering in the design and use of either synthetic or biological materials in leaflet type valve prostheses. The low extensibility of the valve cusps as observed in this investigation agrees well with the studies of Swanson and Clark (1974) using silicone rubber valve casts. They reported that the leaflet length of the valve varies negligibly with applied pressure.

In the explanation of the origin of the first and second heart sounds, some authors are of the opinion that these sounds originate from the vibrations of the atrioventricular and semilunar valves on closure (Dock, 1933; Leatham, 1954). More recent views suggest that these sounds are produced by the accelerations and decelerations of blood which give rise to vibrations of the heart walls and the major blood vessels (Rushmer, 1970; Luisada et al, 1974; Chandraratna et al, 1975). Guyton (1971) suggested that the observed differences in the frequencies of the first and second heart sounds could, in part, be due to the differences in the elastic moduli of the atrioventricular and semilunar valves. He suggested that the lower frequency of the first sound could be due to the lower elastic modulus of the atrioventricular valves and the walls of the ventricles compared to the elastic modulus of the semilunar valves and the arterial walls. He appears to have simplified the problem, which if analyzed in detail will undoubtedly be very complex. For structures like the aortic and mitral valves, the characteristic vibrations associated with their closure will be dependent on the load on the valve, valve geometry and tissue mechanical properties. Since loading of the aortic valve at diastole is quite comparable to that of the mitral valve at systole, the remaining major factors governing the vibrational frequency would be valve geometry on closure and the elastic moduli of the valve tissues. The results presented here and those reported in chapter 6 on the mitral valve show that the elastic modulus of the mitral leaflets is greater than that of the aortic. Figure 7.4 compares the storage elastic modulus for both the mitral and aortic valves. These 2 sets of data were obtained by the same technique and under the same experimental conditions and they clearly show that the storage elastic

Figure7.4. A comparison of the storage modulus, E', of the mitral valve leaflet and the aortic valve cusps. The vertical bars indicate the standard error. Note that the mitral valve leaflets are almost twice as stiff as the aortic valve cusps.

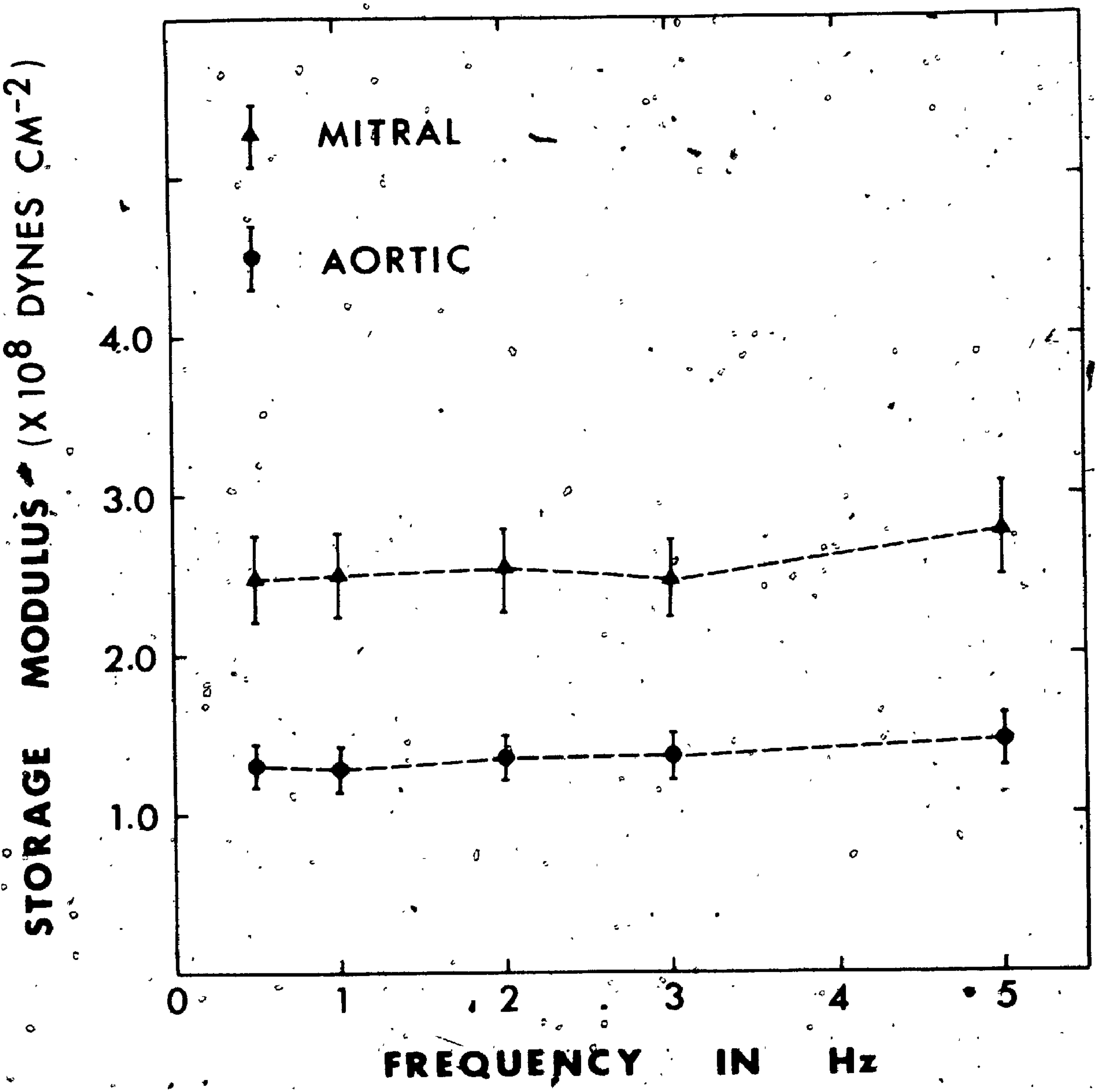
MITRAL
AORTIC
STORAGE MODULUS (X 10^8 DYNES CM^{-2})
4.0
3.0
2.0
1.0
0
1
2
3
4
5
FREQUENCY IN Hz

modulus of the mitral is nearly twice as great as that for the aortic. Since the observed frequencies of the second heart sound are higher than those of the first, while the difference in tissue elastic moduli would suggest the reverse, the differences in valve geometry may be the overriding factor if the origin of these heart sounds is in fact due to the vibrations of the heart valves. However, should it be proven that valve geometry is not the major governing factor then the results presented here would support those who deemphasize the role of the cardiac valves as the sole origin of the heart sounds. Any definitive statement however, must await a detail study of the configuration of the valves at closure.

5. SUMMARY

Membranous samples of human aortic valve cusps were subjected to sinusoidal fluid pressure variations (frequency range, 0.5 to 5 Hertz) to assess their dynamic viscoelastic properties. The storage and loss moduli and phase lag between the stressing function and response were found to be independent of the frequencies applied. The respective average values were 1.35 (SE = 0.06) x 10^8 dynes cm^{-2}, 4.14 (SE = 0.28) x 10^6 dynes cm^{-2} and 0.033 (SE = 0.002) radians. The small phase lag indicates that the tissue would recover very rapidly to its

original state on removal of any applied stress and this and the relatively low extensibility should be considered in the design of leaflet type valve prostheses. The storage modulus of the aortic valve cusps when compared with that of the mitral leaflet shows the mitral to be almost twice as stiff as the aortic. If one were to assume comparable loading and configuration for both the mitral and aortic valves on closure, this finding would lead to the conclusion that the vibrations of these two cardiac valves alone cannot contribute in any significant way to the production of the observed lower frequency of the first and higher frequency of the second heart sounds. However, the validity of the assumption of comparable valve configuration at closure has yet to be verified.

CHAPTER 8

CONCLUSIONS

The intention of this thesis was to investigate the mechanical response of the two very important valves in the human heart, the mitral and aortic valves. The results obtained should be of interest to investigators, designers and manufacturers of leaflet type valve prostheses, as the successful design of these prostheses must incorporate mechanical characteristics that are comparable to those of the normal valvular tissues.

A few studies on the mechanical properties of the valvular tissues of animals and humans have been reported, but these preliminary investigations dealt primarily with the static properties which, though important, are inadequate for a complete characterisation of the manner in which these tissues respond under normal conditions of dynamic stress. The approach in this thesis, however, has been to examine the more important dynamic response of these tissues and the experimental conditions were designed to simulate much of the in vivo state. The frequency range used in the study included the normal stressing frequency of the in vivo condition and whole membranous samples of the valve leaflets instead of valve strips were used as the cut edges of strips can possibly weaken the tissue.

This study not only quantitated the mechanical response of the valvular tissues but it was also extended to relate tissue properties to tissue structure wherever it was found necessary and possible.

The findings of this thesis showed that the valvular tissues (both mitral and aortic) are relatively inextensible and their loss (viscous) moduli are small in comparison to their storage (elastic) moduli. These findings, besides being of interest for prosthetic valve design, have also provided additional information on some hitherto postulated, but poorly substantiated, causes of certain cardiac events. The relatively inextensible nature of the mitral valve tissue and chordae tendineae has cast doubts on the cause of the atrial pressure 'c' wave. In addition, if one were to assume that the geometries of the mitral and aortic valves on closure are not significantly different then the observed greater stiffness of the mitral valve leaflet when compared to that of the aortic valve cusps has led to the conclusion that the observed frequencies of the first and second heart sounds cannot be attributed primarily to the vibrations of these valve structures.

The results obtained in this study also indicated that the structure and mechanical properties of these valvular tissues bear a good relation to their anatomical function. The network of collagen fibrils in the core of chordae tendineae ensures that these fibrils are not excessively strained in normal function. The rather elastic nature of these tissues is also a much desired feature, since they are all under constant dynamic stress. The overall mechanical properties of the many different sized chordae tendineae and valve leaflets act to provide a proper and coordinated function of these two important cardiac valves.

CHAPTER 9

SUGGESTIONS FOR FUTURE RESEARCH

As part of a continuing search for an ideal tissue valve substitute, a systematic comparison between the mechanical properties of the different tissues used in valve substitutes is desirable. It has previously been suggested that failure of artificial tissue valves could be partly due to inadequate preservation techniques. The study could, therefore, be extended to include tests on the properties of these various tissues stored in different solutions of preservative for different periods of time. The tissues most commonly tried for artificial valves are homologous, heterologous or autologous fascia lata, dura and pericardium. A companion study on the internal structures of these tissues could also be done using the scanning electron microscope, thereby providing additional information on the suitability or unsuitability of these biological materials as valve substitutes. A comparison between the surface features of these tissues with that of mechanical valve prostheses can also be useful in a study of the frequency of thrombus formation on these mechanical devices.

Rigby et al (1959) in their experiments on rat tail tendons reported that changes in mechanical properties occurred at a temperature of about 37^{o}C. Since cardiac valves, like tendons, are essentially of collagen, the effect of temperature on normal human valvular tissue properties is worthwhile pursuing. The results could have significant importance in patients suffering from high fever. The effect of pH on the valve tissues would be a further extension of the study. The changes, if any, induced by vibrations is also worth examining. This may have significant implications in cases where high frequency heart murmurs occur. For completeness, stress relaxation and creep tests should also be done on these tissues so that their mechanical response can be more fully characterised.

To confirm the contention that left atrial pressure 'c' wave is not due to the bulging of the mitral valve, studies can be performed to examine the relation between the amplitudes of the 'c' wave and the left ventricular pressure. This could be done on experimental animals by artificially monitoring their left ventricular pressure.

Finally, a theoretical approach to the question of valve vibration would be worth pursuing. Through stress and vibration analysis and considering the valve leaflets as vibrating membranes, a relation between the possible vibrational frequencies and other valve characteristics such as elasticity, dimensions, and loading conditions, could be derived. From it, the expected frequency can be predicted and compared to the values observed for the first and second heart sounds.

APPENDIX

The terms 'stress' and strain' used in chapters 3 and 5 were defined as follows:

$$\text{stress} = \frac{\text{force}}{\text{original cross-sectional area}}$$

$$\text{strain} = \frac{\text{extension}}{\text{original length}}$$

The term " final modulus' in chapter 3 was used to denote the slope of the linear portion of the stress-strain curve after the point of transition but before the proportional limit.

REFERENCES

Barratt-Boyes, B.G. (1964). Homograft aortic valve replacement in aortic incompetence and stenosis. Thorax 19: 131-150.

Bergel, D.H. (1961). The Dynamic Elastic Properties of the Arterial Wall. J. Physiol. 156: 458-469.

Bonchek, L.I., and Starr, A. (1975). Ball Valve Prostheses: Current Appraisal of Late Results. Am. J. Cardiol. 35: 843-854.

Bowes, V.F., Datta, B.N., Silver, M.D., and Minielly, J.A. (1974). Annular injuries following the insertion of heart valve prosthesis. Thorax 29: 530-533.

Bristow, J.D., and Kremkau, E.L. (1975). Hemodynamic Changes After Valve Replacement with Starr-Edwards Prostheses. Am. J. Cardiol. 35: 716-724.

Brock, R.C. (1952). The Surgical and Pathological Anatomy of the Mitral Valve. Br. Heart J. 14: 489-513.

Burch, G.E., and DePasquale, N.P. (1965). Time Course of Tension in Papillary Muscles of Heart: Theoretical Considerations. J. Am. Med. Assoc. 192: 117-120.

Burton, A.C. (1954). Relation of Structure to Function of the Tissues of the Wall of Blood Vessels. Physiol. Rev. 34: 619-642.

Campbell, R.C. (1967). Statistics for Biologists. University Press, Cambridge. pp. 134 and 120.

Caulfield, J.B., Page, D.L., Kastor, J.A., and Sanders, C.A. (1971). Connective Tissue Abnormalities in Spontaneous Rupture of Chordae Tendineae. Arch. Pathol. 91: 537-541.

Chandraratna, P.A.N., Lopez, J.M., and Cohen, L.S. (1975). Echocardiographic Observations on the Mechanism of Production of the Second Heart Sound. Circulation 51: 292-296.

Clark, R.E. (1973). Stress-strain Characteristics of fresh and frozen human aortic and mitral leaflets and chordae tendineae: Implications for clinical use. J. Thorac. Cardiovasc. Surg. 66: 202-208.

Denton, G.R. (1950). A Plastic Prosthesis Without Moving Parts for the Atrioventricular Valves. pp. 239-245. In Proc. Surg. Forum, Clinical Congress, College of Surgeons. W.B. Saunders, Philadelphia.

Dock, W. (1933). Mode of Production of the First Heart Sound. Arch. Intern. Med. 51: 737-746.

Faber, J.J. (1964). Origin and Conduction of the Mitral Sound in the Heart. Circ. Res. 14: 426-435.

Fenoglio, J.J. Jr., Pham, T.D. Wit, A.L., Bassett, A.L. and Wagner, B.M. (1972). Canine Mitral Complex: Ultrastructure and Electromechanical Properties. Circ. Res. 31: 417-430.

Ferry, J.D. (1961). Viscoelastic Properties of Polymers. John Wiley, New York. pp.277.

Flugge, W. (1960). Stresses in Shells. Springer-Verlag, Berlin.

Gallie, W.E. (1948). Fascial Grafts. Br. Surg. Pract. 4:70-83.

Gessel, R.A. (1911). Auricular Systole and its Relation to Ventricular Output. Am. J. Physiol. 29: 32-63.

Ghista, D.N., and Rao, A.P. (1972). Structural Mechanics of the Mitral Valve: Stresses sustained by the valve; non-traumatic determination of the stiffness of the in vivo valve. J. Biomech. 5: 295-307.

Gibson, T., Stark, H., and Evans, J.H. (1969). Directional Variation in Extensibility of Human Skin in vivo. J. Biomech. 2: 201-204.

Glagov, S., and Wolinsky, H. (1963). Aortic Wall as a 'Two-phase' Material. Nature 199: 606-608.

Grimm, A.F., Lendrum, B.L., and Lin, H.L. (1975). Papillary Muscle Shortening in the Intact Dog. Circ. Res. 36: 49-57.

Guyton, A.C. (1971). Textbook of Medical physiology, 4th ed. W. B. Saunders, Philadelphia. pp 152 and 349.

Hall, R.H. (1951). Variations with pH of the Tensile Properties of Collagen Fibers. J. Int. Soc. Leather Trades' Chemists 35: 195-210.

Harken, D.E., Saroff, H.S., Taylor, W.J., Lefemine, A.A., Gupta, S.K., and Lunzer, S. (1960). Partial and Complete Prostheses in Aortic Insufficiency. J. Thorac. Cardiovasc. Surg. 40: 744-762.

Hylen, J.C. (1972). Mechanical Malfunction and Thrombosis of Prosthetic Heart Valves. Am. J. Cardiol. 30: 396-404.

Ionescu, M.I., Pakrashi, B.C, Mary, D.A.S., Bartek, I.T., Wooler, G.H., and McGoon, D.C. (1974). Long-term evaluation of tissue valves. J. Thorac. Cardiovasc. Surg. 68: 361-379.

Ionescu, M.I., and Ross, D.N. (1969). Heart-valve Replacement with Autologous Fascia Lata. Lancet 2: 335-338.

Joseph, S., Somerville, J., Emanuel, R., Ross, D. and Ross, K. (1974). Aortic valve replacement with frame-mounted autologous fascia lata. Long-term results. Br. Heart J. 36: 760-767.

Kaltman, A.J. (1971). Late Complications of Heart Valve Replacement. Annu. Rev. Med. 22: 343-354.

Kloster, F.E. (1975). Diagnosis and Management of Complications of Prosthetic Heart Valves. Am. J. Cardiol. 35: 872-885.

Kosek, J.C., Iben, A.B., Shumway, N.E., and Angell, W.W. (1969). Morphology of fresh heart valve homografts. Surgery 66: 269-274.

Lakier, J.B., Fritz, V.H., Pocock, W.A., and Barlow, J.B. (1970). The Left Sided Components of the First Heart Sound: A Preliminary Communication. South African J. Med. Sc. 35: 85-92.

Lakier, J.B., Kinsley, R.H., Pocock, W.A. and Barlow, J.B. (1972). Left Atrial C Wave and Mitral Leaflet Size. Cardiovasc. Res. 6: 585-588.

Lam, J.H.C., Ranganathan, N., Wigle, E.D., and Silver, M.D. (1970). Morphology of Human Mitral Valve. I. Chordae Tendineae: A New Classification. Circulation 41: 449-458.

Leatham, A. (1954). Splitting of the First and Second Heart Sounds. Lancet 2: 607-613.

Lee, S.J.K., Lees, G., Callaghan, J.C., Couves, C.M., Sterns, L.P., and Rossall, R.E. (1974). Early and late Complications of Single Mitral Valve Replacement. A Comparison of Eight Different Prostheses. J. Thorac. Cardiovasc. Surg. 67: 920-925.

Lefemine, A.A., Millar, M., and Pinder, G.C. (1974). Chronic hemolysis produced by cloth-covered valves. J. Thorac. Cardiovasc. Surg. 67: 857-862.

Lincoln, J.C.R., Riley, P.A., Revignas, A., Geens, M. Ross, D.N., and Ross, J.K. (1971). Viability of autologous fascia lata in heart valve replacement. Thorax 26: 277-283.

Luisada, A.A., MacCannon, D.M., Kumar, S., and Feigen, L.P. (1974). Changing views on the mechanism of the first and second heart sounds. Am. Heart J. 88: 503-514.

MacCannon, D.M., Bruce, D.W., Lynch, P.R., and Nickerson, J.L. (1969). Mass excursion parameters of first heart sound energy. J. Appl. Physiol. 27: 649-652.

Massumi, R.A., Zelis, R., Ali, N., and Mason, D.T. (1973). External Venous and Arterial Pulses. In non-invasive Cardiology, edited by Weissler, A.M. Grune and Stratton, New York.

McArthur, L.L. (1901). Autoplastic Suture in Hernia and other Diastases - Preliminary Report. J. Am. Med. Assoc. 37: 1162-1165.

McKusick, V.A. (1958). Cardiovascular Sound in Health and Disease. Williams and Wilkins Co., Baltimore, pp. 3.

Mercer, J.L., Benedicty, M., and Bahnson, H.T. (1973). The geometry and construction of the aortic leaflet. J. Thorac. Cardiovasc. Surg. 65: 511-518.

Mitton, R.G. (1945). Mechanical Properties of Leather Fibers. J. Int. Soc. Leather Trades' Chemists 29: 169-194.

Morgan, F.R., and Mitton, R.G. (1960). Mechanical Properties of Raw Collagen Fibres. J. Int. Soc. Leather Trades' Chemists 44: 2-23.

Mundth, M.D., Wright, J.E.C., and Austen, W.G. (1971). Development of a Method for Stress/Strain Analysis of Cardiac Valvular Tissue. Curr. Top. Surg. Res. 3: 67-75.

Murray, G. (1956). Homologous Aortic-Valve-Segment Transplants as Surgical Treatment for Aortic and Mitral Insufficiency. Angiology 7: 466-471.

Newman, T.L., and Low, F.N. (1973). The Effects of Enzymes on Extracellular Connective Tissue Components in the Developing Chick Aorta. Am. J. Anat. 136: 407-426.

Nitter-Hauge, S., Sommerfelt, S.C., Hall, K.V., Froysaker, T, and Efskind, L. (1974). Chronic intravascular hemolysis after aortic disc valve replacement. Comparative study between Lillehei-Kaster and Bjork-Shiley Disc valve prostheses. Br. Heart J. 36: 781-785.

Nixon, P.G.F., and Polis, O. (1962). The Left Atrial X Descent. Br. Heart J. 24: 173-179.

Patel, D.J., Tucker, W.K., and Janicki, J.S. (1970). Dynamic elastic properties of the aorta in radial direction. J. Appl. Physiol. 28: 578-582.

Petch, M., Somerville, J., Ross, D., Ross, K., Emanuel, R., and McDonald, L. (1974). Replacement of the mitral valve with autologous fascia lata. Br. Heart J. 36: 177-181.

Rigby, B.J., Hirai, N., Spikes, J.D., and Eyring, H. (1959). The Mechanical Properties of Rat Tail Tendon. J. Gen. Physiol. 43: 265-282.

Roach, M.R., and Burton, A.C. (1957). The Reason for the Shape of the Distensibility Curves of Arteries. Canad. J. Biochem. Physiol. 35: 681-690.

Roberts, W.C., and Cohen, L.S. (1972). Left Ventricular Papillary Muscles. Description of the Normal and a Survey of Conditions Causing them to be Abnormal. Circulation 46: 138-158.

Roberts, W.C., Fishbein, M.C., and Golden, A. (1975). Cardiac Pathology After Valve Replacement by Disc Prosthesis. A study of 61 Necropsy Patients. Am. J. Cardiol. 35: 740-760.

Ross, D.N. (1962). Homograft Replacement of the Aortic Valve. Lancet 2: 487.

Ross, D. N. (1967). Replacement of Aortic and Mitral Valves with a Pulmonary Autograft. Lancet 2: 956-958.

Ross, J. K., and Johnson, D.C. (1974). Mitral valve replacement with homograft, fascia lata and prosthetic valves. A long term assessment of valve function. J. Cardiovasc. Surg. 15: 242-248.

Rushmer, R.F. (1970). Cardiovascular Dynamics, 3rd Ed. W.B. Saunders, Philadelphia. Chapt. 10.

Rushmer, R.F., Finlayson, B.L., and Nash, A.A. (1956). Movements of the Mitral Valve. Circ. Res. 4: 337-342.

Salisbury, P.F., Cross, C.E., and Rieben, P.A. (1963). Chorda tendinea tension. Am. J. Physiol. 205: 385-392.

Senning, A. (1967). Fascia lata replacement of aortic valves. J. Thorac. Cardiovasc. Surg. 54: 465-470.

Shaw, T.R.D., Gunstensen, J., and Turner, R.W.D. (1974). Sudden mechanical malfunction of Hammersmith mitral valve prostheses due to wear of polypropylene. J. Thorac. Cardiovasc. Surg. 67: 579-583.

Silver, M.D., and Trimble, A.S. (1972). Structure of Autologous Fascia Lata Heart Valve Prostheses. Arch. Pathol. 93: 109-115.

Silverman, M.E., and Hurst, J.W. (1968). The mitral complex. Interaction of the anatomy, physiology, and pathology of the mitral annulus, mitral valve leaflets, chordae tendineae and papillary muscles. Am. Heart J. 75: 399-418.

Smith, H.L., Essex, H.E., and Baldes, E.J. (1950). A Study of the movements of heart valves and of heart sounds. Ann. Intern. Med. 33: 1357-1359.

Starr, A. (1960). Total Mitral Valve Replacement: Fixation and Thrombosis. Surg. Forum 11: 258-260.

Starr, A., and Edwards, M.L. (1961). Mitral Replacement: clinical Experience with a Ball-Valve Prosthesis. Ann. Surg. 154: 726-740.

Swanson, W.M., and Clark, R.E. (1974). Dimensions and Geometric Relationships of the Human Aortic Valve as a Function of Pressure. Circ. Res. 35: 871-882.

Vfidik, A. (1973). Functional Properties of Collagenous Tissues. Int. Rev. Connect. Tissue Res. 6: 127-215.

Wallace, R.B. (1975). Tissue Valves. Am. J. Cardiol. 35: 866-871.

Walmsley, T. (1929). In The Heart, Quain's Elements of Anatomy, 11th Ed., Vol. IV. Pt. III. Longmans, Green and Co., London. pp. 46.

Watters, W.B., and Buck, R.C. (1971). An improved simple method of specimen preparation for replicas or scanning electron microscopy. J. Microsc. 94: 185-187.

Wiggers, C.J. (1915). Modern Aspects of the Circulation in Health and Disease. Lea and Febiger, Philadelphia. pp. 186.

Wiggers, C.J. (1934). Physiology in Health and Disease; 1st Ed. Lea and Febiger. Philadelphia. pp. 564.

Wolinsky, H., and Glagov, S. (1964). Structural Basis for the Static Mechanical Properties of the Aortic Media. Circ. Res. 14: 400-413.

Wood, S.J., Robel, S.B., and Sauvage, L.R. (1963). A Technique for Study of Heart Valves. J. Thorac. Cardiovasc. Surg. 46: 379-385.

Wright, J.E.C., and Ng, Y.L. (1974). Elasticity of human aortic valve cusps. Cardiovasc. Res. 8: 384-390.

Wynn, A., Matthews, M.B., McMillan, I.K.R., and Daley, R. (1952). The Left Auricular Pressure Pulse in Normals and in Mitral Valve Disease. Lancet 2: 216-219.

Yamada, H. (1970). In Strength of Biological Materials, edited by Evans, F.G., Williams and Wilkins Co., Baltimore. pp. 108-109.